

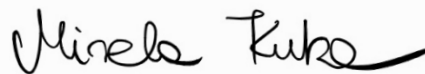
UNIVERSITA' VITA-SALUTE SAN RAFFAELE

**CORSO DI DOTTORATO DI RICERCA
INTERNAZIONALE IN MEDICINA MOLECOLARE**

**CURRICULUM IN BASIC AND APPLIED IMMUNOLOGY
AND ONCOLOGY**

Understanding the determinants of T_H1 versus T_{FH}
development upon viral infections: the role of IFN- γ

DoS: Dr. Mirela Kuka



Second Supervisor: Dr. Michelle Linterman

Tesi di DOTTORATO di RICERCA di Eleonora Sala

matr. 014360

Ciclo di dottorato XXXIV

SSD BIO/13

Anno Accademico 2020/ 2021

CONSULTAZIONE TESI DI DOTTORATO DI RICERCA

Il/la sottoscritto/I	Eleonora Sala
Matricola / <i>registration number</i>	014360
nat_ a/ <i>born at</i>	Vimercate
il/on	17/12/1993

autore della tesi di Dottorato di ricerca dal titolo / *author of the PhD Thesis titled*

Understanding the determinants of T_H1 versus T_{FH} development upon viral infections: the role of IFN- γ

NON AUTORIZZA la Consultazione della tesi per 12 mesi /DOES NOT AUTHORIZE the public release of the thesis for months

a partire dalla data di conseguimento del titolo e precisamente / *from the PhD thesis date, specifically*

Dal/*from* 01/04/2022 a/*to* 01/04/2023

Poiché/*because*:

ci sono parti di tesi che sono già state sottoposte a un editore o sono in attesa di pubblicazione / *Parts of the thesis have been or are being submitted to a publisher or are in press;*

E' fatto divieto di riprodurre, in tutto o in parte, quanto in essa contenuto / *Copyright the contents of the thesis in whole or in part is forbidden*

Data /Date 23/02/2022

Firma /Signature

Eleonora Sala

DECLARATION

This thesis has been composed by myself and has not been used in any previous application for a degree. Throughout the text I use both 'I' and 'We' interchangeably.

The first part of the results (Figure 14 to Figure 21) and part of the “Material and Methods” section have already been published in the paper “De Giovanni M, Cutillo V, Giladi A, et al. Spatiotemporal regulation of type I interferon expression determines the antiviral polarization of CD4+ T cells. *Nat Immunol.* 2020;21(3):321-330” in which I am a co-author.

In particular, regarding the published data:

1. *Flow cytometry experiments and analysis and NICHE-sequencing (Results, Chapter 6, Figure 15 and 16), were performed prior to my arrival in the lab by my former colleague Marco De Giovanni (Ph.D, Dynamics of immune responses, San Raffaele Scientific Institute, Milan, Italy) and other colleagues.*
2. *qPCR analysis and flow cytometry experiments (Results, Chapter 8.1, 8.2, Figures from 17 to 22) were performed in collaboration with my former colleagues Marco De Giovanni and other colleagues.*
3. *DC-scRNA-seq experiment and analysis (Results, Chapter 8.2, Figure 23) were performed in collaboration with my former colleague Marco De Giovanni and with our collaborators from Ido Amit Lab (Professor of Immunology, Weizmann Institute of Science, Israel).*

Regarding the second part with unpublished data, all the results presented here were obtained by myself, except for:

1. *SMARTA- scRNA-seq experiment (Results, Chapter 8.3.3, Figure 29) that was performed in collaboration with my colleagues: Dr. Cristian Gabriel Beccaria G., (Ph.D, Dynamics of immune responses, San Raffaele Scientific Institute, Milan, Italy), Dr. Chiara Laura (bioinformatician), (PhD Student, Dynamics of immune*

responses, San Raffaele Scientific Institute, Milan, Italy) and our collaborators from Ido Amit Lab (Professor of Immunology, Weizmann Institute of Science, Israel).

All sources of information are acknowledged by means of reference.

ABSTRACT

Although humoral and cellular immunity upon viral infections usually co-exist, sometimes one of the two responses emerges as dominant and is responsible for most of the antiviral activity. For example, vesicular stomatitis virus (VSV) infection induces early and potent neutralizing antibody (nAb) responses, whereas lymphocytic choriomeningitis virus (LCMV) infection induces strong cellular responses, but weak nAb responses. Preliminary data obtained in our laboratory showed that unbalance is observed also at the level of CD4 T cells responses, with VSV inducing strong T_{FH} polarization that support nAb responses, and LCMV in contrast promoting T_{H1} differentiation. Here we dissected the determinants of CD4⁺ T cell differentiation upon viral infections. Analysis of the VSV and LCMV priming niches led to identification of the spatiotemporal regulation of type I (Interferon) IFN expression as a critical regulator of antiviral T_{FH} cell polarization. In particular, in the context of VSV infection, early type I IFNs sensing by dendritic cells induced production of the cytokine IL-6 and drove T_{FH} cell polarization, whereas late exposure to type I IFN in the context of LCMV infection resulted in impaired T_{FH} cell differentiation. Moreover, we unveiled a profound heterogeneity among the T_{H1} cells that arise in response to LCMV infection, that comprise a TCF-1⁺ subset and a GzmB⁺ subset. We proved that the development of these T_{H1} is independent of IL-12 and type I IFNs. Instead, we identified IFN- γ as an important determinant of CD4⁺ T cell differentiation, partially inducing T_{H1} differentiation and suppressing T_{FH} development and germinal centers B cell responses. The molecular mechanism is still under investigation, but preliminary data suggest a role of IFN- γ in suppressing the commitment of the TCF-1⁺ population into T_{FH} . Our results shed light on new mechanisms underlying the inefficient nAbs production in response to non-cytopathic viruses such as LCMV.

TABLE OF CONTENTS

3 ACRONYMS AND ABBREVIATIONS	4
4 LIST OF FIGURES AND TABLES	7
5 INTRODUCTION	9
5.1 LCMV and VSV viral infections: polar models to study the two extreme outcomes of adaptive immune responses	9
5.1.1 LCMV.....	10
5.1.2 VSV	13
5.2 Antiviral immune responses in the secondary lymphoid organs	15
5.2.1 The Lymph nodes: filter stations that limit pathogen spread thanks to a multi-layered innate immune response.....	16
5.3 Subcapsular sinus macrophages as “flypaper” that prevent early dissemination of pathogens	18
5.4 B cell activation	21
5.5 Antigen presentation by dendritic cells shapes CD4⁺ T helper responses	24
5.5.1 T _{FH}	28
5.5.2 T _{H1}	31
5.5.3 Transcriptional and environmental cues for T _{FH} and T _{H1} commitment	33
5.6 Type I IFNs: The Jekyll and Hyde of the immune response to viral infections	40
5.6.1 Type I IFNs hinder antiviral B cell responses upon LCMV infection.....	43
6. RATIONALE	46
7. AIM OF THE WORK	50
8. RESULTS	51
8.1. Different kinetics of type I interferon induction in rVSV/rLCMV infections affect CD4⁺ T cell polarization	51

8.2 Early type I IFN sensing by DCs and IL-6 induction drive T_{FH} cell differentiation	54
8.3 Dissecting the determinants of T_{H1} polarization upon LCMV infection	59
8.3.1 IL-12 and type I IFNs are not required for T _{H1} differentiation upon LCMV infection	60
8.3.2 IFN- γ promotes T _{H1} at the expense of T _{FH} differentiation	63
8.3.3 Sc-RNA-seq and flow cytometry highlight heterogeneity within Ag-specific CD4 ⁺ T cells upon LCMV infection.....	66
8.4 Molecular mechanism whereby IFN-γ induces T_{H1} polarization and suppresses T_{FH} development.....	72
8.4.1 SMARTA-derived IFN- γ is sufficient, but not necessary to drive T _{H1} CD4 ⁺ T cell polarization upon LCMV infection.....	72
8.4.2 The early wave of IFN- γ drives T _{H1} polarization at the expense of T _{FH} differentiation.....	74
8.4.3 Group I ILCs-derived IFN- γ does not influence CD4 ⁺ T cell differentiation upon LCMV infection.....	80
8.4.4 Confocal analysis identifies DCs as early producers of IFN- γ upon LCMV infection	81
8.5 Dissecting a possible cross-inhibition between the T_{H1} and T_{FH} subsets	83
8.5.1 IFN- γ does not affect expression of T _{FH} polarizing cytokines	83
8.5.2 B cells as possible mediators of T _{FH} inhibition	84
8.5.3 IL-6 blocks IFN- γ -mediated induction of T _{H1} polarization upon VSV infection	86
9. DISCUSSION.....	90
10. MATERIALS AND METHODS.....	97
10.1. Mice.....	97
10.2. Bone marrow transplantation	97
10.3. Infections and immunizations	98
10.4. T cell isolation and adoptive transfer	98

10.5 Cell labelling.....	98
10.6 Ex Vivo Restimulation of SMARTA CD4+ T cells.....	99
10.7 Administration of antibodies and toxins	99
10.8 Organ processing to obtain cell suspension.....	99
10.8.1 Peripheral Blood	99
10.8.2 Spleen.....	100
10.8.3 Lymph Nodes.....	100
10.9 Flow Cytometry	100
10.10. Immunofluorescence Staining	103
10.11. qPCR.....	104
10.12. Statistical analyses	105
10.13 DCs Single-cell RNA sequencing.....	105
10.13.1 Massively parallel single-cell RNA sequencing library preparation	105
10.13.2 Clustering of dendritic cells.....	106
10.14 SMARTA Single-cell RNA sequencing.....	107
10.14.1 MARS-seq low level data processing.....	107
10.15 GP-1-IgG ELISA	107
<i>11 REFERENCES</i>	<i>109</i>

3 ACRONYMS AND ABBREVIATIONS

AID	Activation-induced cytidine deaminase
APC	Antigen Presenting Cell
BATF	Basic Leucine Zipper ATF-Like Transcription Factor
Bcl-6	B-Cell Lymphoma 6
BCR	B Cell Receptor
BLIMP	B lymphocyte-induced maturation protein
CCL	Chemokine (C-C motif) ligand
CCR	CC-chemokine receptor
CD	Cluster Differentiation
CD62L	L-Selectin
cDCs	Conventional dendritic cells
CR	Complement receptor
CSF-1	Colony stimulating factor-1
CSR	Class switch recombination
CTL	Cytotoxic T lymphocytes
CXCL	C-X-C motif Ligand
CXCR	C-X-C motif Receptor
DC	Dendritic cell
dLNs	Draining lymph nodes
DTR	Diphtheria Toxin Receptor
DC-SIGN	Dendritic cell-specific intercellular adhesion molecule-3 grabbing non-integrin
EBI2	Epstein-Barr virus-induced gene 2
FcγRs	Receptors for the Fc region of IgG
FDC	Follicular Dendritic Cell
FLT3L	FMS-like tyrosine kinase 3 ligands
FOXP3	Forkhead box protein P3
FRCs	Fibroblastic reticular cells
GC	Germinal Centre
GP	Glycoprotein

GzmB	Granzyme B
HBSS	Hank's Balanced Salt Solution
HEVs	High endothelial venules
i.m.	Intramuscular
i.p.	Intraperitoneal
IAV	Influenza virus
ICOS	Inducible T Cell Costimulator
ID2	Inhibitor of DNA Binding 2
IFN	Interferon
Ig	Immunoglobulin
IL	Interleukin
ILC	Innate lymphoid cell
IRF	IFN-regulatory factor
ISGs	IFN-stimulated genes
JAK	Janus kinase
LCMV	Lymphocytic choriomeningitis virus
LCs	Langerhans cells
LNs	Lymph Nodes
MCMs	Medullary cord macrophages
MHC	Major Histocompatibility Complex
MoDCs	Monocyte-derived dendritic cells
MSMs	Medullary sinus macrophages
nAbs	Neutralizing antibodies
NK	Natural Killer
NK1.1	Natural Killer cell associated marker
NP	Nucleoprotein
OAS	Oligoadenylate synthetase
PC	Plasma Cells
PD	Programmed cell death protein
pDCs	Plasmacytoid dendritic cells
PI3K	Phosphoinositide 3-kinase
PRRs	Pattern recognition receptors

PSGL-1	P-selectin glycoprotein ligand-1
RdRp	RNA-dependent RNA polymerase
RIG-I	Retinoic acid-inducible gene I
s.c.	Subcutaneous
S1P	Sphingosine- 1-phosphate
S1PR1	Sphingosine- 1-phosphate receptor 1
SCS	Subcapsular sinus
SHM	Somatic hypermutation
SIRP	Signal Regulatory Protein
SLAM	Signaling lymphocytic activation molecule
SLO	Secondary Lymphoid Organ
SOCS	Suppressor of cytokine signaling
SSM	Subcapsular sinus macrophages
STAT	Signal transducer and activator of transcription
T-bet	T-box expressed in T cells
TCF	T cell factor
TCR	T cell Receptor
TIM-3	T cell immunoglobulin and mucin domain-containing protein 3
T _{FH}	T Follicular Helper
T _{H1}	T Helper 1
TLR	Toll-like receptor
TRAIL	TNF-related apoptosis-inducing ligand
TYK	Tyrosine-protein kinase
UMAP	uniform manifold approximation and projection
VSV	Vesicular Stomatitis Virus
WT	Wild Type
YFP	Yellow Fluorescent Protein
XCR1	X-C Motif Chemokine Receptor 1
ZBTB	Zinc finger and BTB domain containing

4 LIST OF FIGURES AND TABLES

Figure 1. The course of acute LCMV infection.	12
Figure 2. The course of acute VSV infection	15
Figure 3. Lymph node structure and migration of immune cells.....	18
Figure 4. Schematic of LN showing main areas and lymphatic sinuses and suggested nomenclature for macrophage subsets.	19
Figure 5. Schematic model for macrophage antigen presentation to B cells.....	20
Figure 6. Schematic of the different ways through which the antigen is presented to B cells in the lymph node.....	22
Figure 7. Spatiotemporal dynamics of B cell activation.....	24
Figure 8. Schematic model for dendritic cell type and their specific markers.	26
Figure 9. CD4 ⁺ T helper cell subsets	28
Figure 10. The multistep process of T _{FH} differentiation	31
Figure 11. T _{FH} and T _{H1} bifurcation.	35
Figure 12. Environmental cues that instruct CD4 ⁺ T cell differentiation.	40
Figure 13. The pleiotropic roles of type I IFNs upon viral infection.....	42
Figure 14. Type I interferon-mediated suppression of antibody responses.	45
Figure 15. VSV and LCMV infections result in distinct antiviral CD4 ⁺ T cell polarization.	47
Figure 16. Characterization of the antiviral CD4 ⁺ T cell priming niche.....	48
Figure 17. Type I IFNs kinetics differ upon rVSV and rLCMV infection	52
Figure 18. Type I IFNs sensing is essential for the induction of T _{FH} differentiation upon rVSV infection	53
Figure 19. Early type I IFNs sensing is essential for the induction of T _{FH} polarization	54
Figure 20. Type I IFNs sensing by DCs is instrumental for the induction of T _{FH} polarization upon rVSV infection	55
Figure 21. IL-6 expression requires type I IFN sensing	56
Figure 22. Early IL-6 induction is essential for antiviral T _{FH} differentiation.	57
Figure 23. scRNA-seq analysis of LN DCs upon viral infection.	59
Figure 24. IL-12 and type I IFNs are induced upon subcutaneous LCMV infection	60
Figure 25. IL-12 is not required in the induction of T _{H1} polarization upon LCMV infection	61
Figure 26. Type I IFNs are not required in the induction of T _{H1} polarization upon LCMV infection	63

Figure 27. IFN- γ induces SMARTA T _{H1} differentiation and suppresses SMARTA T _{FH} development upon LCMV infection.	64
Figure 28. IFN- γ induces endogenous T _{H1} differentiation at the expense of T _{FH} development upon LCMV infection.	66
Figure 29. Single-cell RNA-seq identifies two clusters of SMARTA CD4 ⁺ T cells upon LCMV infection.....	68
Figure 30. Effector CD4 ⁺ T cells polarize into TCF-1 ⁺ ad TCF-1 ⁻ GzmB ⁺ populations and the GzmB ⁺ population represent the major IFN- γ producer.	70
Figure 31. IFN- γ inhibits T _{FH} differentiation suppressing the differentiation of the TCF-1 ⁺ population towards CXCR5 ⁺ PD-1 ⁺ T _{FH}	71
Figure 32. SMARTA-derived IFN- γ is sufficient, but not necessary, to drive T _{H1} CD4 ⁺ T cell polarization upon LCMV infection.....	74
<i>Figure 33. The early sensing of IFN-γ influences CD4⁺ T cell polarization upon LCMV infection</i>	<i>75</i>
Figure 34. IFN- γ blockade does not affect the expansion of neutrophils, inflammatory monocytes or cDCs	76
Figure 35. IFN- γ producers upon rLCMV infection.....	78
Figure 36. IFN- γ expression by Group I ILCs in dLNs upon LCMV infection	79
Figure 37. Group I ILCs-derived IFN- γ does not influence CD4 ⁺ T cell polarization upon LCMV infection.....	80
Figure 38. IFN- γ expression by DCs in dLNs upon LCMV infection.....	82
Figure 39. IFN- γ does not affect the expression of type I IFNs and IL-6.....	84
Figure 40. IFN- γ suppresses GC-B cell development and hinder humoral response upon LCMV infection.....	86
Figure 41. T _{H1} polarizing cytokines expression is induced upon rVSV infection	87
Figure 42. The early production of IL-6 upon rVSV infection antagonizes the IFN- γ mediated induction of T _{H1} polarization.....	88
Figure 43. Spatiotemporal regulation of type I interferon expression determines the antiviral polarization of CD4 ⁺ T cells	90
Figure 44. Graphical Abstract showing the role of IFN- γ in shaping CD4 ⁺ T cell responses	92

INTRODUCTION

5 INTRODUCTION

The dynamicity and diversity of the immune system supports efficient protection of the individual from an array of different pathogenic entities. Effective viral clearance is achieved mainly through the elimination of infected cells by antigen-specific cytotoxic T lymphocytes and the neutralization of infectious virus by antigen-specific B cells (Hangartner *et al*, 2006). These two arms of the adaptive immune system usually coexist in a state of competitive equilibrium to maximize viral clearance (Arnaout & Nowak, 2000); however, some viruses can favor one branch at the expense of the other, leading one response to emerge as dominant and disrupting this dynamic equilibrium (Hangartner *et al*, 2006). The differentiation of CD4⁺ T cells into specialized helper subsets actively participates in the balance between humoral and cellular adaptive immunity (Sheikh & Groom, 2020), but the molecular mechanisms that drive distinct T effector subsets are incompletely understood. This introduction will give an overview of how antiviral cellular and humoral responses are generated in the secondary lymphoid organs in response to viral infection, with a particular focus on CD4⁺ T cell differentiation and its role in supporting humoral and cellular immunity.

5.1 LCMV and VSV viral infections: polar models to study the two extreme outcomes of adaptive immune responses

Viruses are obligate intracellular pathogens, and as a consequence, they require host cells for their replication. Despite their relatively simple structure (an RNA or DNA genome surrounded by a virus-coded protein coat), viruses can trigger the immune system in different ways. They can activate intracellular pattern recognition receptors (PRRs) through their RNA/DNA content and induce the production of type I interferons (IFNs), which control early viral replication (Mueller & Rouse, 2008). Besides the activation of innate immunity, viruses trigger also adaptive immune responses. Efficient coordination of humoral and cellular responses results in the elimination of infectious virions on one hand, and infected cells on the other. Taking into consideration that each virus is different from the other, there can be immune responses that are different in modality and/or timing. Indeed, depending on the nature of the virus, humoral responses and cellular

responses might outcompete each other, resulting in a wide range of outcomes (Hangartner *et al*, 2006).

When we talk about viruses and immune responses, one of the most fascinating aspects is the virus-host adaptation. It's in the interest of a virus that the host survives, as the survival of the host guarantees the virus to be able to transmit and propagate. A host that dies before this happens means the death of the virus itself. This is why some viruses are controlled very efficiently by the immune system whereas others have evolved to interfere with generation of immune responses in multiple ways. This results in a wide spectrum of antiviral adaptive immune responses. On one hand, cytopathic viruses, which provoke extreme damage in infected tissues and have to be rapidly controlled by a strong neutralizing antibody (nAb) response to ensure the host survival; on the other hand, poorly cytopathic viruses that do not induce direct cell damage, usually elicit robust cytotoxic cellular responses that control viral titers but cause immunopathology (Rouse & Sehrawat, 2010). As a result, a fine balance between humoral and cellular responses would be desirable to ensure an efficient viral clearance without excessive immunopathology (Arnaout & Nowak, 2000). In this context, lymphocytic choriomeningitis virus (LCMV) and vesicular stomatitis virus (VSV) represent model viruses for the two extremes of the spectrum of adaptive immune responses and they are widely used to study the different outcomes of the adaptive immune response (Hangartner *et al*, 2006).

5.1.1 LCMV

LCMV was originally isolated in 1933 by Charles Armstrong in patients with aseptic encephalitis and two years later the house mouse (*Mus musculus*) was recognized as the natural reservoir host of the virus (Vilibic-Cavlek *et al*, 2021). LCMV is an enveloped Old-World arenavirus, with a negative-strand RNA genome, ambisense coding strategy, with ~10.7 kb genome formed of 2 RNA segments (Smelt *et al*, 2001);(Eschli *et al*, 2006). The structure of the virus comprises a helical nucleocapsid with an RNA genome containing two ambisense RNA segments (S and L) that encode for four viral proteins: nucleoprotein (NP), envelope precursor glycoprotein (GPC), which is cleaved into two subunits (GP1 and GP2), matrix zinc-binding (Z) protein and the large (L) RNA-dependent RNA polymerase (RdRp). NP represents the main structural protein and is

essential for both transcription and replication. LCMV glycoproteins belong to typical class I viral fusion proteins, so they form heterodimeric trimers containing the peripheral receptor-binding subunit glycoprotein 1 (GP-1) that binds to the surface receptor α -dystroglycan and the transmembrane subunit GP-2, which mediates viral membrane fusion (Kunz *et al*, 2003). LCMV-neutralizing antibodies (nAbs) are directed against a single site on GP-1 protein, preventing the binding of the virus to the cell (Vilibic-Cavlek *et al*, 2021).

LCMV is widely used in the field of immunology as a valuable model to investigate viral pathogenesis and adaptive cellular responses. Indeed, LCMV has been used in some of the most fundamental studies and has contributed to research that has later gone on to win several Nobel prizes (Zhou *et al*, 2012); (Abdel-Hakeem, 2019) (Guo, 2018). Among the most important conceptual discoveries, we find the Major Histocompatibility Complex (MHC) restriction phenomenon, T cell memory, persistent infections, and T cell exhaustion (Zhou *et al*, 2012);(Zinkernagel & Doherty, 1975).

But why is LCMV such a useful tool to study cellular immune responses? First, LCMV is a poorly cytopathic virus, so it does not cause direct damage to cells and tissues, thus enabling a thorough analysis of the cytotoxic activity of immune cells. Another important feature of the virus is the high degree of diversity coupled to the rapid evolution, which resulted in the isolation of several well-characterized viral strains that differ in their replicative capacity, cell tropism, and experimental routes of infection, providing a wide spectrum of immune responses (Vilibic-Cavlek *et al*, 2021). The most widely used strains are the Armstrong strain and the Clone 13 (Cl-13) strain, which lead to acute and chronic infection, respectively (Bergthaler *et al*, 2010).

In the acute system, the virus reaches its peak typically at day 3-4 post-infection, then CD8⁺ T cells proliferate to large numbers upon the priming phase in the secondary lymphoid organs (SLOs). CD8⁺ T cells reach their peak few days later after the peak of the virus and once CD8⁺ T cell starts to emerge the level of the virus declines down toward undetectable levels and CD8⁺ T cells shrink quite substantially leaving a long-lived memory response (Althaus *et al*, 2007); (Zhou *et al*, 2012). These CD8⁺ T cells are very efficient in the clearance of the virus because they are oligoclonal, so they target different peptides, they secrete a high amount of IFN- γ , which is an essential antiviral cytokine and they are highly proliferative (Anderson *et al*, 1985). In this way, the virus is completely

eliminated, and it cannot acquire mutations that drive its escape. However, CD8⁺ T cell can proliferate and control the virus in the early phase upon infection, but in absence of CD4 or B cell help, a few weeks upon infection, the virus will reemerge and CD8⁺ T cells become exhausted leading to an increase viremia (Misumi & Whitmire, 2014). In addition, LCMV, like other poorly cytopathic viruses, lacks an early and potent nAbs response, typical of cytopathic viruses such as VSV (Hangartner *et al*, 2006). Indeed, nAbs are undetectable during the acute phase of infection and only develop in the late phase of the immune response (at 50-80 days) (Hangartner *et al*, 2006) (**Figure 1**). For this reason, LCMV is also used as a model to investigate why poorly cytopathic viruses fail to induce an efficient nAbs response; several studies shed light on many of the factors responsible for this phenomenon.

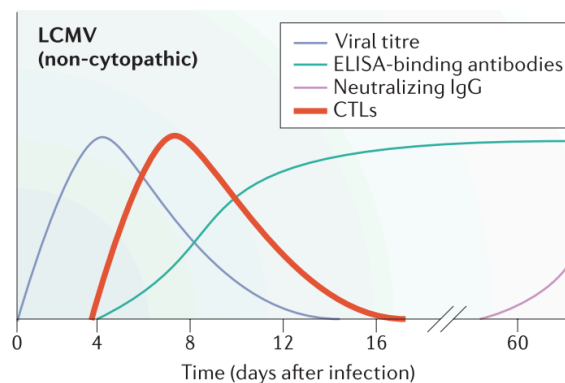


Figure 1. The course of acute LCMV infection.

*Schematic representation of the immunological profile of acute LCMV infection. LCMV induces a vigorous CTL response that peaks at 7 days post-infection, which is trivial in clearing the virus below detectable levels. Neutralizing-antibody responses usually do not contribute during the acute phase of infection and only develop after 50–80 days. (Figure adapted from Hangartner *et al*, Nature Review Immunology, 2006 _ License Number: 5247081454245)*

One of the factors is the frequency of germ line-encoded immunoglobulin variable regions specific for accessible sites, that greatly influence the immunogenicity properties of the virus. In the context of LCMV infection, the neutralizing epitope of the surface glycoprotein was shown to be poorly immunogenic in wild-type mice (Pinschewer *et al*, 2004). On the contrary, mice transgenic for the heavy chain of the LCMV-neutralizing monoclonal antibody KL25, which carry lots of B cells specific for the neutralizing

epitope, develop an early and efficient T-independent neutralizing antibody response, suggesting that, in wild-type mice, the frequency of antigen-specific B cell precursors should be very low (Seiler *et al*, 1998). Another factor that is linked to a weak nAbs response in the context of LCMV infection is the induction of impaired T helper responses, which result in the activation of B-cells regardless of their specificity and in an increased hypergammaglobulinemia (Hunziker *et al*, 2003). These B cells localize in the same niche of the rare neutralizing B cells and contend for survival factors (Hunziker *et al*, 2003).

In addition, the exacerbated CD8⁺ CTLs responses lead to the disruption of the architecture of secondary lymphoid organs and the elimination of antigen-presenting cells, further impairing the neutralizing-antibody response (Borrow *et al*, 1995);(Odermatt *et al*, 1991). Finally, during the last years type I IFNs have emerged as new important suppressors of anti-viral humoral immune responses at multiple levels (Wilson *et al*, 2013);(Osokine *et al*, 2014); (Moseman *et al*, 2016). Their role in hindering B cell responses will be explained in detail in paragraph 5.6.1.

5.1.2 VSV

VSV is a negative-strand RNA virus, and a member of the *rabdoviridae* family. It exhibits a strong neurotropism that can result in paralytic symptoms in mammals, including mice. For this reason, it is widely used as an ideal model for investigating immunity to human neurotropic viruses like rabies virus. In contrast to LCMV, it is highly cytopathic, causing extreme damage in infected tissues and it has to be efficiently controlled by the immune system to ensure the host's survival (Hangartner *et al*, 2006). The single-stranded negative-sense RNA genome of VSV is associated with nucleoprotein (N), phosphoprotein(P), and RNA-dependent polymerase (L). The genome is arranged in a helical fashion with a lipid-glycoprotein envelope that encloses the nucleoprotein core. This comprises the glycoprotein (G) protein, which anchors to target cells, and the structural protein matrix (M), which drives budding of virus particles from the host plasma membrane. (Whelan, 1972);(Hastie *et al*, 2013). There are two main VSV serotypes, Indiana (IND) and New Jersey (NJ), which are endemic to parts of the United States as well as much of Central and South America (Hastie *et al*, 2013).

Different studies on VSV viral pathogenesis have shown different outcomes of infection dependent on the dose and the route of administration (Johnson *et al*, 2007). For example, intranasal (i.n.) injection in mice or non-human primates has been used as a model for experimental encephalitis (Summers, 2009). Other routes of administration, such as intramuscular (i.m.), subcutaneous (s.c.), or intraperitoneal (i.p.), generally end in very mild disease and limited virus replication (Hastie *et al*, 2013). Indeed, viral spreading is kept under control thanks to an early, strong, T-cell-independent, neutralizing IgM response that turns into a T-cell-dependent IgG response after 4–6 days (Hangartner *et al*, 2006) (**Figure 2**). This rapid induction of early T-independent nAbs is critical for the control of viral infection since it gives time to CD4⁺ T cells to be primed by dendritic cells (DCs), to undergo clonal expansion and differentiation toward T Follicular Helper (T_{FH}), that support the delayed T-dependent Germinal Centre (GC) reaction. Although there is an efficient induction of CTLs upon VSV infection, they are not essential to control infection. Mice that lack CTLs can control viral spreading to the same extent as CTL-competent mice (Whelan, 1972);(Andersen *et al*, 1999).

But how is fatal neuroinvasion prevented upon peripheral infection? In mice, immunity to VSV engages a vigorous, multi-layered cellular and humoral response that limits viral replication after infection. This involves the induction of an efficient type I IFN response regulated by viral sensing pattern recognition receptors (PRRs), mainly endosomal Toll-like receptor-7 (TLR7), and cytosolic retinoic acid-inducible gene I (RIG-I) receptors (Solmaz *et al*, 2019). SCS macrophages represent crucial gatekeepers for the viral spread because they capture and retain lymph-borne virions and present them intact to B cells, ensuring their early activation (Iannacone *et al*, 2010);(Junt *et al*, 2007). In addition, an interesting study identified subcapsular sinus (SCS) macrophages as crucial players in preventing the access of VSV to the central nervous system (CNS). Specifically, SCS macrophages sense VSV through TLR7, which represents the main sensing receptor for this virus and is crucial in controlling lymph-borne VSV infection (Solmaz *et al*, 2019). As a consequence, they constitute one of the main cellular sources of the early wave of type I IFNs (Iannacone *et al*, 2010). Experiments in bone marrow chimeric mice showed that type I IFN acts on both haematopoietic and stromal compartments, including the intranodal nerves, to prevent lethal infection with VSV. In addition, SCS macrophages are also capable to secrete waves of chemokines that attract plasmacytoid DCs (pDC),

which migrate from the deep cortex towards the SCS and medulla, where they encounter VSV, secrete high levels of type I IFNs and promote the survival of Ag-specific CTLs, thus controlling viral burden and preventing viral spread in LN peripheral nerves (Swiecki *et al*, 2010);(Detje *et al*, 2009).

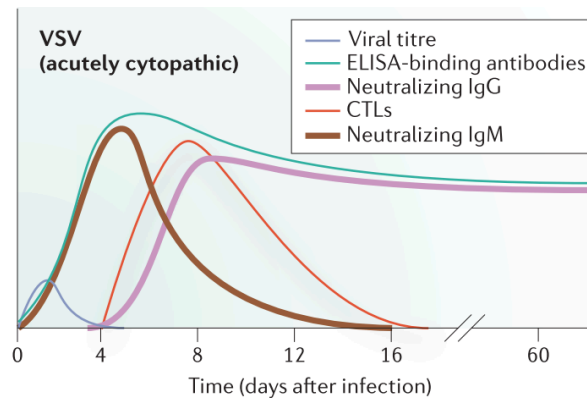


Figure 2. The course of acute VSV infection

*Schematic representation of the immunological profile of acute VSV infection. VSV is rapidly controlled by a strong, early, initially T-cell-independent, neutralizing IgM response that switches to a T-cell-dependent IgG response after 4–6 days. Although virus-specific CTLs are induced during VSV infections, they are neither necessary nor sufficient to control infection (Figure adapted from Hangartner *et al*, Nature Review Immunology, 2006_ License Number: 5247081454245)*

5.2 Antiviral immune responses in the secondary lymphoid organs

Adaptive immune responses are generated in secondary lymphoid organs (SLOs), which include spleen and lymph nodes (LNs). Blood-borne antigens are captured and processed mostly in the spleen, whereas lymph-born antigens are recognized in the LNs. Many viruses, including the ones that have been used in my PhD project, enter the organism principally through the skin and the mucous membranes that represent the first barrier against pathogen invasion. (Kuka & Iannacone, 2014). Taking into account this physiologic route of infection, our studies focus on the analysis of adaptive immune responses in the draining LNs after subcutaneous viral infection.

Mediators of innate immunity, such as innate cells and interferons contribute decisively in establishing the “antiviral state” that contains the viral spread at the entry site. The innate arm of the immune system is activated very quickly upon infection and

keeps the infection in check while it stimulates the more specialized adaptive arm. However, some viruses evade this first barrier and enter the lymph through the lymphatic vessels that drain fluid from tissues. From here, the virus reaches the draining lymph nodes, bean-shaped organs that behave as lymph filters and avoid systemic pathogen spread. Recent works have revealed a multilayered spatial organization of lymph nodes that are colonized by different immune cells localized in specific niches to maximize pathogen clearance (Kastenmüller *et al*, 2012);(Iannacone *et al*, 2010);(Gerner *et al*, 2015a). The detailed structure of LNs is described in the paragraphs below.

5.2.1 The Lymph nodes: filter stations that limit pathogen spread thanks to a multi-layered innate immune response

The lymph node is surrounded by a protective fibrous capsule constituted mainly by collagen (**Figure 3**). After reaching this capsule, afferent lymphatic vessels, which contain cells of the immune system and tissue-derived antigens, deliver lymph to the subcapsular sinus (SCS), a cavity underneath the collagen capsule. Lymph then flows from the cortical sinuses to the medullary sinuses and into the efferent lymphatic vessels (Von Andrian & Mempel, 2003);(Girard *et al*, 2012). The SCS and the medullary sinus floors display a network of lymphatic endothelial cells expressing lymphatic vessel endothelial hyaluronic acid receptor 1 (LYVE1). At the level of LN sinuses, there are two populations of macrophages that are surrounded by the lymph: CD169⁺ SCS macrophages and medullary macrophages (Gray & Cyster, 2012).

Underneath the subcapsular sinus is the cortex, the outer region of the LNs, which consists of aggregates of B lymphocytes, known as primary follicles. B cell follicles represent the main site of humoral responses since they are home to GCs reactions during T cell-dependent immune responses (Allen *et al*, 2007). They are shaped by different chemokine cues provided by a network of stromal cells that guides the migration of the B cells (Katakai *et al*, 2004);(Huang *et al*, 2018). This network is composed mainly of a population of radiation-resistant follicular dendritic cells (FDCs) that express high levels of the adhesion molecules vascular cell-adhesion molecule 1 (vCAM1) and intercellular adhesion molecule 1 (ICAM1), as well as complement and Fc receptors (Wang *et al*, 2014). Despite their dendritic-shaped structure, FDCs are of stromal origin and thus are distinct from classical DCs (Jarjour *et al*, 2014).

Naïve B and T cells enter the LNs through HEVs, and migrate to different niches based on the chemokine receptors they express. Naïve B cells are guided to enter the follicles thanks to the expression of C-X-C chemokine receptor type 5 (CXCR5), the receptor for the CXCL13 chemokine, produced by FDCs (De Guinoa *et al*, 2011). Naïve T cells and DCs express the receptor CCR7, so they are directed to the paracortex by CCL19 and CCL21 chemokines gradients produced in the T cell area by fibroblastic reticular cells (FRCs) (Gunn *et al*, 1998). FRCs provide an infrastructure along which lymphocytes can traffic and they are key players in orchestrating T- DC interactions (Anderson & Anderson, 1975). The T cell area also includes a channel of collagenous conduit fibers that consent the movement of low-molecular-weight factors of the lymph, such as chemokines, from the subcapsular sinus to HEVs (Ma *et al*, 2007). The medulla, innermost layer, is mainly constituted by efferent lymph vessels that collect filtered lymph that they put back into the circulation. This area contains both B and T cells that are localized in the medullary cords and many other immune cells such as DCs, macrophages, plasma cells (PC), and memory B cells. In addition, recent work has identified a new subset of stromal cells called medullary FRCs (MedRCs) that sustains the PC niche in the medulla guiding PC migration and residence, but also sustaining PC homeostasis (Huang *et al*, 2018) (**Figure 3**).

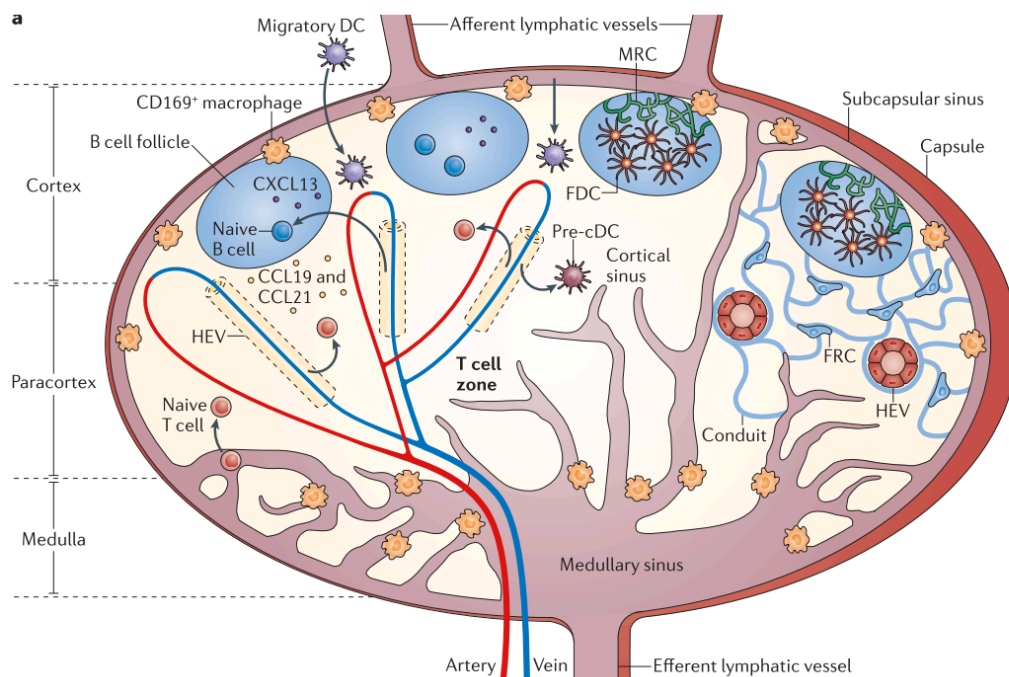


Figure 3. Lymph node structure and migration of immune cells

Schematic representation of a lymph node showing the three different areas: the cortex, the paracortex, and the medulla. The route of entry of naive lymphocytes includes high endothelial venules (HEVs) or afferent lymphatic vessels, instead, the route of exit includes cortical sinuses, medullary sinuses, and the efferent lymphatic vessel in the medulla. The cortex contains B cells and follicular dendritic cells (FDCs) organized to form B cell follicles. T cells are located mainly in the T cell area of the paracortex. The fibroblastic reticular cells (FRCs) in the T cell areas provide the conduit system along which lymphocytes can traffic. (Figure adapted from Girard et al., Nature Review Immunology, 2012 __Licence number: 5247080594171)

5.3 Subcapsular sinus macrophages as “flypaper” that prevent early dissemination of pathogens

The advent of new powerful technologies such as intravital imaging has changed our vision and understanding of adaptive immune responses, enabling the real-time view of the interplay between viruses and the immune system (Hickman, 2017). One example is the characterization of the early steps of antigen recognition in the dLNs. Viral particles and other antigens are carried to the dLNs through afferent lymph vessels and once they have entered the SCS, they can be handled in different ways depending on their size. Antigens of the size of a virus (higher than 70 kDa) are too big to diffuse directly through the SCS lumen; they instead are captured and retained by SCS macrophages (SSM) (Iannacone et al, 2010);(Louie & Liao, 2019). Macrophages are hematopoietic cells deriving either by bone marrow-derived monocytes or from fetal liver-derived precursors: they require colony stimulating factor-1 (CSF1) for their development (Gray & Cyster, 2012). Macrophages can enter damaged tissues from the circulation, and recognize, engulf and degrade cellular debris and pathogens. Inside the lymph node, there are three different populations of macrophages: subcapsular sinus macrophages (SSMs), medullary sinus macrophages (MSMs), and medullary cord macrophages (MCMs) (Gray & Cyster, 2012) (**Figure 4**). They cooperate in limiting the viral dissemination but they hold different aptitudes to capture lymph-borne molecules; MSMs are less discriminatory in their filtering skills and avidly bind any lymph-borne antigen that filter through the SCS and cortical sinuses and is trapped in the medullary sinuses; by contrast, SSMs are less phagocytic and efficient at binding particulate antigens, with the significant exception of viruses and immune complexes. These macrophage subtypes are also different in terms

of susceptibility to viruses (Clark, 1962);(McDevitt *et al*, 1966). Indeed, several works have shown that in the case of VSV infection, the virus replicates in SSMs but not in MCMs (Sammicheli *et al*, 2016);(Junt *et al*, 2007). The reasons behind these differences are still incompletely understood but they could rely on several phenotypic and functional features.

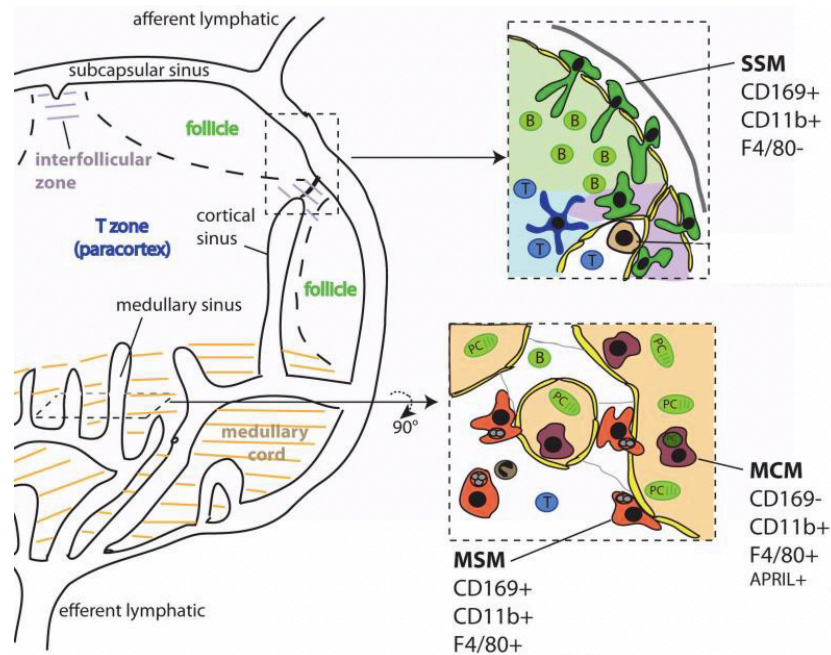


Figure 4. Schematic of LN showing main areas and lymphatic sinuses and suggested nomenclature for macrophage subsets.
(Figure adapted from Gray et al., J Innate Immun, 2012_License Number:5247091427132)

Several milestone studies have defined SSMs as the bridge that links lymph-borne antigens and follicular B cells (Junt *et al*, 2007); (Carrasco & Batista, 2007); (Phan *et al*, 2007). Thanks to 2-photon microscopy it has been possible to visualize the unique structure of these macrophages, with a ‘head’ directed toward the sinus and long ‘tail’ protrusions that are inserted into the follicles (Cyster, 2010) (**Figure 5**).

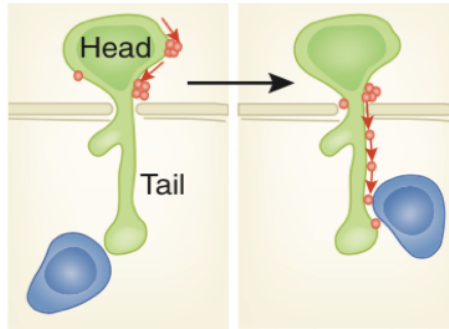


Figure 5. Schematic model for macrophage antigen presentation to B cells.

Subcapsular sinus macrophages are characterized by a unique structure with a ‘head’ directed toward the sinus and long ‘tail’ protrusions that are inserted into the follicles. They translocate viral particles across the subcapsular sinus floor to present them to B cells inside the follicle (Figure adapted from Cyster, Nat Imm, 2010_ License Number: 5247080863775)

Junt et al., used a fluorescently labeled ultraviolet-inactivated VSV and thanks to multiphoton intravital microscopy in popliteal draining lymph nodes they were able to spot the virus at the level of the SCS floor within minutes after injection. VSV signal colocalized with CD11b⁺, MHC-II⁺, CD169⁺ cells in the SCS, defining SSMs as the cells that capture the virus early upon VSV infection (Junt *et al*, 2007). These macrophages have also the ability to translocate viral particles across the subcapsular sinus floor to present them to B cells inside the follicle. Follicular B cells migrate through the dense carpet of macrophages’ tails, often making direct contact with them (Carrasco & Batista, 2007);(Phan *et al*, 2007);(Junt *et al*, 2007) (**Figure 5**). In this way, cognate B cells can acquire and process the antigen through the B cell receptor (BCR) and start the process of activation before the migration to the T-B border, where they may receive specific T-cell help. In addition, the fundamental role of SSMs is evident when they are depleted through treatment with clodronate-loaded liposomes; in their absence VSV is no more captured and contained, so it spreads systemically (Iannacone *et al*, 2010).

In some conditions, CD169⁺ macrophages themselves could be infected, therefore representing an early reservoir for pathogen replication (Iannacone *et al*, 2010);(Sammicheli *et al*, 2016). For example, SSMs are the only cellular target infected by the virus upon subcutaneous VSV infection (Sammicheli *et al*, 2016); as a consequence, they are the major producers of type I IFNs, which prevent VSV from invading peripheral nerves within LNs (Iannacone *et al*, 2010).

5.4 B cell activation

Early B cell activation is characterized by two spatiotemporal defined events: first, specific recognition of native antigens by the BCR initiates intracellular signaling and antigen internalization (Cyster, 2010); second, antigen processing and presentation to helper T cells boosts B-cell activation and ultimately drives the development of high-affinity nAbs (Crotty, 2014).

B cells recognize antigens in their native conformation without the need of processing and presentation by antigen-presenting cells (APCs). However, display of native antigens by other cell type enhances physical cross-linking of the BCR and renders B cell activation more efficient. As previously mentioned, SSMs capture, retain and translocate viral particles across the SCS floor to display it for B cells. This is true only for antigens of the size of a virus, since low-molecular weight antigens may gain access to the follicles without requiring cell-mediated presentation, through direct diffusion via FRCs conduits. Antigen display to B cells could be mediated by dendritic cells and follicular dendritic cells (Chen et al, 1978),(Suzuki et al, 2009) (**Figure 6**). Antigen captured by DCs is either stably exposed on the cell surface or is resistant to intracellular degradation. This is achieved thanks to the expression of Fc γ RIIB and DC-SIGN, which direct the internalization of antigen-containing immune complexes into either non-degradative intracellular compartments or in neutral endosomes, respectively (Bergtold *et al*, 2005). On the other hand, FDCs are widely considered the first players in antigen presentation to B cells in SLOs in the follicles mediating the retention of antigen in the form of immune complexes (with antibody and/or complement fragments) through two different mechanisms. The first relies on the expression of high levels of complement receptor 1 (CR1) and CR2 (also known as CD35 and CD21, respectively), which bind to various fragments of C3 and the second on Fc γ RIIB that is expressed on the surface of FDCs in germinal centers (Mandels *et al*, 1980); (Chen *et al*, 1978); (Tpw *et al*, 1980).

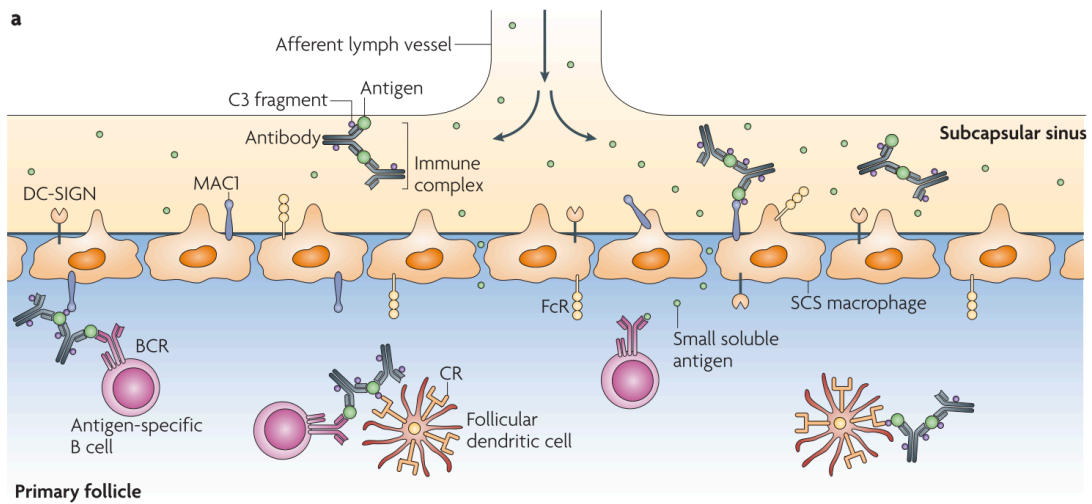


Figure 6. Schematic of the different ways through which the antigen is presented to B cells in the lymph node.

*Small soluble antigens present in the lymph diffuse directly to the B cell follicles. Large antigens, immune complexes and viruses can be presented to follicular B cells at the macrophage-rich SCS. In addition, follicular B cells may recognize antigen that is presented on the surface of FDCs. (Figure adapted from Batista *et al*, *Nature Review Immunology*, 2009_ License Number: 5247081053659)*

Shortly after antigen recognition through the BCR, B cells upregulate CCR7 (the receptor for CCL19/ 21 chemokines, which are secreted in the T cell area) and downregulate CXCR5, thus migrating to the T-B border to seek for T cell help (Okada *et al*, 2005) (**Figure 7**). In addition to the modulation of CXCR5 and CCR7, B cell access to the outer parts of the follicle is fostered by the chemoattractant receptor Epstein-Barr virus-induced gene 2 (EBI2), which binds to the oxysterol 7a,25-HC, produced by stromal cells. In this way, EBI2 helps B cell positioning in the outer follicle, and leads to improvement of T-dependent antibody responses (Cyster *et al*, 2014); (Gatto & Brink, 2013). This first B cell migration step occurs also upon viral infections that do not trigger an early and potent nAb response, such as LCMV in mice (Sammicheli *et al*, 2016).

At the T-B border, CXCR5⁺ EBI2^{lo} antigen-specific B cells can interact with cognate CD4⁺ T cells through peptide-MHCII (pMHCII): T cell receptor (TCR) engagement, a process that can drive their full activation and the initiation of GC reactions. Alternatively, a first wave of T-independent IgM antibodies is generated after B cell differentiation towards extrafollicular plasmablasts (**Figure 7**). The two abovementioned fates are not mutually exclusive. For example, in the context of VSV infection, T-

independent IgMs produced as early as four days after infection rapidly control viral spread. Later, higher affinity T-dependent IgGs arise after GC reactions (Hangartner *et al*, 2006); (Ochsenbein *et al*, 2000).

The GC is a highly peculiar structure containing several immune cell subsets: GC-T_{FH}, B cells, FDCs, macrophages and stromal cells. At this stage, T-B interactions, differently from the ones occurring at the T-B border, are very short in duration but they comprise an extensive area of interaction (entanglement) (Liu *et al*, 2015). GCs can be divided into a dark (DZ) and a light zone (LZ), originally named so based on their appearance upon histological staining. The dark zone is filled by densely packed GC B cells, whereas the light zone contains FDCs, T_{FH} cells, and more sparsely distributed GC B cells. FDCs present non-processed antigens and serve as long-term antigen deposits, therefore taking part in the B cell selection process. By secreting CXCL13 they attract CXCR5 expressing GC B cells and T_{FH} cells into the light zone. On the contrary, CXCL12 expressed by reticular cells retains CXCR4 expressing GC B cells in the dark zone. The interplay of those two cytokines and their receptors orchestrates the zonal distribution of the GC B cells, yet they regularly transit between both zones (Allen *et al*, 2008);(Schwickert *et al*, 2007). Indeed, the GC reaction progresses as a cyclic process. In the DZ, B cells undergo proliferation and activation-induced cytidine deaminase (AID)- driven somatic hypermutation (SHM), a process that generates BCRs with different affinities towards the antigen (Barreto *et al*, 2005). The hypermutated GC cells recycle to the light zone where they interact with FDCs and T_{FH} cells, which are important for the selection of high-affinity GC B cells. GC B cells with higher affinity BCRs capture and display more antigen leading to an advantage in the competition for T_{FH} cell help, which drives their selection. After positive selection, the GC cells re-enter the dark zone, where they undergo cell division leading to the expansion of the high-affinity clones. This results in a feedforward loop where GC cells expressing high-affinity BCRs repeatedly recirculate to the dark zone where they proliferate and undergo additional rounds of SHM (Victora & Nussenzweig, 2012). Although GC B cells are not directly involved in antibodies secretion, they take part to long-lasting humoral responses by polarizing into PCs and memory B cells (Victora & Nussenzweig, 2012). Several works have shown that PC polarization is aided by higher affinity, both in the early plasmablast wave and within GCs, whereas lower-affinity B cells are preferentially differentiated toward memory B

cells (Phan *et al*, 2006). The last step of the GC process is the GC dissolution, which usually occurs 21 days upon infection or later. GCs start to disappear with a decrease in B cell numbers inside the follicles. The timing of GC dissolution is very variable, differing from several infections (Victora, 2014). Little is known about the factors that initiate GC dissolution, but a recent paper published by the group of Victora showed how the resolution of GCs is linked to the upregulation by T_{FH} of the master transcriptional regulator FoxP3, which acts as an essential determinant of GC lifespan (Jacobsen *et al*, 2021).

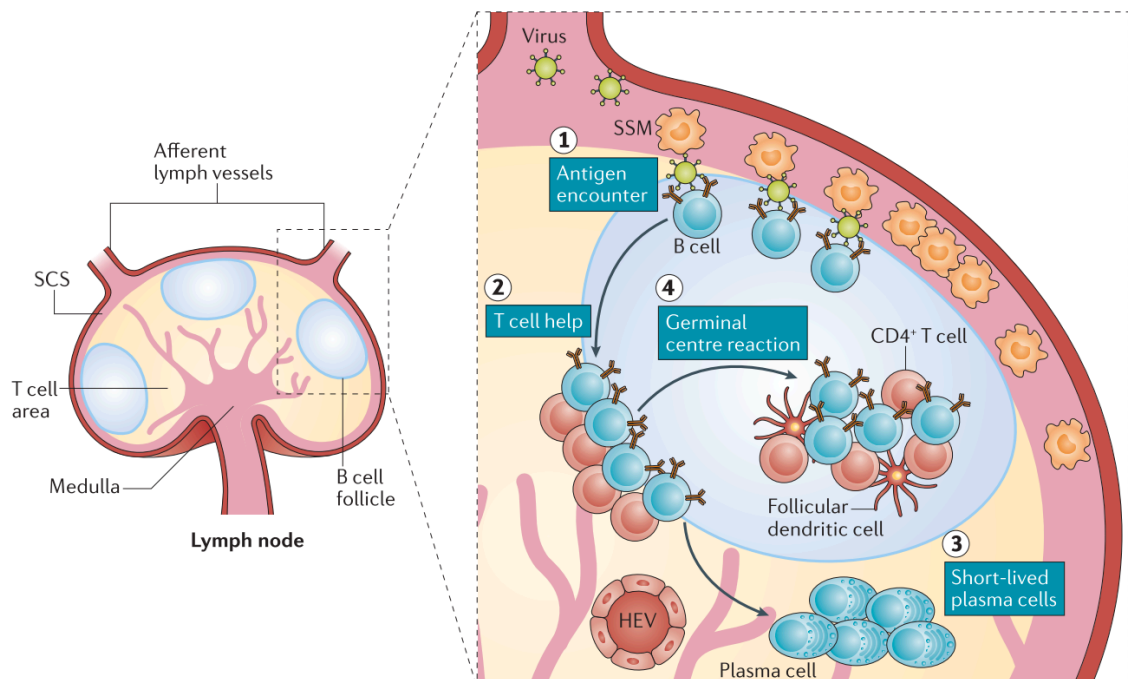


Figure 7. Spatiotemporal dynamics of B cell activation.

*Macrophages translocate viral particles captured from the afferent lymph across the subcapsular sinus floor and present them to B cells inside the follicle (step 1). After antigen encounter, naive B cells undergo early activation and proliferation and migrate to the T-B border to search for T cell help (step 2). Interaction with cognate $CD4^+T$ drives B cells either to develop into short-lived plasma (step 3) or to return to the follicle to give rise to germinal center reaction (step 4). (Figure adapted from Kuka *et al*, Nature Reviews Immunology, 2017_ License Number: 5247081254689)*

5.5 Antigen presentation by dendritic cells shapes $CD4^+$ T helper responses

Discovered by Steinman and Cohn in 1973, DCs represent the key nexus between the innate and the adaptive arm of an immune response, being the most efficient APCs in priming naive T cells (Steinman & Cohn, 1973). Antigen presentation by DCs activates

both CD4⁺ and CD8⁺ T cells, but in the next paragraph I will focus specifically on CD4⁺ T cell responses since they are the main object of my thesis project.

DCs start T cell activation by processing and presenting pathogen-derived peptides on MHC molecules (signal 1) and by delivering costimulatory signals (signal 2) mediated by the interactions between CD80/CD86 and CD28 receptor on T cells. The combination of these two signals drives the activation, the clonal expansion and provides pro-survival signals to the antigen-specific T cells. DCs represent also the source of the signal 3 that consist in the release of cytokines that guide the complete activation of T cells and their commitment toward different effector programs (Cabeza-Cabrero *et al*, 2021). Several works have brought to the classification of DCs in several subtypes, based on their origin, localization, differentiation requirements and their functionality. The most recent classification of DCs gained thanks to high-throughput techniques divides them into subclasses based on their ontogeny that is often correlated to their function. In this way, DCs are categorized into conventional (also known as classical) DCs (cDCs), pDCs and monocyte-derived DCs (MoDCs) (Eisenbarth, 2019) (**Figure 8**).

In this paragraph I will give an overview of the different populations of cDCs and their unique capacity to integrate signals from pathogens and bystander cells to guide the differentiation of naive CD4⁺ T cells into different effectors.

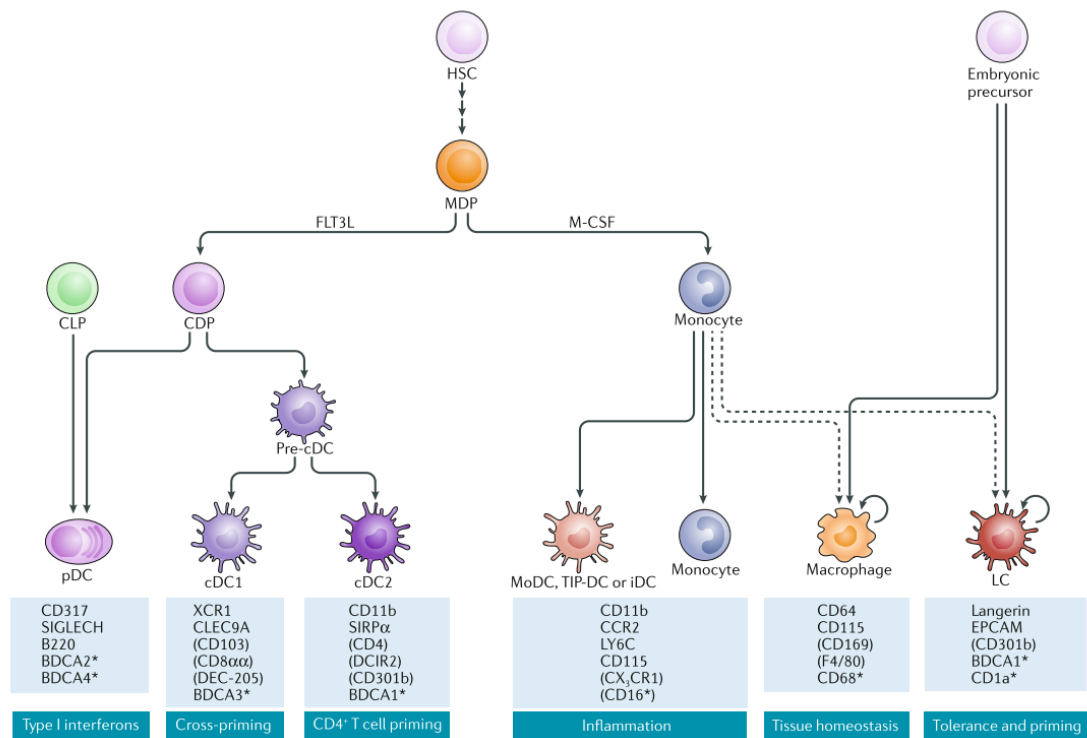


Figure 8. Schematic model for dendritic cell type and their specific markers.

Monocyte- macrophage DC progenitors (MDPs) differentiate into monocytes and common dendritic cell progenitors (CDPs). CDPs in turn give rise to both pDCs and pre-cDCs. that require the transcription factor FMS-like tyrosine kinase 3 ligand (FLT3L) for development. All other MDP- derived cells develop into monocyte-derived cell that can share phenotypic markers with cDCs, especially under inflammatory conditions and they are called non-conventional DCs. (Figure adapted from Eisenbarth et al, Nature Reviews Immunology, 2019_ License Number: 5247090288897)

cDCs rise from a common DC precursor (CDP) in the bone marrow (BM). They need the transcription factor FMS-like tyrosine kinase 3 ligand (FLT3L) for their development (Onai et al, 2007) and they express the transcription factor Zinc finger and BTB domain containing (ZBTB46). This transcription factor is selectively expressed by cDCs and it is widely used to discriminate cDCs from monocytes and pDCs (Meredith et al, 2012). cDCs are distinguished in cDC1 and cDC2, based on the differential expression of surface molecules and functions. cDC1 and cDC2 are further categorized into SLOs-resident cells and migratory cells. Resident cDCs continually gain access to the LNs from the blood and receive antigen from the lymph or from bystander cells to present it to CD4+ and CD8+ T cells. On the contrary, migratory cDCs localize in parenchymal tissues and must migrate to LNs to get in touch with naive T cells. In mice resident cDC1s require the

transcription factors Batf3, IRF8, and Inhibitor of DNA Binding 2 (ID2) for their development and express different markers, such as CD8a, X-C Motif Chemokine Receptor 1 (XCR1) and CD24, whereas migratory cDC1 are distinguished from the resident because they lose the expression of CD8a, express the peripheral marker CD103 and higher levels of MHC class II. From the functional point of view, cDC1s are the primary population responsible for the cross-presentation of extracellular antigens on MHC class I to CD8⁺ T cells. On the other side, CD8⁺ T cells are also able to attract cDC1 through the secretion of X-C Motif Chemokine Ligand 1 (XCL1), the chemoattractant ligand of the receptor XCR1. Resident cDC2s represent the most heterogeneous and numerous DC subset in SLOs. They express CD4, CD11b, and SIRP α (Signal Regulatory Protein α) and they are specialized in priming CD4⁺ T cells by presenting antigenic fragments associated with MHC class II (Cabeza-Cabrerizo et al, 2021). Several studies tried to identify markers to discriminate resident from migratory cDC2 showing that, at steady-state conditions, migratory cDC2 express higher levels of MHC class II, CD11c, and migratory markers such as CCR7 (Min et al, 2018).

The advent of high-resolution imaging techniques such as histocytometry brought to the definition of different cDC niches in LNs that are finely orchestrated in the course of immunization or infection (Eisenbarth, 2019). At steady state, cDC1s prevalently reside in the T cell zone, whereas resident cDC2s in the outer cortex and migratory cDC2s in the interfollicular area, nearby the T-B border (Kamath *et al*, 2000); (Braun *et al*, 2011). cDC1 and cDC2 positioning reflects the geography of CD8⁺ and CD4⁺ T cells that are guided by distinct chemokine gradients. Thanks to their localization, resident cDC2 capture antigen faster and they are more efficient in priming CD4⁺ T cells with respect to cDC1 (Gerner *et al*, 2015b). The cytokine milieu in SLOs plays a critical role in the developmental fate of CD4⁺ T cells. DCs can express or secrete an array of different factors shaped by the several pathogens that they could encounter, molding their transcriptional and cytokine profile to optimize the immune response

Different CD4⁺ T helper cells subsets fine-tune the antiviral adaptive immune responses (**Figure 9**) (Swain *et al*, 2012). In particular, viral infections usually stimulate the generation of both T helper 1 (T_H1) and T_{FH} (Hale *et al*, 2013).

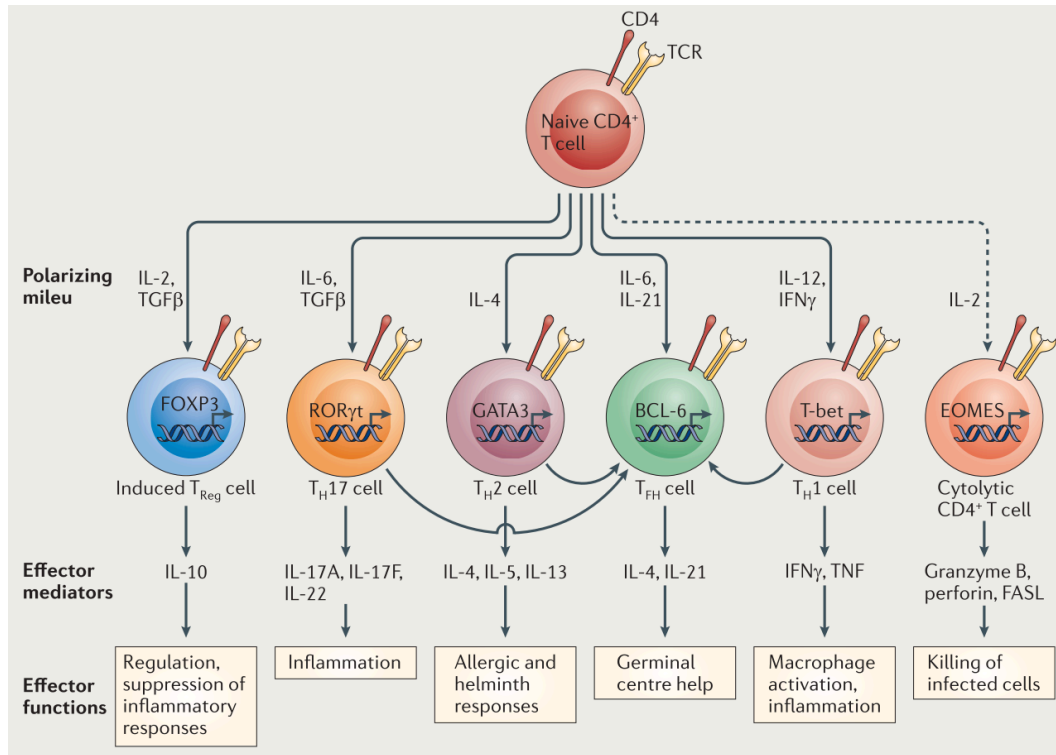


Figure 9. CD4⁺ T helper cell subsets

Depending on the nature of antigen stimulation signal received from APCs, naive CD4⁺ T cells differentiate into distinct effector T-helper cell subsets, which are characterized by expression of lineage-specific transcriptional regulators, cell surface markers, and secretion of key cytokines

In the next paragraphs, I will give an overview of the development and the function of TH1 and TH2 during viral infection and how this dichotomy is tipped by multi-layered transcriptional networks and inflammatory milieu.

5.5.1 TH2

The development of effective nAbs ensures clearance of the infection since the early phase and it is a key goal for vaccination. For many years, the mechanism whereby T cells contribute to the development of an efficient humoral response by supporting B cell activation was unknown. CD4⁺ T cells were among the best candidates that could be actively involved in GC B cell responses, given their pleiotropic roles in shaping the adaptive immune response. In 1986 the identification of T helper 1 (TH1) and TH2 cells by Mosmann and Coffman, raised the hypothesis that one or both of these T helper subsets could be the interacting partners of B cells that promote their proliferation and

immunoglobulin class switching. (Mosmann *et al*, 1986). Although there are several studies that have demonstrated the ability of both T_{H1} and T_{H2} cells to support B cell responses (Noelle *et al*, 1989); (DeKruyff *et al*, 1989);, the latter were widely believed to be the principal players, as the canonical T_{H2} cytokine interleukin-4 (IL-4) is implicated in various stages of B cell proliferation and promotes IgG1/IgE class switching differentiation (Croft & Swain, 1991); (Purkerson & Isakson, 1992).

Even though T_{H1} cells are usually associated with cell-mediated immunity, and generally regarded as less important for B cell responses, IgG2a isotype switching is promoted by IFN- γ (Huang *et al*, 1993); the prototypical T_{H1} cytokine, which inhibits also switching to IL-4-dependent isotypes, such as IgE, (Snapper & Paul, 1987). These results suggest that T_{H2} cells are not unique in their ability to induce T-dependent B cell responses, but the mechanisms by which T_{H1} and T_{H2} help B cell responses remain to be elucidated, particularly *in vivo*. However, T_{H2} cells are not essential for B cell proliferation and differentiation, as IL-4 or IL-5 knockout (KO) mice, which have deficient T_{H2} responses, have readily detectable Ab production and germinal center formation (Del Prete *et al*, 1988); (Pene *et al*, 1988).

A CD4⁺ T helper cell subset that expresses high levels of CXCR5 was discovered only in 2009. Later, this new T helper cell subset was categorized as a distinct subset of T helper cells, specialized in B cell help. These CD4⁺ T cells are now commonly named T follicular helper (T_{FH}) cells (Breitfeld *et al*, 2000); (Kim *et al*, 2001); (Schaerli *et al*, 2000). T_{FH} cells directly interact with B cells in the B cell follicles, becoming essential mediators of the humoral immune response (Garside *et al*, 1998);.

T_{FH} cell differentiation is a multistage, multifactorial process (Crotty, 2011) (**Figure 10**), and can largely be modeled as an early cell fate decision between becoming a T_{FH} cell and a non-T_{FH} effector cell. The canonical T_{FH} cell commitment starts when naive CD4⁺ T cells in the T cell area of SLOs encounter activated antigen-presenting DCs. During this process, T cells receive a variety of different stimuli that include the engagement of the T cell receptor (TCR), costimulatory molecules from DCs and specific cytokines derived from the microenvironment (Hilligan & Ronchese, 2020). Upon priming by DCs, CD4⁺ T cells sense T_{FH}-polarizing cues that lead to the initial upregulation of the T_{FH} master transcription factor Bcl-6 (B-Cell Lymphoma 6) (Nurieva *et al*, 2009). This enables the early upregulation of the chemokine receptor CXCR5 and the downregulation

of CCR7, guiding the migration of these pre-T_{FH} to the T-B border (Hardtke *et al*, 2005). This step is also aided by the fine-tuned regulation of a set of different migration receptors and integrins such as the migration receptor P-selectin glycoprotein ligand-1 (PSGL1), the chemoattractant receptor EBI2, Sphingosine- 1-phosphate (S1P) receptors, Signaling lymphocytic activation molecule (SLAM) family receptors, and integrins (Crotty, 2019). DC priming is essential for the first step of pre-T_{FH} induction but is not sufficient for the generation of the full polarized GC-T_{FH}. To this end, T_{FH} require signals from cognate B cells, which exert a key role in the maintenance and full polarization of pre-T_{FH} to GC-T_{FH} (Baumjohann *et al*, 2013); (Crotty, 2014).

The T-B border represents the initial meeting point for cognate T-B interactions since antigen-activated B cells migrate towards this area thanks to the upregulation of CCR7 that enables their journey towards CCL19 and CCL21 cues produced mainly by stromal cells in the T cell zone (Hardtke *et al*, 2005). Antigen-specific T cells and B cells interact in the T-B border engaging in long-lasting contacts. The interaction between these two cognate players induces several signals that result in the initiation of GC reactions, and in the production of high affinity nAbs responses. On one side these signals comprise CD40-CD40 ligand interactions on activated B cells and T_{FH}, respectively that drive a massive B cell proliferation (Takahashi *et al*, 1998). On the other side, the interaction between ICOSL expressed by the B cell and ICOS expressed by the T_{FH} further increases CXCR5 expression and inhibits CCR7, PSGL- 1, and CD62L (also known as L- selectin) expression (Akiba *et al*, 2005); (Weber *et al*, 2015). In this way T_{FH} become more sensitive to CXCL13 gradients and increase their migration into the follicle in a Phosphoinositide 3-kinase (PI3K)- dependent manner (Preite *et al*, 2019). During this process T_{FH} cells acquire a more differentiated phenotype through the upregulation of CXCR5, Bcl-6 and Programmed cell death protein 1 (PD-1), becoming fully differentiated GC-T_{FH} (Crotty, 2011). Indeed, the combination of these markers is used in mice to identify this peculiar population (Espéli & Linterman, 2015).

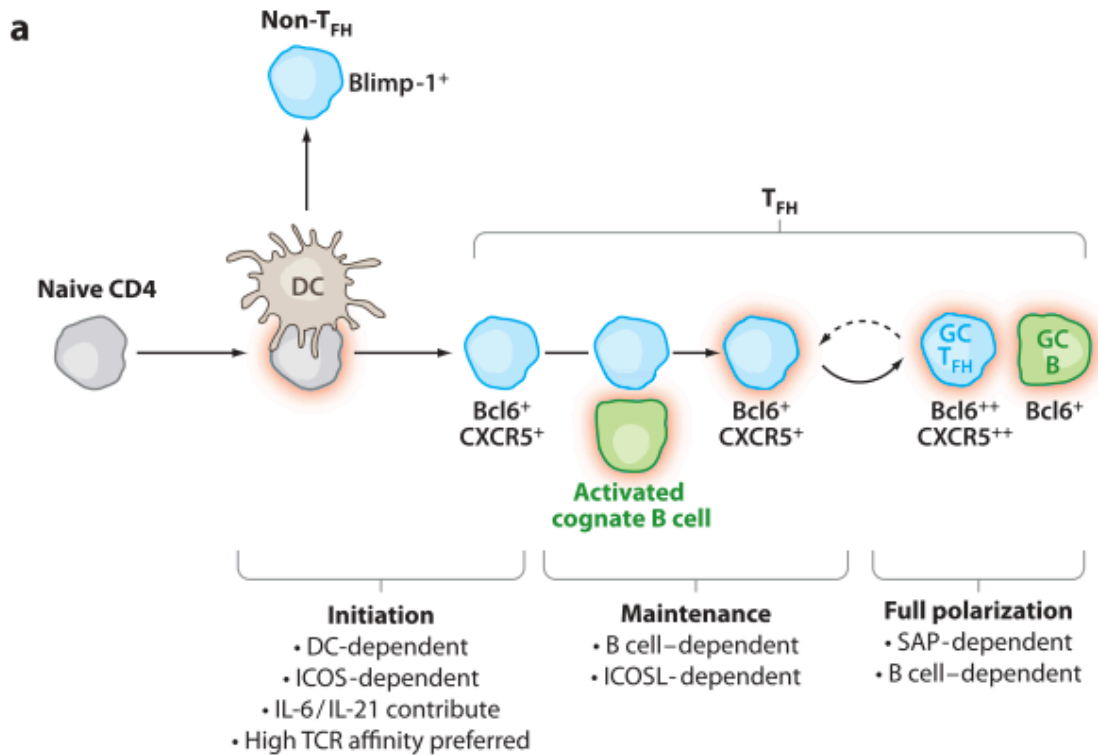


Figure 10. The multistep process of T_{FH} differentiation

Multiple stages of T_{FH} differentiation, involving initiation, maintenance, and full polarization.

(Figure adapted from Crotty, Annu. Rev. Immunol., 2011 _ License requested)

5.5.2 T_{H1}

T_{H1} cells play an important role in mediating cellular immunity against infections by intracellular pathogens, such as viruses. They do so mainly by enhancing mononuclear phagocyte and $CD8^+$ T cell activation thanks to their capacity to secrete a high amount of $IFN-\gamma$. Upon infection, during the priming phase, $CD4^+$ T cells undergo clonal expansion and differentiation and are exposed to different cytokines secreted by the surrounding environment, mainly infected cells and stromal cells. When $CD4^+$ T cell sense T_{H1} polarizing cytokines, they upregulate the expression of T-bet, the T_{H1} master transcription factor that represents one of the major drivers of $IFN-\gamma$ production (Zhu et al, 2012). Before going into the details of which factors drive T_{H1} polarization, it is worth pointing out that T_{H1} cells might be endowed with a degree of heterogeneity, so their phenotype is continually shaped by the different cytokine cues that vary among the infections (Cano-Gamez et al, 2020); (Kiner et al, 2021); (Tuzlak et al, 2021). This

property increases the complexity in finding common T_H1 polarizing modules that are shared by different infections. IL-12 represents one of the biggest examples of the context-dependent role of some well-known T_H1 polarizing cytokines, since it is essential in inducing T_H1 polarization in the context of bacterial infections, but not in the case of some viral infections (Krueger et al, 2021); (Oxenius et al, 1999); (Schijns et al, 1998). With regard to this, Krueger et al., recently revealed how the early generation of T_H1 cells is IL-12 independent in both influenza virus (IAV) infection and *Salmonella enterica* (Se) infection, however, T_H1 generated upon Se infection undergo a two-module differentiation. The second module is IL-12-dependent and gives rise to CX3CR1-expressing cytotoxic T_H1 endowed with high protective properties and increased IFN- γ production. On the contrary, the early T_H1 generated in the context of IAV infection do not develop into the cytotoxic subset and progress in competitive equilibrium with T_{FH} cells (Krueger et al, 2021). This two-step differentiation process is in line with a model proposed by Schulz et al. built on the basis of cell culture experiments. This model entails a first stage in which T-bet and IL-12 receptor expression are driven by TCR engagement independently from IL-12 signaling, resulting in a T_H1 cell population, which produces low level of IFN- γ . In a second step, IL-12 receptor signaling activates STAT4, driving further T-bet expression, IFN- γ production capacity and commitment toward the T_H1 lineage (Schulz et al, 2009). T-bet binds directly to the *Ifng* locus driving the expression of the canonical T_H1 cytokine IFN- γ (Thieu et al, 2008). This early source of IFN- γ acts as a first booster for the immune system inducing T-bet expression in naive CD4⁺ T cells, in a STAT1-dependent manner. In this way, this cytokine acts in an autocrine-positive fashion to drive further T_H1 differentiation. In addition to the role in supporting and maintaining T_H1 cell differentiation, IFN- γ induces the IFN-stimulated chemokines C-X-C motif Ligand 9 and 10 (CXCL9, CXCL10), leading to further recruitment of CXCR3⁺ T cells into regions of inflammation (Groom et al, 2012).

Several publications provide evidence of a key role of T_H1 in helping B cells. In fact, they promote isotype switching to IgG2c and IgG2a and their depletion leads to an increase IgG1 class switching in response to some viral infections such as LCMV and Zika (Liang *et al*, 2019); (Barnett *et al*, 2016). In addition to their role in isotype switching, T_H1 could act directly on B cells inducing T-bet expression through IFN- γ mediated pathway. A recent paper published by the group of Rudentsky shows that T-

bet⁺ CD4⁺ T cells that comprise both T_{H1} and T-bet⁺ T_{FH}, and T-bet⁺ B cell form a spatial circuit that acts as a unique module in inducing IgG2c class switching (Mendoza *et al*, 2021). In this context, T_{H1} alone are able to induce IgG2c class switching and T_{FH} instead support germinal center formation, elucidating a new important function of T_{H1} in supporting extrafollicular humoral responses. However, it remains unknown how these extrafollicular nAbs generated independently of T_{FH} are efficient in protecting the host from a viral infection in respect to the T_{FH}-dependent nAbs.

5.5.3 Transcriptional and environmental cues for T_{FH} and T_{H1} commitment

Since their discovery, the predominant model of T helper (T_H) cell definition has relied on a distinction based on the expression of lineage-defining master regulator transcription factors. However, recent data clearly suggest that many of the lineage-defining factors are expressed in multiple subsets of T_H cells (Zhou *et al*, 2009);(O' Shea and Paul, 2010). For example, the T_{H1} master transcription factor T-bet is expressed not only in T_{H1} but at variable levels also in T_{FH} cells. (Wang *et al*, 2019). A large body of literature defines T_{FH} cells as a highly heterogeneous population skewed by the inflammatory environment and able to shape B cell responses. A recent concept paper proposed a new nomenclature to define the different T_{FH} subsets based on the cytokines/chemokines profile, the transcriptional signature and the functional characteristics (Tuzlak *et al*, 2021). These different T_{FH} subsets could promote different immunoglobulin isotype switching, suggesting a key role in shaping humoral responses. The developmental trajectories of these cytokine-skewed T_{FH} cells are still under investigation with some study that propose a linear differentiation pathway from naïve CD4⁺ T and other that define them as a transitional state between T_{FH} cells and other T effector subsets (Sheikh & Groom, 2020). T_{FH1} for example, develop upon type I inflammatory responses and display some T_{H1} features, such as the expression of the T_{H1} master transcription factor T-bet and the secretion of IFN- γ (Olatunde *et al*, 2021); (Wang *et al*, 2019). They are induced concomitantly with T_{H1} and they share some transcriptional trajectories. Recent works shed light on IL-12 as an early polarizing cytokine for both T_{FH1} and T_{H1} thanks to its ability to induce T-bet and Bcl-6 (Nakayamada *et al*, 2011). The competitive equilibrium between these two master transcription factors determines the developmental fate toward

T_H1 or T_{FH}, with Bcl6 that is required for the maintenance of T_{FH} differentiation in parallel with T-bet silencing (Oestreich *et al*, 2012).

Interestingly, Nakayamada *et al.* showed that T_{FH} and T_H1 share a transitional precursor that expresses both Bcl-6 and T-bet; however, in the late phase of T_H1 differentiation T_{FH}-related genes are silenced leading to the ultimate commitment toward the T_H1 fate (Nakayamada *et al*, 2011). The precise timing of the fate bifurcation is still under investigation. While some studies suggest that CD4⁺ fate decisions are imprinted early upon infection, others indicate that this bifurcation occurs later, between days 2 and 4 post-infection (Sheikh & Groom, 2020). These discrepancies could be linked to different infection models but also to the high degree of plasticity retained by differentiating CD4⁺ T cells. This flexibility enables effector CD4⁺ T cells to adapt their response to different stimuli based on the cytokine milieu to which they are exposed.

The regulatory mechanisms that instruct the differentiation of T_{FH} cells and T_H1, are guided by the coordinated interplay between cell-extrinsic signals (i.e. cytokines or ligand-receptor interactions) and cell-intrinsic transcriptional networks (Sheikh & Groom, 2020) (**Figure 11 and 12**). T_{FH} and T_H1 share a common precursor stage (**Figure 11**), but the timing and the combination of factors that guide the final T_{FH}/T_H1 dichotomy are still under investigation and the field is complicated by the high heterogeneity and plasticity of these populations. In this section I will give an overview of the transcription factors and inflammatory cues that direct T_{FH}/T_H1 fates.

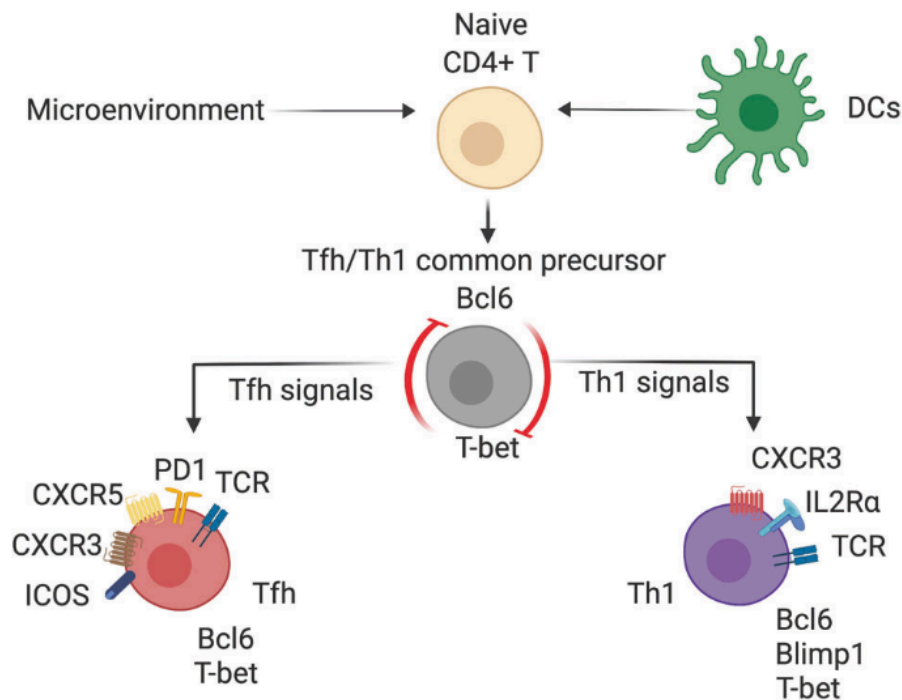


Figure 11. T_{FH} and T_{H1} bifurcation.

Antigen presentation by DCs and inflammatory cues coming from the microenvironment drive the initial development of naïve CD4⁺ T cells into a common precursor that expresses both T_{H1} and T_{FH} markers (T-bet⁺ Bcl-6⁺ CD4⁺ T cell). Later during the differentiation path, T_{FH} cues drive this precursor to differentiate toward T_{FH} cells that start the expression of the chemokine receptors CXCR5 and CXCR3 and of PD-1 and ICOS. Conversely, T_{H1} signals tips the T_{H1}/T_{FH} precursors toward T_{H1} development. These fully differentiated T_{H1} express canonical T_{H1} transcription factors Blimp-1, T-bet and Bcl-6; chemokine receptors CXCR3 and IL-2R (Figure adapted from Sheikh *et al.*, *Cellular and Molecular Immunology*, 2020_ Open Access Article)

5.5.4.1 Transcriptional mediators of T_{H1}/T_{FH} dichotomy

The common precursor of T_{FH}/T_{H1} is a hybrid population that expresses both the lineage defining factors T-bet and Bcl-6. These two transcription factors are expressed in a competitive equilibrium, but ultimately this equilibrium is disrupted and one of the two factors becomes the determinant of the final CD4⁺ T cell polarization (Nakayamada *et al.*, 2011); (Lönnberg *et al.*, 2017).

Bcl-6 is a *proto-oncogene zinc-finger transcriptional repressor* involved in the differentiation pathways and in the function of several immune cells. In particular, Bcl-6 expression is crucial in orchestrating humoral immunity, since it is involved in T_{FH} and GC B cells development (Ye *et al.*, 1997); (Kitano *et al.*, 2011). Indeed, GC B cells express

high levels of Bcl-6, which inhibits their differentiation into plasma and memory cells (Reljic *et al*, 2000). In addition, it also regulates the generation and maintenance of memory CD8⁺ T cells (Ichii *et al*, 2002). Its expression is upregulated by CD28 activation, STAT1 and STAT3-mediated pathways and by IL-21 and IL-4 secreted by T_{FH} (Arguni *et al*, 2006); (Choi *et al*, 2013); (Chevrier *et al*, 2017). Moreover, Bcl-6 promotes the expression of both IL-21R and CXCR5 in CD4⁺ T-cells facilitating their migration toward the follicle, further promoting T_{FH} differentiation in a positive feedback fashion (Hatzi *et al*, 2015). Bcl-6 expression counteracts Blimp-1 expression and vice versa in both GC B cells and T_{FH} cells. In fact, the overexpression of Blimp-1, in non-T_{FH} CD4⁺ T cells, inhibits CD4⁺ T cells to acquire the T_{FH} phenotype via the inhibition of the expression of canonical markers, including CXCR5, ICOS, and PD-1 (Johnston *et al*, 2009). One of the most critical roles of Bcl-6 as the T_{FH} master transcription factor, in addition to the establishment of T_{FH} commitment, is the concomitant inhibition of alternative pathways of T helper differentiation by the epigenetic silencing of promoters and enhancers linked to T_{H1}, T_{H2} and T_{H17} differentiation (Hatzi *et al*, 2015).

T-bet is a T_{H1}-specific T box transcription factor, involved in the induction of IFN- γ expression (Szabo *et al*, 2000). After its discovery, several papers were published describing the expression of this transcription factor on several immune cells and highlighting its key role in orchestrating antiviral immune responses (Lighvani *et al*, 2001); (Kallies & Good-Jacobson, 2017); (Sheikh *et al*, 2019). In fact, T-bet exerts its function on CD8⁺ T cells, where it induces the development of effector at the expense of memory precursors (Hamilton & Jameson, 2007), but also on GC B cells, where it directs their localization to the GC dark zone (Ly *et al*, 2019). It plays a key role also in innate lymphoid cell (ILC)s differentiation, inducing IFN- γ expression (Zhang *et al*, 2018). Besides these pleiotropic roles, T-bet is best recognized for its vital role in T_{H1} cell differentiation, since it promotes the expression of the canonical T_{H1} cytokine IFN- γ (Szabo *et al*, 2000). Going into the details of the mechanism of IFN- γ induction, T-bet induces this cytokine to some extent through remodeling the *Ifng* gene and among others by upregulating IL-12R β 2 expression, thus promoting both IFN- γ expression and selective T_{H1} cell expansion in response to IL-12 (Nakayamada *et al*, 2011); (Schulz *et al*, 2009). Like Bcl-6, T-bet supports the T_{H1} fate by preventing T helper cell precursors from adopting non-T_{H1} effector fates and negatively regulating the transcription of

lineage-defining transcription factors (Lazarevic *et al*, 2011). Indeed, T-bet is also involved in the regulation of the chemokines CCL3 and CCL4 and the chemokine receptor CXCR3, which are involved in the migration of T_{H1} in the T cell zone (Groom *et al*, 2012).

Bcl-6 and T-bet should not be seen as two separate identities involved in the differentiation of T_{FH} and T_{H1}, but as a fine-tuned complex molded by the environmental cues. The regulation of this Bcl-6/T-bet module is extremely multifaceted and involves the recruitment of the Bcl6-T-bet complex to the *Ifng* locus and to the SOCS1 and SOCS3 (suppressor of cytokine signaling) promoters. SOCS1 signaling is involved in the suppression of IFN- γ and STAT1 pathways, in this way the Bcl-6/T-bet complex curtails the IFN- γ mediated immunopathology (Oestreich *et al*, 2011). Another factor involved in this complex network of interaction is B-lymphocyte-induced maturation protein 1 (Blimp1), a transcription factor highly expressed by T_{H1} cells that inhibits Bcl-6 expression, tipping the balance between T_{FH} and T_{H1} towards T_{H1} (Johnston *et al*, 2009).

In addition to the T_{FH} master transcription factor Bcl-6, during the last years, several papers identified new transcription factors implied in the induction of T_{FH} transcriptional trajectories, including T-cell factor 1 (TCF-1), and a number of STAT factors.

TCF-1 belongs to the HMG family of transcription factors and it is encoded by the *Tcf7* gene. Recent works highlighted an essential role of this transcription factor in promoting and maintaining T_{FH} differentiation via several pathways (Wu *et al*, 2015). First of all, upon LCMV infection it directly induces Bcl-6 expression and suppresses *Il2ra* and *Prdm1* transcription in a negative feedback loop (Shao *et al*, 2019); (Xu *et al*, 2015). Second, TCF-1 enhances the expression of IL-6R α and gp130, increasing ICOS expression, further promoting T_{FH} development (Choi *et al*, 2013). TCF-1 is also involved in the generation of GC reactions since its ablation impairs GC B cell development (Xu *et al*, 2015).

5.5.4.2 Cytokine mediators of T_{H1}/T_{FH} dichotomy

Several works raised the concept that each viral infection stimulates unique cytokines modules that regulate the transcriptional networks at the basis of T_{H1}/T_{FH} bifurcation. Among the different cytokines, IL-6, IL-21, IL-2, IL-12 and IFN- γ have been reported to be involved in either T_{FH} or T_{H1} cell commitment (**Figure 12**).

IL-6, together with IL-21, is the best known T_{FH} polarizing cytokine and it is produced by several cellular sources including DCs, T and B cells, macrophages, fibroblasts, endothelial cells, glial cells and keratinocytes (Sheikh & Groom, 2020). IL-6 signaling involves the activation of STAT3 that in turn elicits Bcl-6 expression and drives T_{FH} differentiation. However, during LCMV infection IL-6 is able to induce T_{FH} differentiation also in absence of STAT3 signaling (Hotson *et al*, 2009), but the alternative pathways need further investigation. T_{FH} differentiation is strongly impaired only when STAT1 and STAT3 are missing, suggesting that the cooperation of these two pathways is essential in inducing T_{FH} commitment (Choi *et al*, 2013). In line with this role in supporting T_{FH} development, IL-6 is also involved in the generation of nAbs in the context of GC reactions, but it is still unclear whether it is directly sensed by GC-B cells or it is an indirect effect of the increased T_{FH} differentiation (Harker *et al*, 2011). Another pathway through which IL-6 induces T_{FH} differentiation is through the induction of **IL-21**, which represents the most abundant cytokine produced by T_{FH}. Its main function is to promote GC reactions and IgG1 class switch recombination (Ozaki *et al*, 2002). In the context of T_{FH} differentiation IL-21 alone is dispensable in inducing T_{FH} commitment, but it acts in concert with IL-6 promoting STAT3-mediated signaling (Eto *et al*, 2011). Among the cytokines that are known to suppress T_{FH} development **IL-2** is considered one of the best antagonists. Its mechanism of action relies on the induction of the expression of Blimp1 and the inhibition of STAT3 binding to the Bcl-6 locus, thus promoting at the same time T_{H1} development and T_{FH} suppression (Johnston *et al*, 2012); (Ballesteros-tato *et al*, 2013). In fact, during T_{FH} development, CD25 (the α chain of the high-affinity IL-2 receptor) is negatively regulated in order to protect the developing T_{FH} from the suppressive signals mediated by the IL-2 pathway. In line with this, T_{H1} precursors express a higher level of CD25 and they are defined as “IL-2 consumers”. In the context of LCMV infection, in absence of IL-2 consumers, as in T-bet deficient mice, early-T_{FH} precursors are more exposed to the inhibitory signals of the IL-2, thus resulting in the impairment of both T_{H1} and T_{FH} commitment (Ditoro *et al*, 2018). On the contrary, in a different setting such as Influenza infection, the absence of T_{H1} does not result in the decrease of T_{FH} differentiation because the concomitant induction of IL-6 drives T_{FH} development (Sheikh *et al*, 2019). To summarize these studies, like many other cytokines,

the role of IL-2 is context-dependent and is tightly regulated in a spatiotemporal dependent manner.

Among the factors that drive T_{H1} commitment, for many decades **IL-12** has been categorized as the best T_{H1} -polarizing cytokine, due to its ability to induce STAT4-dependent pathways that result in the induction of T-bet (Schulz *et al*, 2009). Nevertheless, as explained in the previous paragraph, T-bet could be expressed in a transient or permanent way also by T_{FH} , which share a transcriptional precursor with T_{H1} . Indeed, IL-12 not only induces the expression of T-bet and IFN- γ , but also of IL-21 and Bcl-6 on $CD4^+$ T cells (Nakayamada *et al*, 2011). However, the role of this cytokine is context and time-dependent. A recent paper published by the group of Jenkins showed how IL-12 is dispensable for the early induction of T_{H1} polarization upon both Salmonella and Influenza infection. Conversely, at the late stage of Salmonella infection, T_{H1} become more sensitive to IL-12, which increases their cytotoxic potential and their capacity to produce IFN- γ . This T_{H1} phenotype-switch does not happen in the context of Influenza infection and other works highlight the concept that upon viral infection IL-12 is dispensable in inducing T_{H1} , but there must be other unknown polarizing factors responsible for T_{H1} differentiation (Nakayamada *et al*, 2011).

Another cytokine that can act in concert with IL-12 to induce T_{H1} polarization is **IFN- γ** (Schulz *et al*, 2009). IFN- γ has always been considered the canonical effector T_{H1} cytokine, a key player in orchestrating innate and adaptive immunity against intracellular pathogens. IFN- γ producers include T_{H1} , $CD8^+$, NK and NKT cells, macrophages, DCs and B cells, even if T cells represent the major source during adaptive immunity. IFN- γ exerts its function interacting with its heterodimeric IFN γ R composed of a ligand-binding α subunit (IFNGR1) and a signal-transducing β subunit (IFNGR2). IFN- γ signaling pathway starts with the phosphorylation of JAK1-JAK2 activation, which in turn activates STAT1. STAT1 homodimers translocate to the nucleus, where they promote the transcription of IFN- γ associated genes and of T-bet, which delineates the onset of T cell polarization for commitment to T_{H1} lineage (Schroder *et al*, 2004). IFN- γ acts also in a positive feedback loop to further enhance T_{H1} differentiation and IFN- γ production (Wakil *et al*, 1998).

While its role in maintaining the T_{H1} phenotype and in increasing the pool of memory T cells is widely accepted (Whitmire *et al*, 2007), its role in driving T_{H1} polarization needs further investigation.

In vitro studies showed how IFN- γ induces an early wave of T-bet expression via STAT1 signaling followed by further T_{H1} polarization mediated by IL-12 (Schulz *et al*, 2009), however, *in vivo* the transcriptional and cytokine networks are more complex and the molecular mechanism is still unknown.

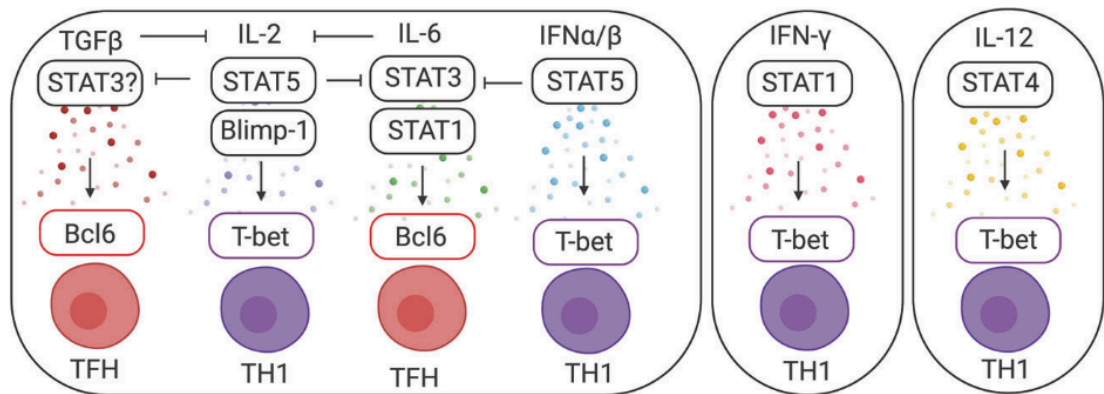


Figure 12. Environmental cues that instruct $CD4^+$ T cell differentiation.

*Selective cytokines and transcription factors that tip the balance between T_{H1} and T_{FH} differentiation (Figure adapted from Sheikh *et al.*, Cellular and Molecular Immunology, 2020_ Open Access Article)*

5.6 Type I IFNs: The Jekyll and Hyde of the immune response to viral infections

When analyzing determinants of adaptive immune responses to viral infections, it is important to keep into account a family of innate molecules, which have been found to play a crucial role in shaping both innate and adaptive immune responses: type I IFNs. Type I IFNs are cytokines secreted in response to a viral infection that restrict viral replication within the host cell through the induction of several IFN-stimulated genes (ISGs). The type I IFN family is a multi-gene cytokine family composed of IFN- β and several IFN- α isoforms that signal through the heterodimeric receptor constituted of Interferon Alpha and Beta Receptor Subunit (IFNAR1 and IFNAR2) subunits. Type I IFN-mediated pathway leads to the activation of several intracellular programs that

impact both the innate and the adaptive immune responses. Indeed, type I IFNs exert a context-dependent role upon viral infections and their functions might translate into beneficial or detrimental outcomes for the host (**Figure 13**). These are strictly dependent also on the timing and the magnitude of the production of this cytokine, which could trigger different intracellular pathways and ISGs, leading to pleiotropic effects in the antiviral immune response (McNab *et al*, 2015).

IFN α/β induction is driven by microbial products sensed by receptors placed on the cell surface, in the cytosol or in the endosome, named pattern recognition receptors (PRRs). The signaling transduced through these receptors converges on the activation of a few key factors, such as the IFN-regulatory factor 3 (IRF3) that induce a first wave of transcription of *Ifnb* and *Ifna4* genes that then trigger IRF7 in an autocrine positive loop that enhances type I IFN transcription. Type I IFNs binding to its receptor then leads to the activation of numerous intracellular pathways. The canonical pathways involve the activation of the kinases JAK1 and TYK2 that in turn phosphorylate signal transducer and activator of transcription 1 (STAT1) and STAT2 molecules in the cytosol, leading to their dimerization and translocation in the nucleus where they interact with IRF9, forming the ISG factor 3 (ISGF3) complex. ISGF3 then binds to IFN-stimulated response elements present in the ISG promoters, promoting ISG transcription. This is just one of the intracellular pathways induced by type I IFN that in fact can signal also through STAT1 homodimers that are shared by the IFN- γ -mediated signaling or by other STATs (STAT3, 4 and 5), leading to the transcription of different ISGs (Platanias, 2005). This multi-layered signaling represent one of the main reasons behind the pleiotropic effects of IFN α/β -mediated signaling, as it induces the transcription of other genes behind the ISGs, such as cytokines and chemokines, pro-apoptotic and anti-apoptotic molecules, and molecules related to metabolic processes.

Besides inducing an antiviral state, type I IFNs are key players of the innate and adaptive immune response, acting on different cell types. First of all, they promote antigen presentation and DC maturation through the upregulation of MHC-II expression and costimulatory molecules such as CD80 and CD86. These type I IFN-mediated effects, coupled with the induction of CXC-chemokine ligand 9 (CXCL9) and CXCL10 that act as chemoattractants for T cells, lead to a more efficient T cell stimulation. Type I IFNs induce also the production of the chemokine CCL2 by stromal cells, which in turn drives

the recruitment of CCR2⁺ inflammatory monocytes through the CCL2-CCR2 axis (Dasoveanu *et al*, 2020). Further, NK cells functionality and survival are directly or indirectly influenced by this cytokine. During murine cytomegalovirus (MCMV) infection, type I IFNs induce IL-15, which is essential in supporting the proliferation and the activation of NK cells (Baranek *et al*, 2012). In addition, it enhances IFN- γ production by NK cells through a STAT1-mediated signaling (Marshall *et al*, 2006). As mentioned previously, type I IFN acts not just on the innate arm of the immune system, but also on the adaptive arm. It can directly act on CD4⁺ and CD8⁺ T cells, promoting their survival, proliferation, function, and also their memory potential. The nature of CD4⁺ and CD8⁺ T cell responses is strictly shaped by the spatiotemporal regulation of this cytokine and on the activation of different STAT-mediated signaling upon IFNAR engagement. In the context of LCMV infection, type I IFN dampens T cell-mediated response inhibiting their egression from SLOs, but also promoting an anti-proliferative effect on CD8⁺ T cells. This, in turn, influence the initial proliferation of T cells, determining also the size of the downstream memory T cell pool (Marshall *et al*, 2011).

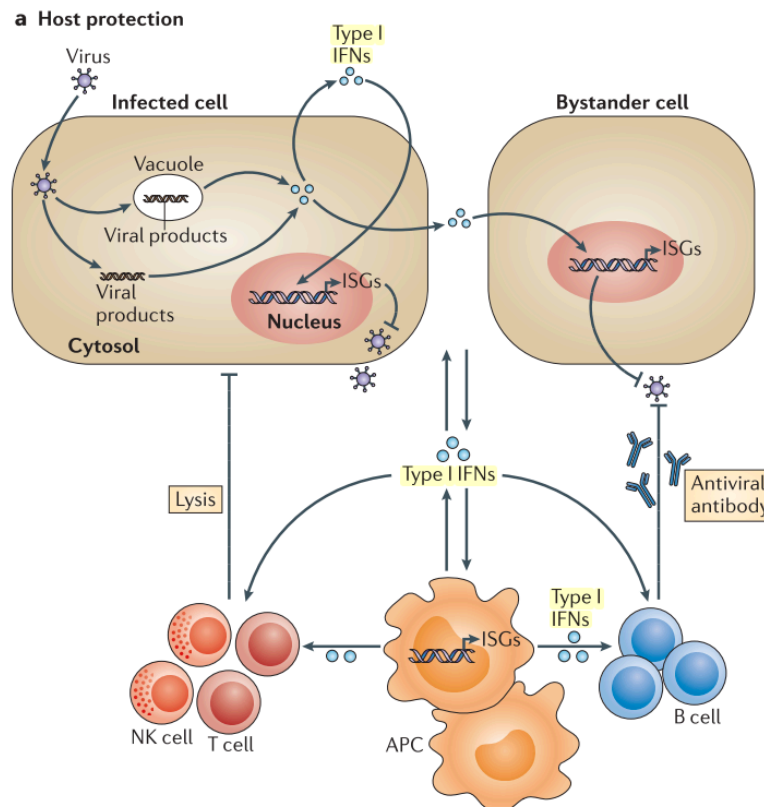


Figure 13. The pleiotropic roles of type I IFNs upon viral infection

Infected cells secrete type I interferons (IFNs) in response to viral infection and/or contact with viral products. Type I IFNs produced by infected cells acts in an autocrine or paracrine fashion on the bystander cells, inducing the transcription of IFN-stimulated genes (ISGs), which inhibit the viral replication cycle. Type I IFNs are also produced and sensed by APCs, enhancing their antigen-presenting capacity. They can also improve the antiviral task of cells of the adaptive arm, such as B cells, T cells, and natural killer (NK) cells. (Figure adapted from McNab et al, Nature Reviews Immunology, 2015 _ License Number: 5247090091242)

Type I IFNs participate also in the polarization of CD4⁺ T cells toward T_H1 or T_{FH}, but its role is context-dependent and it changes in different types of immunization or viral infections. Different viral infections lead to a wide spectrum of type I IFN-induced responses since it could be sensed by different cell types and the level of complexity increases since it involves its spatiotemporal regulation in the different anatomical niches (Kuka *et al*, 2019).

IFNs affects also B cell responses at the level of two important steps: development and proliferation and antibodies secretion, including class switching (Stark *et al.*, 1998). Ig class switching is crucial in molding the immune response to different pathogens as the different isotypes drive diverse effector functions.

Indeed, IFN α/β are crucial in supporting early B cell responses during VSV and Influenza infection. In addition, *in vitro* type I IFNs support mature B cells survival and resistance to Fas-mediated apoptosis (Braun *et al*, 2002). Ultimately, pDCs secrete type I IFNs, which promote the generation of plasma cells and IL-6, which enhances their capacity to release antibodies (Jego *et al*, 2003). However, type I IFNs could also play an immunosuppressive role during viral infections, such as in the context of LCMV infection. This concept will be discussed in the next paragraph.

5.6.1 Type I IFNs hinder antiviral B cell responses upon LCMV infection

Type I IFN plays a dual role in the context of LCMV infection, acting on one side as an antiviral molecule and on the other side as an immunomodulatory cytokine. In this paragraph I will give an overview of the recent discoveries about the detrimental roles of type I IFNs in humoral B cell responses upon LCMV infection. Part of this work was published by our group and took advantage of multiphoton intravital imaging (MP-IVM) to define the spatiotemporal dynamics underlying virus-specific B cells responses upon

subcutaneous LCMV infection compared to VSV infection in the popliteal draining LNs (Sammicheli *et al*, 2016). This study unveiled profound differences in the B cell migration and interaction partners in the two infections. As was shown in previous studies with ultraviolet-inactivated VSV or non-viral Ags (Junt *et al*, 2007); (Carrasco & Batista, 2007), early upon subcutaneous infection (2h), VSV-specific B cells localize in the SCS area where they engage prolonged interaction with infected SSM, they acquire the antigens and migrate to the T-B border (8h). By 72h they undergo activation and clonal expansion and migrate back to the B cell follicles, in line with the early induction of nAbs four days upon infection. On the contrary, LCMV-specific B cells migrate to the T-B interface later upon the infection (24h), they upregulate markers of early activation but at day three they remain stacked in that area without moving back in the B cell follicles. This confinement of LCMV-specific B cells was due to their interaction with a population of CD11b⁺Ly6C^{hi} inflammatory monocytes recruited in the dLNs in a type I IFN and CCR2-dependent fashion. These monocytes are responsible for the B cell apoptosis thanks to their ability to produce nitric oxide (NO) and lead to an impairment of nAbs responses independently of CD4⁺ T cells. Indeed, the ablation of inflammatory monocytes through anti-Gr-1 Abs or the inhibition of their lymph node recruitment (via IFN-I or CCR2 blockade) leads to enhanced survival of LCMV-specific B cells and recovery of virus-nAbs responses (Sammicheli *et al*, 2016). Monocyte-derived NO represent just one of the ways through which inflammatory monocytes could hinder humoral responses. In the context of influenza infection, it was shown that type I IFNs could induce the expression of TNF-related apoptosis-inducing ligand (TRAIL) on inflammatory monocytes and of its receptor DR5 on epithelial cells. In this way, inflammatory monocytes induce the apoptosis of epithelial cells causing an excessive immunopathology (Herold *et al*, 2008). Staniek *et al*. reported the expression of Trail receptors (TRAIL-R) on activated primary human B Lymphocytes (Staniek *et al*, 2019), supporting the hypothesis that the Trail-DR5 axis could be involved in the apoptosis of B cells, but its role upon viral infections remains elusive.

In another study, IFN-I was shown to induce the secretion of different cytokines, such as TNF- and IL-10 by DCs, T cell, and Gr1⁺ cells that, in turn, guide the fate of LCMV-specific B cells into short-lived plasma cells and ultimately drive their deletion (Fallet *et al*, 2016). Finally, LCMV can actively infect antigen-specific B cells, a mechanism that

results in the presentation of viral antigens to cytotoxic T cells (Planz *et al*, 1996) (**Figure 14**). In this case, since type I IFN is required to expand and differentiate T effector cells, blockade of type I IFN receptor signaling protected antiviral B cells by promoting effector CD8⁺ T cell dysfunction (Moseman *et al*, 2016).

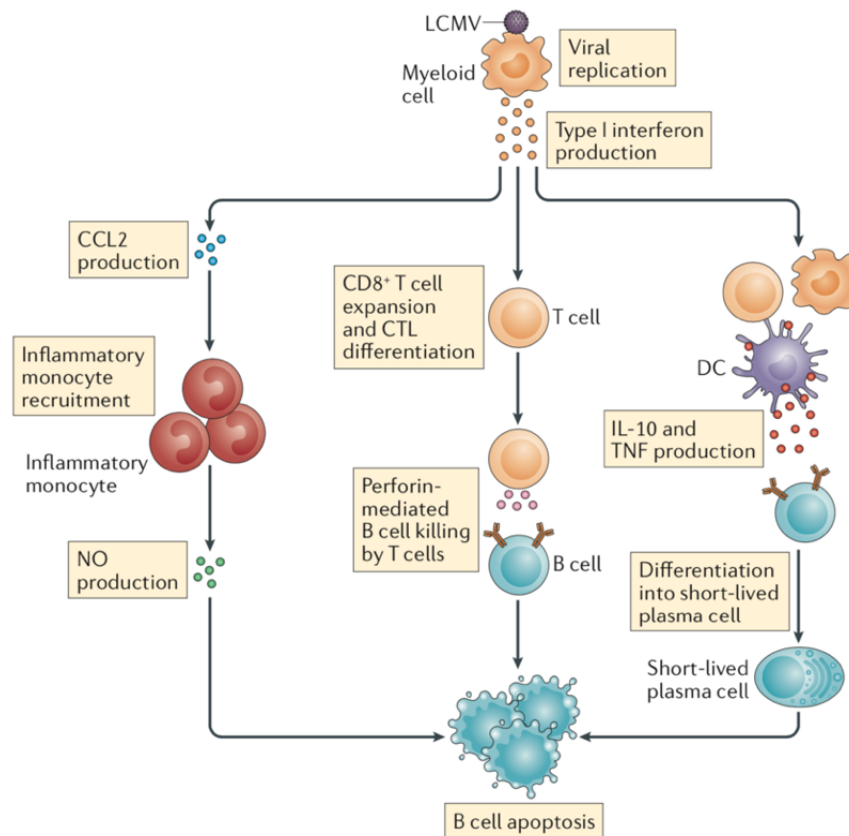


Figure 14. Type I interferon-mediated suppression of antibody responses.

*Type I interferon induces the secretion of CC-chemokine ligand 2 (CCL2) that drives the migration of inflammatory monocytes to the virus-draining lymph node; inflammatory monocytes engage interaction with LCMV-specific B cells, inducing their apoptosis in nitric oxide (NO)-dependent manner. Type I interferon promotes the proliferation and the development of CD8⁺ T cells, which kill LCMV-specific B cells in a perforin-dependent fashion. In conclusion, type I interferon induces IL-10 and TNF production by different cell types, which elicits differentiation of activated LCMV-specific B cells into short-lived plasma cells, eventually resulting in B cell apoptosis. (Figure adapted from Kuka *et al*, Nature Reviews Immunology, 2018_ License Number: 5247081254689)*

RATIONALE

6. RATIONALE

CD4⁺ T cells represent critical mediators of the adaptive immune response, supporting both the cellular and the humoral branch of immunity to pathogens. Although these two faces of the immune response coexist in a state of equilibrium, sometimes one of the two takes over and becomes the major player in the antiviral activity. The clearance of fast-replicating and cytopathic viruses such as VSV is usually controlled by strong nAbs responses, whereas slow replicating and poorly cytopathic viruses such as LCMV induce a massive cellular response mediated by CD8⁺ T cells. One important question is whether the rupture of this equilibrium might be observed also at the level of CD4⁺ T differentiation.

In this paragraph I will show the preliminary data that my colleagues obtained before my arrival in the lab and that constituted the premises of my PhD project. These preliminary data, together with new results that I contributed to generate during my first year have been published in the paper: “De Giovanni M, Cutillo V, Giladi A, et al. Spatiotemporal regulation of type I interferon expression determines the antiviral polarization of CD4⁺ T cells. *Nat Immunol.* 2020;21(3):321-330.

My colleagues investigated the differentiation of antiviral CD4⁺ T cells upon VSV and LCMV infection to test whether they could be involved in the compartmentalization of the two immune responses against the two viruses. To this end, naïve VSV-specific (Tg7) (Maloy *et al*, 1999) or LCMV-specific (SMARTA) (Oxenius *et al*, 1998) transgenic CD4⁺ T cells were adoptively transferred into C57BL/6 mice 24 h before subcutaneous (s.c.) intrafootpad infection with VSV Indiana (VSV Ind) or LCMV WE, respectively. Popliteal draining LNs were collected 5 days after infection and CD4⁺ T cell polarization was assessed by flow cytometric analysis (**Figure 15A**). T follicular helper cells (T_{FH}) were defined as CXCR5⁺ Bcl-6⁺ or as CXCR5⁺T-bet^{low} CD4⁺ T cells, whereas T_{H1} cells as T-bet⁺ CXCR5⁻ CD4⁺ T cells. (**Figure 15A**). On day 5 after VSV infection, the majority (>40%) of Tg7 CD4⁺ T cells had acquired a T_{FH} phenotype, with little or no differentiation into T_{H1} cells (**Figure 15B**). In contrast, SMARTA CD4⁺ T cells induced by LCMV infection maintained a predominant T_{H1} phenotype (>80%) with very few T_{FH} (<15%) (**Figure 15B**).

Since it is well established that heterogeneous T cell antigen receptor (TCR) signals influence the differentiation of CD4⁺ T cells, with high-affinity interactions driving induction of T_{FH} at the expense of T_{H1} in different contexts, it was possible that the observed CD4⁺ T cell compartmentalization was due to a difference in terms of TCR binding affinities. To address this point, C57BL/6 mice were infected with recombinant VSV and LCMV (referred to hereinafter as rVSV and rLCMV, respectively) expressing the same glycoprotein containing the LCMV gp₆₁₋₈₀ epitope recognized by SMARTA CD4⁺ T cells. With this system, the same LCMV-specific CD4⁺ T cells could be analyzed in response to both VSV and LCMV infections. Also in this case, LCMV induced a predominant T_{H1} response, whereas VSV induced a T_{FH} phenotype (**Figure 15C**). These results indicated that features of the viral backbone dictated the cell fate of the CD4⁺ T cells, independently of TCR signal strength.

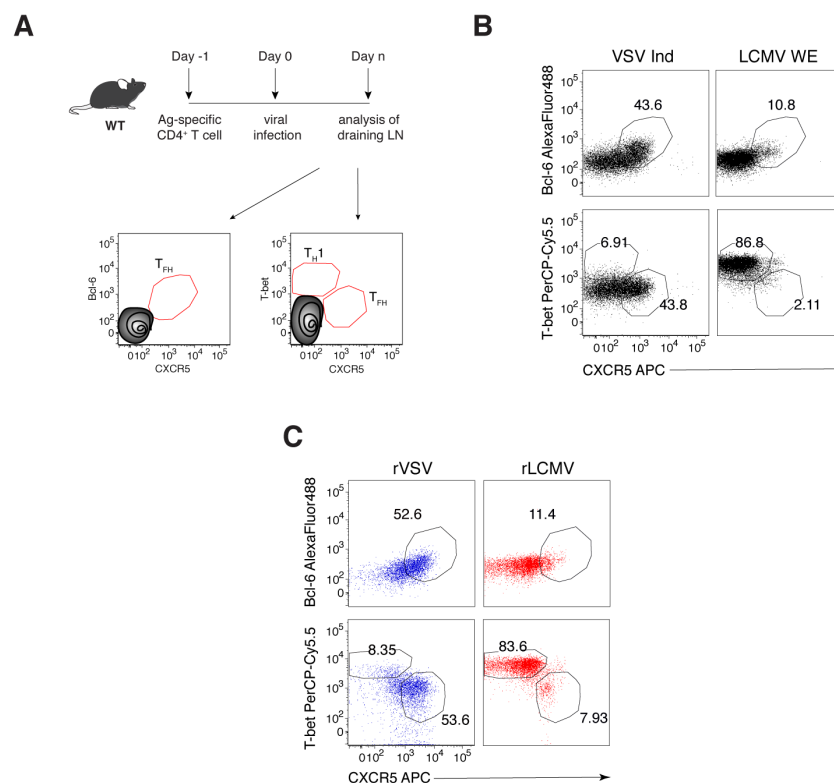


Figure 15. VSV and LCMV infections result in distinct antiviral CD4⁺ T cell polarization. (A) Schematic representation of experimental procedure for the results described in Fig. B–C. 1×10^6 purified Ag-specific (Tg7 when VSV-Ind was used, SMARTA cells in all other cases) CD45.1⁺ CD4⁺ T cells were injected into CD45.2⁺ WT recipients 1 day before intrafootpad infection. dLNs were collected at day 5 after infection and analyzed by flow cytometry. T_{FH} were

defined as either $Bcl-6^+ CXCR5^+$ or $CXCR5^+ T-bet^-$ cells; T_H1 were defined as $T-bet^+ CXCR5^-$ cells.

(B). Representative flow cytometry plots of transferred $CD45.1^+ Tg7 CD4^+$ T cells or $CD45.1^+ SMARTA CD4^+$ T cells (1×10^6 cells each) in the dLNs of $CD45.2^+$ WT recipient mice 5 d after intrafootpad infection with VSV Ind (left) or LCMV WE (right), respectively. Numbers indicate percentages within the indicated gates. Plots are representative of at least five independent experiments.

(C). Representative flow cytometry plots of transferred $CD45.1^+ SMARTA CD4^+$ T cells (1×10^6 cells) in the dLNs of $CD45.2^+$ WT recipient mice 5 d after intrafootpad infection with rVSV (left) or rLCMV (right). Numbers indicate percentages within the indicated gates. Plots are representative of at least five independent experiments.

Next, to gain more insight on the differences in $CD4^+$ T cell priming, VSV and LCMV priming niches were analyzed by NICHE-seq, which combines photoactivation and single-cell RNA sequencing (scRNA-seq) to spatially reconstruct immune niches (Medaglia *et al*, 2017). Even though VSV and LCMV priming niches slightly differed in their cellular composition, by using different conditional knockout and transgenic mice, it was demonstrated that these differences in the priming niches did not initially influence $CD4^+$ T-cell polarization. Instead, NICHE-seq analysis revealed an increased type I IFN signature in cells isolated from the $CD4^+$ T cell priming niche of rLCMV-infected mice as compared to cells from the $CD4^+$ T cell priming niche of rVSV-infected mice on day 2 after infection (**Figure 16 A-B**). These data raised the hypothesis that type I IFNs could potentially play a role in the $CD4^+$ T cell dichotomy observed in the two infections.

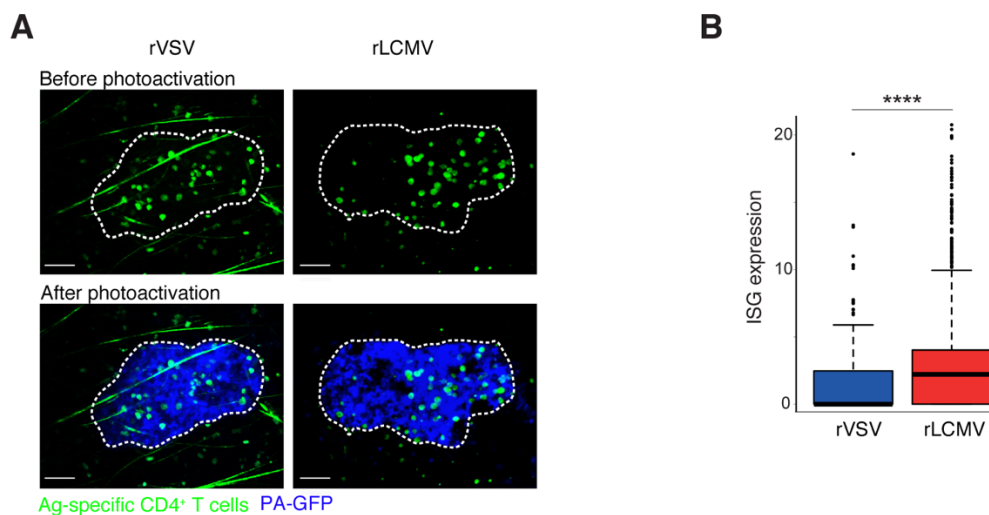


Figure 16. Characterization of the antiviral $CD4^+$ T cell priming niche.

(A) Multiphoton intravital micrographs depicting photoactivation of the CD4⁺ T cell priming niche upon rVSV or rLCMV infection. Images were acquired 2 d after infection. Antigen-specific (SMARTA) CFP⁺ CD4⁺ T cells are depicted in green, and PA-GFP⁺ cells are depicted in blue. Top, before photoactivation; bottom, after photoactivation. Scale bars, 50 μ m. Images are representative of at least two independent experiments.

*(B) Expression profile of selected ISGs (Irf7, Cxcl9, Cxcl10, Oas11, Ifitm3, Oas2 and Isg15) in 2,406 single cells from the photoactivated CD4⁺ T cell priming niches described in (A). Data were pooled from two independent experiments. Kolmogorov–Smirnov test was applied: ****P < 0.0001*

AIM OF THE WORK

7. AIM OF THE WORK

As mentioned earlier, previous work in our lab had identified a striking compartmentalization of CD4⁺ T helper responses upon VSV and LCMV infections. In particular, subcutaneous infection with VSV resulted in polarization of CD4⁺ T cells towards the T_{FH} phenotype. By contrast, LCMV infection resulted in almost complete T_{H1} differentiation, with little or no T_{FH} induction.

The overall aim of my thesis project has been to dissect the determinants of CD4⁺ T cell differentiation upon viral infections. In particular, the present work is structured with a first part focused on the investigation of the molecular determinants of the strong T_{FH} differentiation observed upon VSV infection and a second part in which we investigated the factors involved in the strong T_{H1} polarization observed upon LCMV infection. With particular regard to the second part the following objectives have been addressed:

1. Evaluating whether there are specific polarizing cytokines that drive T_{H1} cell differentiation in the context of LCMV infection.
2. Based on the results of the previous point showing a role of IFN- γ in inducing T_{H1} differentiation and suppressing T_{FH} development upon LCMV infection, I focused on understanding the cellular source and the mechanism whereby this cytokine shapes CD4⁺ T cells differentiation.
3. The strong CD4⁺ T cell compartmentalization observed in the two infections prompted me to consider a possible cross-inhibition between the T_{H1} and T_{FH} subsets.

RESULTS

8. RESULTS

The results showed in the paragraphs 8.1 and 8.2 together with the preliminary data showed in section 6 have been published in the paper: “De Giovanni M, Cutillo V, Giladi A, et al. Spatiotemporal regulation of type I interferon expression determines the antiviral polarization of CD4⁺ T cells. *Nat Immunol.* 2020;21(3):321-330” in which I am a co-author.

PART I

8.1. Different kinetics of type I interferon induction in rVSV/rLCMV infections affect CD4⁺ T cell polarization

Type I IFNs represent one of the most proficient innate immune barriers against viruses and other intracellular pathogens. However, there is growing evidence for a context dependent and controversial role for type I IFNs, with either beneficial or detrimental effects in the fight against infection. This multifaceted role could be linked to the different cellular sources, kinetics and cellular targets for this cytokine (Kuka *et al*, 2019).

Driven by preliminary data obtained through the Niche-Seq analysis, we decided to explore whether type I IFNs might play a role in CD4⁺ T cell polarization upon our viral infection settings. Kinetic analysis of several *Ifna* isoforms (only *Ifna4* shown in the **Figure 17**), *Ifnb* and two representative IFN-stimulated genes (ISGs), *Isg15* and *Oas2*, in total RNA isolated from LNs at 4, 8, 16, 24 and 48 h after infection with rVSV or rLCMV indicated that, although the magnitude of type I IFNs induction was comparable between rVSV and rLCMV infection, the timing was consistently different. Indeed, rVSV induced an earlier and transient wave of type I IFN, which peaked at 8 h after infection, whereas rLCMV induced a delayed (16-24 h) peak, possibly mirroring the different kinetics of viral replication *in vivo* (**Figure 17**). Indeed, it was previously shown that VSV replication is detectable in the subcapsular sinus 1-2 hours after the infection, and reaches its peak at 8 hours. On the contrary, LCMV replication becomes detectable only at 12-18 hours upon infection (Sammicheli *et al*, 2016).

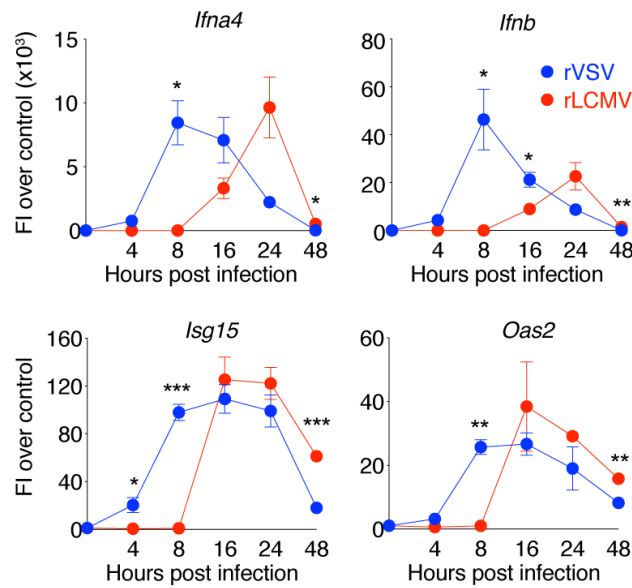


Figure 17. Type I IFNs kinetics differ upon rVSV and rLCMV infection

Analysis of *Ifna4*, *Ifnb*, *Isg15* and *Oas2* gene expression in dLN at 0, 4, 8, 16, 24 and 48 h after rVSV (blue) or rLCMV (red) infection by qPCR. $n = 3$ (0 h), 4 (4 h), 4 (8 h), 4 (16 h), 3 (24 h, rLCMV), 4 (24 h, rVSV) and 4 (48 h). Data were pooled from two independent experiments. The mean \pm s.e.m. is shown. Two-way ANOVA with LSD post test was applied: * $P < 0.05$, ** $P < 0.01$, *** $P < 0.001$. The same sample was measured repeatedly for the four genes. FI, fold increase.

This different kinetic profile of type I IFN expression between the two infections raised the hypothesis that CD4⁺ T cell polarization could be shaped by this particular timing. To address this point, we transferred SMARTA CD4⁺ T cells into WT recipients and treated them with an antibody that blocks IFNAR1 one day prior to rVSV or rLCMV infection (**Figure 18A**).

We found that CD4⁺ T cells polarization in IFNAR1-blocked rLCMV-infected mice was not affected, with SMARTA that differentiated mostly into TH1 cells. By contrast, induction of T_{FH} cells in rVSV-infected mice was severely compromised, with transferred CD4⁺ T cells differentiating into T-bet⁺ CXCR5⁻ TH1 cells (**Figure 18 B-C**).

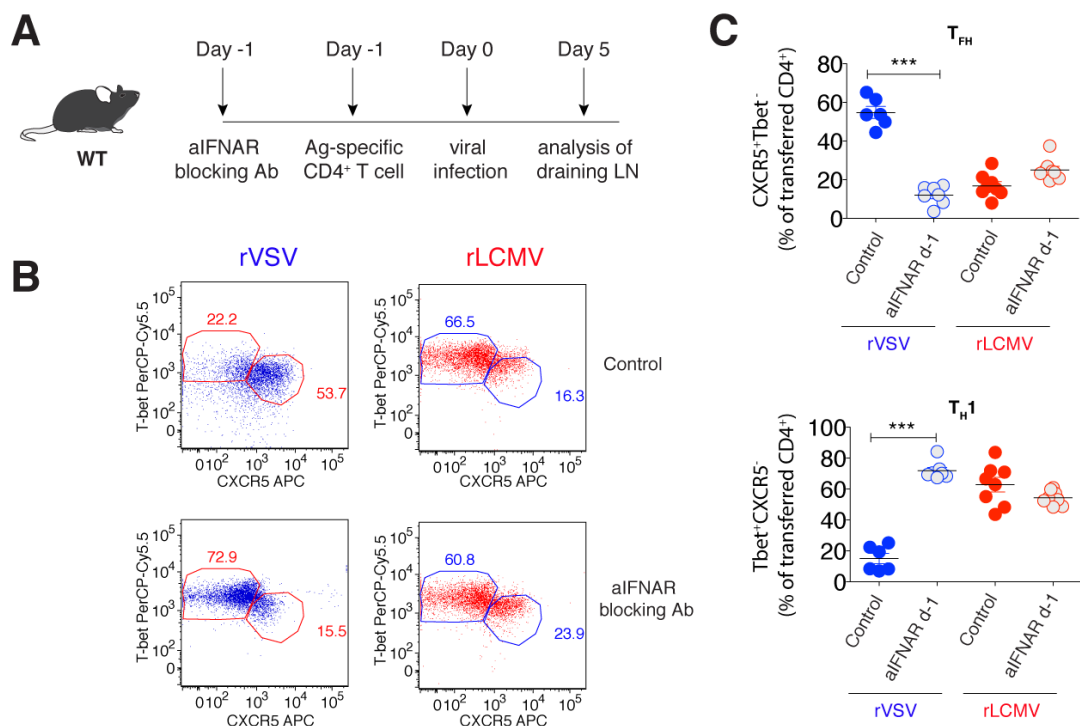


Figure 18. Type I IFNs sensing is essential for the induction of T_{FH} differentiation upon rVSV infection

(A) Schematic representation of experimental procedure for the results described in Fig. B–C. 1×10^6 purified CD45.1⁺ Ag-specific (SMARTA) CD4⁺ T cells were transferred to CD45.2⁺ WT recipients and treated with anti-IFNAR1 1 day prior to rVSV or rLCMV infection.

(B) Representative flow cytometry plots showing T_{FH} and T_{H1} cells among antigen-specific CD4⁺ T cells in dLNs of the mice described in (A). Numbers represent the percentage of cells within the indicated gate.

(C) Quantification of T_{FH} (top) and T_{H1} (bottom) cells, expressed as percentages of antigen-specific CD4⁺ T cells out of total transferred cells, in dLNs of the mice described in (A). The mean \pm s.e.m. is shown. $n=6$ (rVSV) and 8 (rLCMV). Data are representative of at least two independent experiments. One-way ANOVA with Bonferroni's post test was applied: *** $P < 0.001$.

The fact that blocking of type I IFN receptor did not impact LCMV-specific CD4⁺ T cell differentiation, despite the fact that type I IFNs are induced in LCMV-infected mice, suggested that the role of type I IFNs in T_{FH} polarization was limited to the IFNs produced in the first hours after infection (like in rVSV). To test this hypothesis, we administered IFNAR1 blocking Ab either one day prior or one day after infection (**Figure 19A**). Interestingly, we found that when IFNAR1 was blocked the day after infection SMARTA CD4⁺ T cells polarization upon rVSV infection was not affected (**Figure 19B**). These results indicate that type I IFN sensing within the first hours is essential for the induction of T_{FH} cell differentiation.

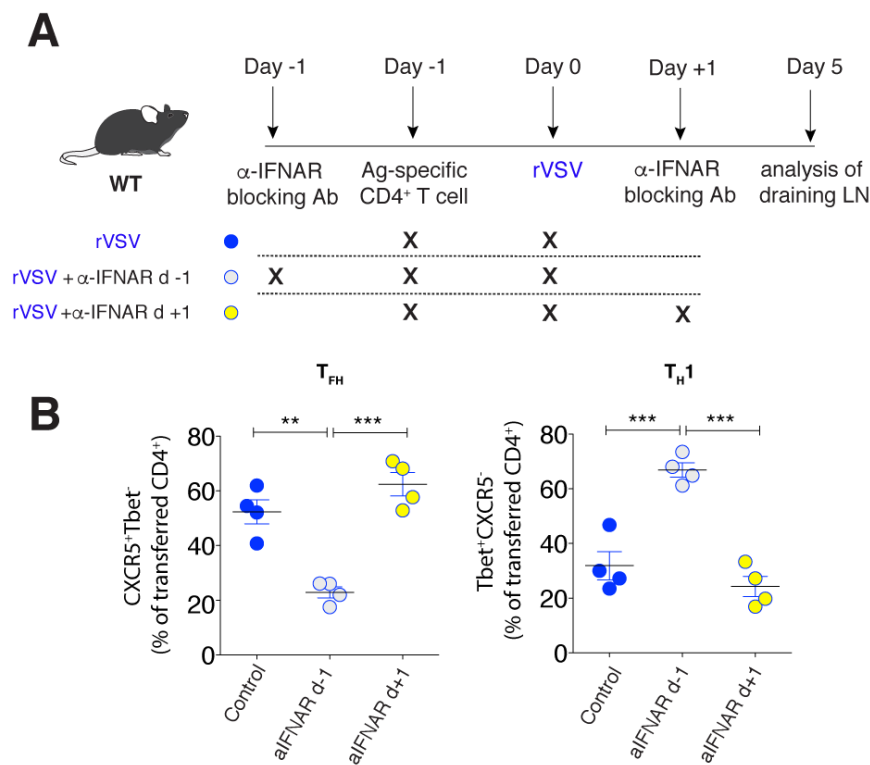


Figure 19. Early type I IFNs sensing is essential for the induction of T_{FH} polarization

(A) Schematic representation of experimental procedure for the results described in (B). 1×10^6 purified $CD45.1^+$ Ag-specific (SMARTA) $CD4^+$ T cells were transferred to $CD45.2^+$ WT recipients and treated anti-IFNAR1 blocking antibody either 1 day prior to (light blue) or 1 day after (yellow) rVSV infection.

(B) Quantification of the percentages of T_{FH} (left) and T_{H1} (right) antigen-specific $CD4^+$ T cells (out of total transferred cells) in dLNs of the mice described in (A). Data are representative of at least two independent experiments. The mean \pm s.e.m. is shown; $n = 4$. One-way ANOVA with Bonferroni's post test was applied: $**P < 0.01$, $***P < 0.001$.

8.2 Early type I IFN sensing by DCs and IL-6 induction drive T_{FH} cell differentiation

We next sought to determine the cellular target(s) of type I IFNs that determined this $CD4^+$ T cell polarization upon viral infection. We first ruled out the direct sensing of type I IFN by SMARTA $CD4^+$ T cells since we did not find any differences in terms of $CD4^+$ T cell differentiation between WT or *Ifnar1*^{-/-} SMARTA $CD4^+$ T cells that were adoptively transferred into WT recipients prior to rVSV infection (*data not shown*).

We next focused on the role of type I IFNs sensing by DCs, since they are involved in the priming of $CD4^+$ T cells and they could directly influence their polarization through the

expression of different costimulatory molecules or the secretion of several polarizing cytokines (Hilligan & Ronchese, 2020). In order to assess this, we adoptively transferred WT SMARTA CD4⁺ T cells into irradiated WT recipients that were reconstituted with *CD11c-Cre* (as control) or *CD11c-Cre x Ifnar1^{fl/fl}* BM (**Figure 20A**). In this setting, mice expressing a Cre recombinase under a DC-specific promoter (*CD11c*) were crossed with mice with a loxP-flanked IFNAR1 (*Ifnar1^{fl/fl}*), generating mice lacking IFNAR1 on DCs. In this model we observed a strong impairment in T_{FH} differentiation upon rVSV infection, mirroring the anti-IFNAR1 blocking Ab experiment (**Figure 20B**).

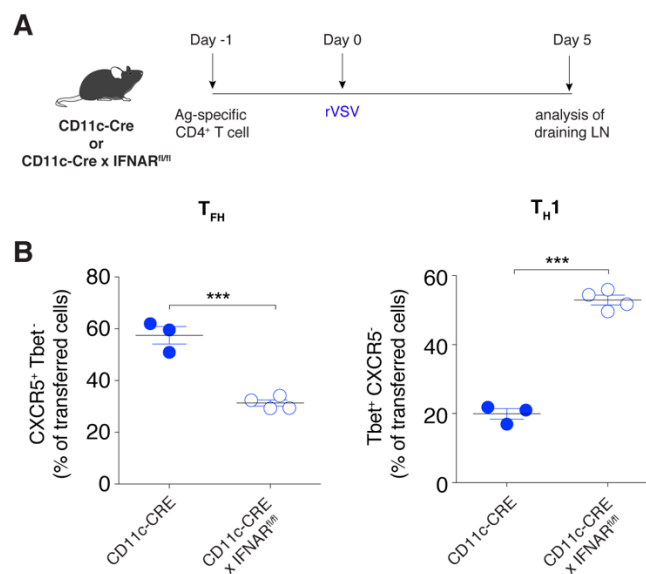


Figure 20. Type I IFNs sensing by DCs is instrumental for the induction of T_{FH} polarization upon rVSV infection

(A) Schematic representation of experimental procedure for the results described in (B). 1×10^6 purified CD45.1⁺ Ag-specific (SMARTA) CD4⁺ T cells were transferred to either CD45.2⁺ *Cd11c-Cre* or CD45.2⁺ *Cd11c-Cre; Ifnar1^{fl/fl}* recipients 1 day prior to rVSV infection.

(B) Quantification of the percentages of T_{FH} and T_{H1} antigen-specific (SMARTA) CD4⁺ T cells (out of total transferred cells) in dLNs of the mice described in (A). Data are representative of three independent experiments. The mean \pm s.e.m. is shown. *Cd11c-Cre*, $n = 3$; *Cd11c-Cre; Ifnar1^{fl/fl}*, $n = 4$. An unpaired two-tailed *t* test was applied: *** $P < 0.001$, **** $P < 0.0001$.

We next investigated the mechanism exerted by type I IFNs on DCs to induce T_{FH} cell differentiation and we focused our attention on IL-6, since it is known to promote T_{FH} differentiation, and its induction is known to be dependent on type I IFNs (Cucak *et al*,

2009). Kinetic analysis of *Il6* expression in LNs from wild-type mice infected with rVSV or rLCMV indicated that induction of *Il6* mRNA mirrors type I IFNs signature, with an early peak (8 h after infection) during VSV infection and a delayed (>16 h) and lower peak during LCMV infection (**Figure 21A**).

These data prompted us to investigate a possible link between type I IFNs expression and the induction of IL-6. To confirm this, we analyzed by qPCR the expression of *Il6* in *Ifnar1*^{-/-} mice. Interestingly, *Il6* mRNA upregulation was completely abrogated in rVSV infected mice in absence of type I IFNs sensing (*Ifnar1*^{-/-} mice) (**Figure 21B**). These data suggest that rVSV-induced *Il6* expression requires type I IFN sensing.

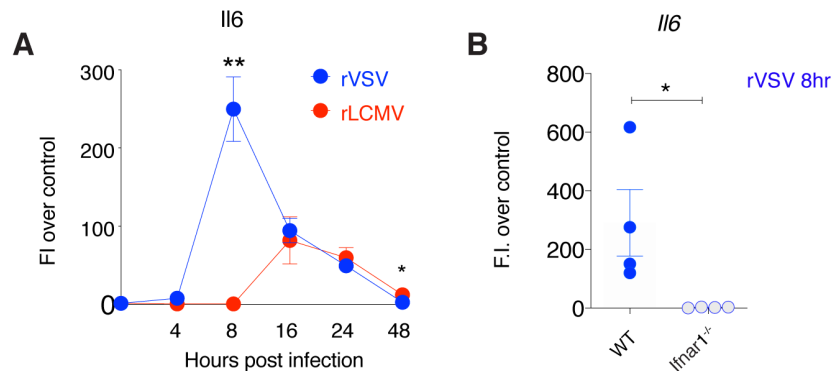


Figure 21. IL-6 expression requires type I IFN sensing

(A) qPCR analysis of the *Il6* gene expression profile at 0, 4, 8, 16, 24 and 48 h in dLNs of mice infected with rVSV (blue) or rLCMV (red). The mean \pm s.e.m. is shown. $n = 4$ (0 h), 4 (4 h), 4 (8 h), 4 (16 h), 3 (24 h, rLCMV), 4 (24 h, rVSV) and 4 (48 h). Data were pooled from two independent experiments. Two-way ANOVA with LSD post test was applied: * $P < 0.05$, ** $P < 0.01$.

(B) qPCR analysis of *Il6* gene expression in wild-type and *Ifnar1*^{-/-} mice in dLNs 8 h after rVSV infection. Data were pooled from two independent experiments. The mean \pm s.e.m. is shown. An unpaired two-tailed *t* test was applied: * $P < 0.05$.

In addition, the early blocking of IL-6 upon rVSV infection significantly disrupted T_{FH} cell differentiation driving a concomitant increase in T_{H1} polarization (**Figure 22A-B**). These observations identify IL-6 as a critical early determinant of the differentiation of antiviral T_{FH} cells.

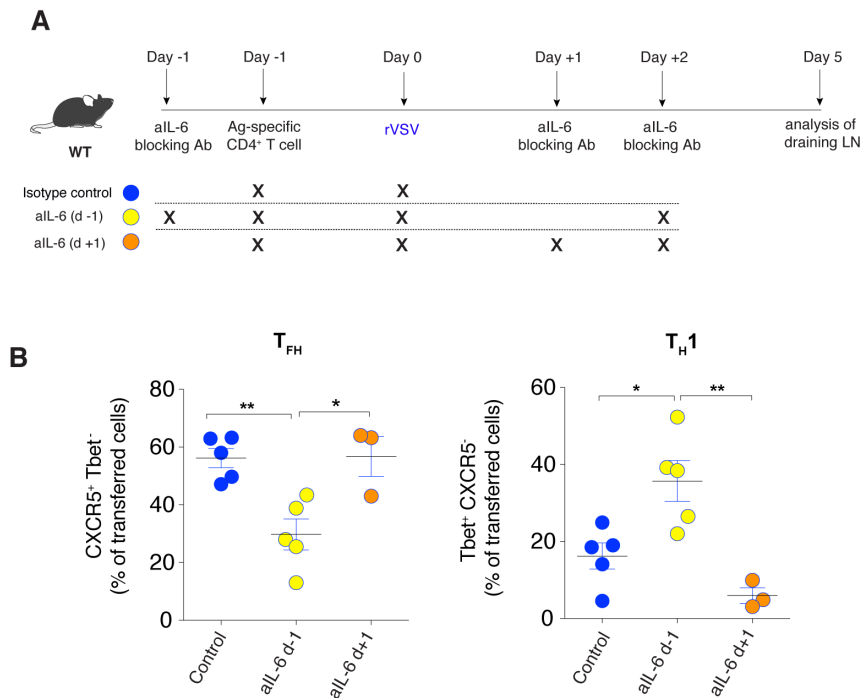


Figure 22. Early IL-6 induction is essential for antiviral T_{FH} differentiation.

(A) Schematic representation of experimental procedure for the results described in Fig. (B). 1×10^6 purified CD45.1⁺ Ag-specific (SMARTA) CD4⁺ T cells were transferred to CD45.2⁺ WT recipients and treated with anti-IL-6 blocking antibody starting either 1 day prior to (yellow) or 1 day after rVSV infection (orange).

(B) Quantification of the percentages of T_{FH} (left) and T_{H1} (right) antigen-specific CD4⁺ T cells (out of total transferred cells) in dLNs of the mice described in (A). Data are representative of at least two independent experiments. The mean \pm s.e.m. is shown. No antibody, $n = 5$; anti-IL-6 1 d before, $n = 5$; anti-IL-6 1 d after, $n = 3$. One-way ANOVA with Bonferroni's post test was applied: * $P < 0.05$, ** $P < 0.01$.

Despite pointing at IL-6 as an important early determinant for T_{FH} differentiation, the abovementioned experiments did not clarify whether IL-6 was produced by DCs in response to type I IFNs. To determine whether type I IFNs induced expression of IL-6 directly on DCs, we analyzed the composition and the transcriptional profile of DCs exposed to early or late type I IFN or lacking the ability to sense this cytokine (*Ifnar1*^{-/-} mice). scRNA-seq on CD11c⁺MHC-II^{hi} sorted from the LNs of wild-type or *Ifnar1*^{-/-} mice at 8 or 48 h after infection with rVSV or rLCMV and unbiased analysis using the MetaCell package (Baran *et al.*, 2018) indicated that CD11c⁺MHC-II^{hi} DCs could be subsetted into migratory cDC2s, cDC1s, cDC2s, moDCs and a small subset of contaminant macrophages (Figure 23A).

Experimental conditions where type I IFN signaling was maximal (8 h after rVSV infection and 48 h after rLCMV infection) showed an enrichment of DC subsets (migratory cDC2s and moDCs) that have been reported to support T_{FH} cell differentiation (Chakarov & Fazilleau, 2014) (**Figure 23B**). Furthermore, ISGs induced by type I IFN were upregulated in DCs from wild-type, but not *Ifnar1*^{-/-} mice, particularly in experimental conditions (8 h after rVSV and 48 h after rLCMV infection) where type I IFN signaling was maximal (**Figure 23C-D**), indicating that DCs responded to type I IFN. Notably, migratory cDC2s and moDCs express *Il6* at 8 h after rVSV infection of wild-type but not *Ifnar1*^{-/-} mice (**Figure 23E**); by contrast, after rLCMV infection, *Il6* mRNA had very low expression in migratory cDC2s and moDCs from wild-type and *Ifnar1*^{-/-} mice, even at 48 h after infection when other ISGs were maximally induced (**Figure 23E**). Thus, DCs express *Il6* and drive T_{FH} cell polarization in response to early (rVSV) but not late (rLCMV) type I IFN signaling.

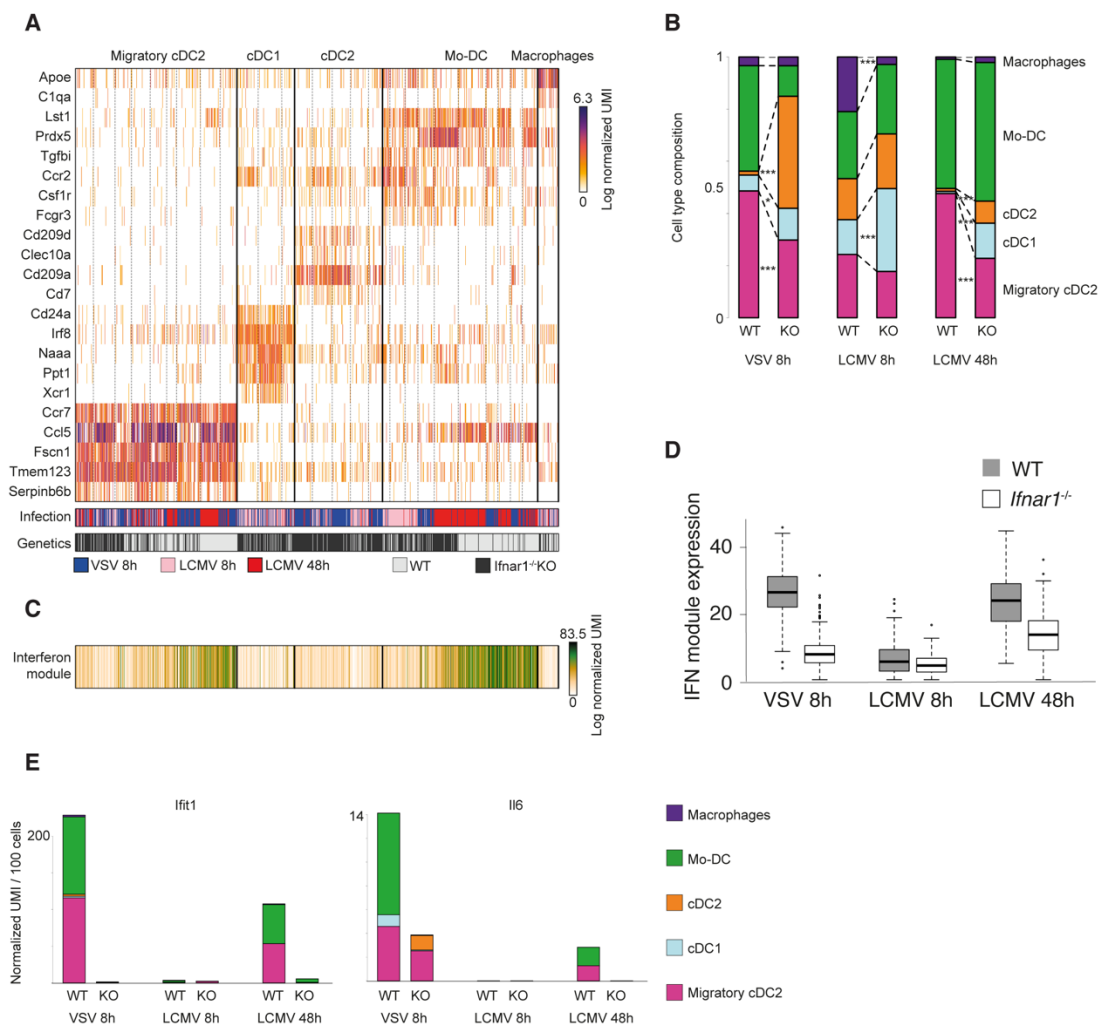


Figure 23. scRNA-seq analysis of LN DCs upon viral infection.

(A) Gene expression profiles of 2,179 single LN $CD11c^+MHC-II^{hi}$ cells passing quality control grouped in five clusters. The color bars indicate each cell's origin (blue, cells from the popliteal LN of mice 8 h after intrafootpad rVSV infection; pink, cells from the popliteal LN of mice 8 h after intrafootpad rLCMV infection; red, cells from the popliteal LN of mice 48 h after intrafootpad rLCMV infection; light gray, wild-type mice; black, *Ifnar1*^{-/-} mice).

(B) Relative abundance of different DC clusters 8 h after rVSV infection, 8 h after rLCMV infection and 48 h after rLCMV infection. Lines show differences in cluster abundance between wild-type and *Ifnar1*^{-/-} mice under the same infection condition. Significant differences in abundance are highlighted. Two-sided FDR-adjusted Fisher's exact test: * $P < 0.05$, *** $P < 0.001$.

(C) Color bar showing total size-normalized (by total number of UMIs in each cell) expression of ISGs in the cells in (A).

(D) Distribution of total size-normalized expression of ISGs in $CD11c^+ MHC-II^{hi}$ cells grouped by experimental condition.

(E) Total expression of the ISG *Ifit1* and the T_{FH} cell-promoting cytokine *Il6* in different experimental conditions. Values represent size-normalized total transcripts per 100 cells. Colors represent relative contribution from the five different DC subsets.

PART II

8.3 Dissecting the determinants of T_{H1} polarization upon LCMV infection

Although the abovementioned results defined the spatiotemporal regulation of type I IFN and IL-6 expression as a critical determinant of T_{FH} differentiation during VSV infection, they did not fully explain the strong $CD4^+$ T cell compartmentalization during VSV and LCMV viral infections. Specifically, absence of T_{H1} cells in the context of VSV infection remained elusive. Moreover, lack of an early type I IFN and IL-6 expression upon LCMV infection could explain the impaired T_{FH} differentiation, but not the extreme T_{H1} polarization in this setting.

Several *in vitro* studies lead to the identification of a complex gene network that comprises cytokines and transcription factors that govern T_{H1} cell differentiation (Sheikh & Groom, 2020); (Schulz *et al*, 2009), however the molecular and cellular determinants of $CD4^+$ T cell differentiation into T_{H1} *in vivo* are incompletely understood. Based on these previously described polarizing factors, LCMV might induce T_{H1} cell differentiation through induction of IL-12, type I IFNs or IFN- γ , all cytokines that have been involved, at least partially, in T_{H1} differentiation (Schulz *et al*, 2009); (Nguyen *et*

al, 2002); (Bradley *et al*, 1996). The current section will show experiments aimed at evaluating which are the polarizing cytokines that drive T_H1 cell differentiation upon LCMV infection.

8.3.1 IL-12 and type I IFNs are not required for T_H1 differentiation upon LCMV infection

The physiological role of IL-12 in inducing type 1 cytokine responses upon protein immunizations, bacterial and parasitic infections has been described (Novelli & Casanova, 2004), but its function upon viral infection requires further investigation. Previous studies have shown how IL-12 drives T_H1 polarization inducing T-bet expression via STAT1 signaling, and IFN- γ production via STAT4 (Zhang *et al*, 2001b); (Schulz *et al*, 2009). Interestingly, like IL-12, also type I IFNs signal through STAT4 to induce IFN- γ , leading to an extremely complex and redundant regulation of IFN- γ expression (Cho *et al*, 1996).

To evaluate which T_H1 polarizing cytokines are involved in the strong T_H1 polarization observed upon LCMV infection we based our investigation on preliminary data that were obtained in the lab showing that all the above mentioned T_H1 polarizing cytokines, besides the alpha subunit of IL-12 (*Il12a* or *Il12p35*) are expressed in the LNs of rLCMV subcutaneously-infected mice and peak at 24 hours post infection (**Figure 24**).

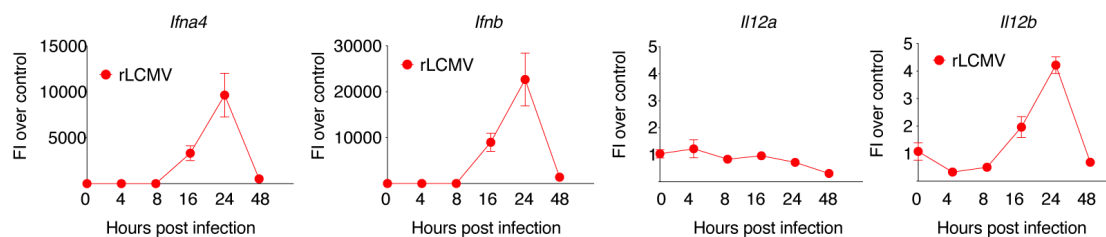


Figure 24. IL-12 and type I IFNs are induced upon subcutaneous LCMV infection
 Analysis of *Ifna4*, *Ifnb*, *Il12a* and *Il12b* gene expression in dLN at 0, 4, 8, 16, 24 and 48 h after rLCMV infection by qPCR. $n = 3$ (0 h), 4 (4 h), 4 (8 h), 4 (16 h), 3 (24 h), and 4 (48 h). Data were pooled from two independent experiments. The mean \pm s.e.m. is shown. The same sample was measured repeatedly for the four genes. FI, fold increase.

To test the role of IL-12 in promoting T_H1 cell polarization in the context of LCMV infection, naïve SMARTA were adoptively transferred into C57BL/6 mice 24 hours before subcutaneous (s.c.) intrafootpad infection with rLCMV. Recipient mice were also

treated with an antibody neutralizing IL-12 or with a control isotype antibody as indicated in **Figure 25A**. Popliteal draining LNs were collected 5 days after infection and SMARTA CD4⁺ T cell polarization was analyzed by flow cytometry. T_H1 and T_{FH} cells were identified as T-bet⁺ CXCR5⁻ and CXCR5⁺ T-bet⁻ CD4⁺ T cells, respectively. Administration of the blocking antibody against IL-12 did not impact SMARTA CD4⁺ T cell polarization in comparison to untreated controls (**Figure 25B-C**), suggesting that IL-12 is dispensable for T_H1 differentiation upon LCMV infection. However, it must be taken into account that in this experimental setup we were not able to formally prove the efficiency of antibody blockade. Unfortunately, we don't have the possibility to test *in vivo* the neutralization with other pathogens that induce T_H1 polarization. Future *in vitro* experiments will formally address this point. Nonetheless, an important body of literature supports that T_H1 arising upon viral infections are IL-12 independent; on the contrary IL-12 plays a more prominent role in the context of bacterial infections (Schijns *et al*, 1998); (Oxenius *et al*, 1999); (Krueger *et al*, 2021).

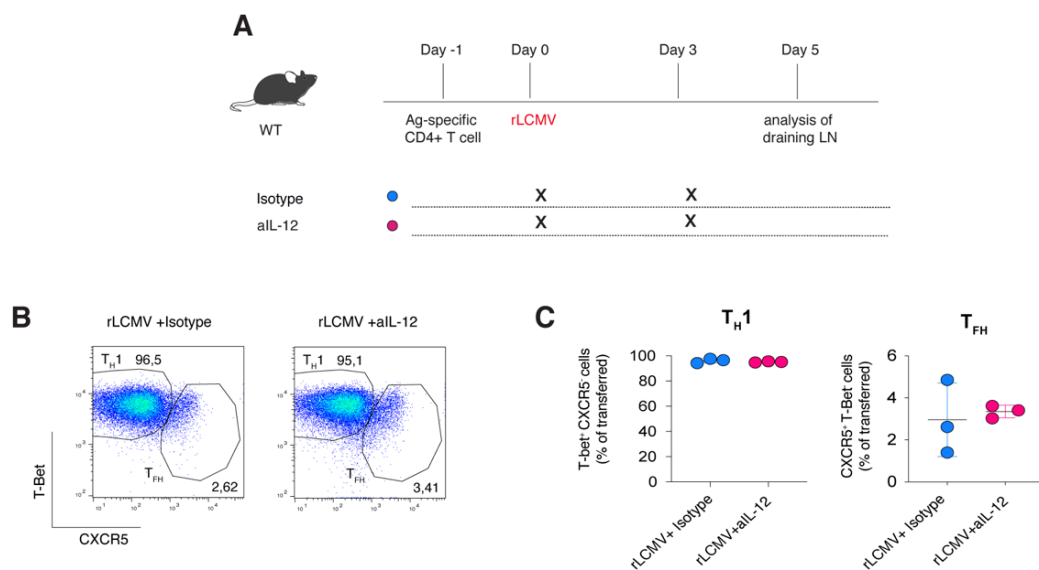


Figure 25. IL-12 is not required in the induction of T_H1 polarization upon LCMV infection
(A) Schematic representation of experimental procedure for the results described in Fig. **B-C**. 1×10^6 purified CD45.1⁺ SMARTA CD4⁺ T cells were transferred into CD45.2⁺ WT recipients 1 day before s.c. intrafootpad rLCMV infection (2×10^5 F.F.U). CD45.2⁺ WT recipient mice were also treated with anti-IL-12 blocking antibody (or isotype control) at d0 and d3 after infection. pLNs were analyzed 5 days post infection.
(B) Representative flow cytometry plots showing T_H1 (T-bet⁺ CXCR5⁻) and T_{FH} (T-bet⁻ CXCR5⁺) cells among antigen-specific CD4⁺ T cells in dLNs of the mice described in **(A)**. Numbers represent the percentage of cells within the indicated gate.

(C) Quantification of T_{H1} (left) and T_{FH} (right), expressed as percentages of antigen-specific $CD4^+$ T cells out of total transferred cells, in dLNs of the mice described in (A). $n=3$. Mean \pm s.e.m. is shown. Data are representative of at least two independent experiments.

The fact that both IL-12 and type I IFNs can induce T_{H1} polarization through STAT4 phosphorylation, raised the possibility that upon IL-12 blocking, type I IFNs could possibly compensate for the lack of IL-12. To address this point we took advantage of *Ifnar1*^{-/-} mice, which lack the receptor for type I IFNs. WT or *Ifnar1*^{-/-} mice were treated with IL-12 blocking antibodies or isotype control and infected with rLCMV (**Figure 26A**). Popliteal draining LNs were collected 7 days after infection (a timepoint that represents the peak of endogenous T cell activation) and endogenous $CD4^+$ T cells were analyzed by flow cytometry for expression of T_{H1} and T_{FH} cell markers. In line with previous experiment, $CD4^+$ T cell differentiation was not impaired in absence of IL-12, however $CD4^+$ T cells preserved their phenotype also in absence of type I IFN sensing (*Ifnar1*^{-/-} mice) and in absence of both IL-12 and Type I IFN (*Ifnar1*^{-/-} mice treated with anti-IL-12) (**Figure 26B**).

Taken together, these data strongly indicate that IL-12 and type I IFNs are not key drivers of the strong T_{H1} polarization observed upon LCMV infection.

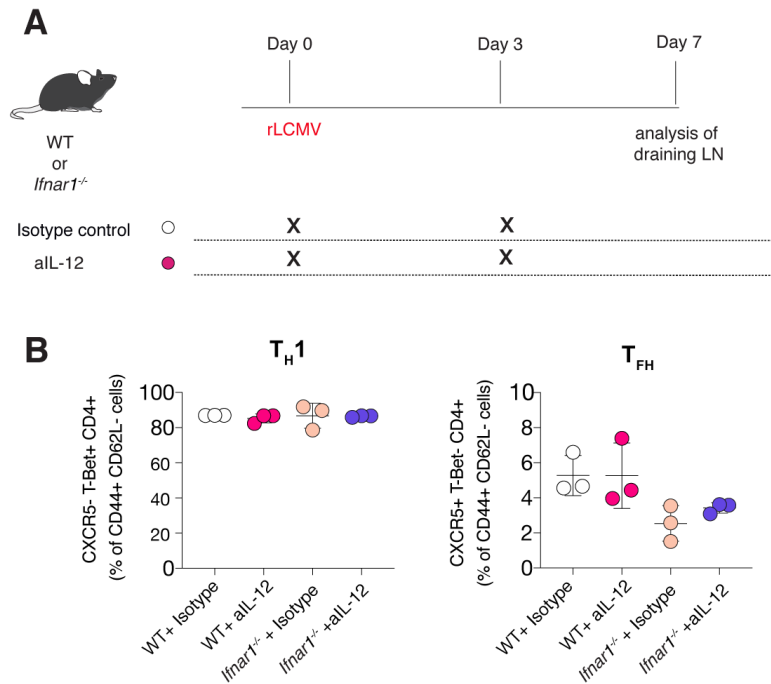


Figure 26. Type I IFNs are not required in the induction of T_{H1} polarization upon LCMV infection

(A) Schematic representation of experimental procedure for the results described in **(B)**. CD45.2⁺ WT and *Ifnar1^{-/-}* recipients were infected s.c. with rLCMV (2×10^5 F.F.U) and were also treated with anti-IL-12 blocking antibody (or isotype control) at d0 and d3 after infection. pLNs were analyzed 7 days post infection.

(B) Quantification of T_{H1} (left) and T_{FH} (right), expressed as percentages out of CD44⁺ CD62L⁻ effector CD4⁺ T cells, in dLNs of the mice described in **(A)**. $n=3$. Mean \pm s.e.m. is shown. Data are representative of at least two independent experiments.

8.3.2 IFN- γ promotes T_{H1} at the expense of T_{FH} differentiation

IFN- γ , the main cytokine produced by T_{H1}, acts in a positive feedback loop to reinforce the T_{H1} identity, but can also induce T-bet in the early phases of T_{H1} differentiation in synergy with TCR-derived stimuli (Schulz *et al*, 2009). Consequently, IFN- γ can play a dual role as effector cytokine and autocrine T_{H1} cell differentiation signal. We found that this cytokine is expressed early in the LNs of rLCMV-infected mice and its expression peaks at 24 hours post infection (**Figure 27A**).

Previous findings showing that IFN- γ cooperates with IL-12 in inducing T_{H1} polarization (Wenner *et al*, 1996); (Schulz *et al*, 2009), led to the hypothesis that, in absence of IL-12, IFN- γ could possibly rescue T_{H1} polarization also in our setting. To address this,

SMARTA CD4⁺ T cells were adoptively transferred in C57BL/6 mice treated with blocking antibodies against IL-12 and IFN- γ alone or in combination. Mice were then infected sc with rLCMV and SMARTA CD4⁺ T cell polarization in the dLNs was assessed at day 5 upon infection by flow cytometry. In vivo neutralization of IL-12 showed again no effect on SMARTA CD4⁺ T cell polarization while IFN- γ blockade resulted in a slight decrease of T_H1 cell differentiation (**Figure 27B-C**). Surprisingly, the impaired T_H1 cell differentiation correlated with an increased T_{FH} cell development leading to a partial shift in the equilibrium between T_{FH} and T_H1 towards T_{FH} in absence of IFN- γ (**Figure 27D**). The blockade of both IL-12 and IFN- γ resulted in a SMARTA CD4⁺ T polarization that resembled the condition in which just IFN- γ was blocked (**Figure 27B-D**), indicating that IFN- γ , but not IL-12, is relevant for T_H1 differentiation upon rLCMV infection.

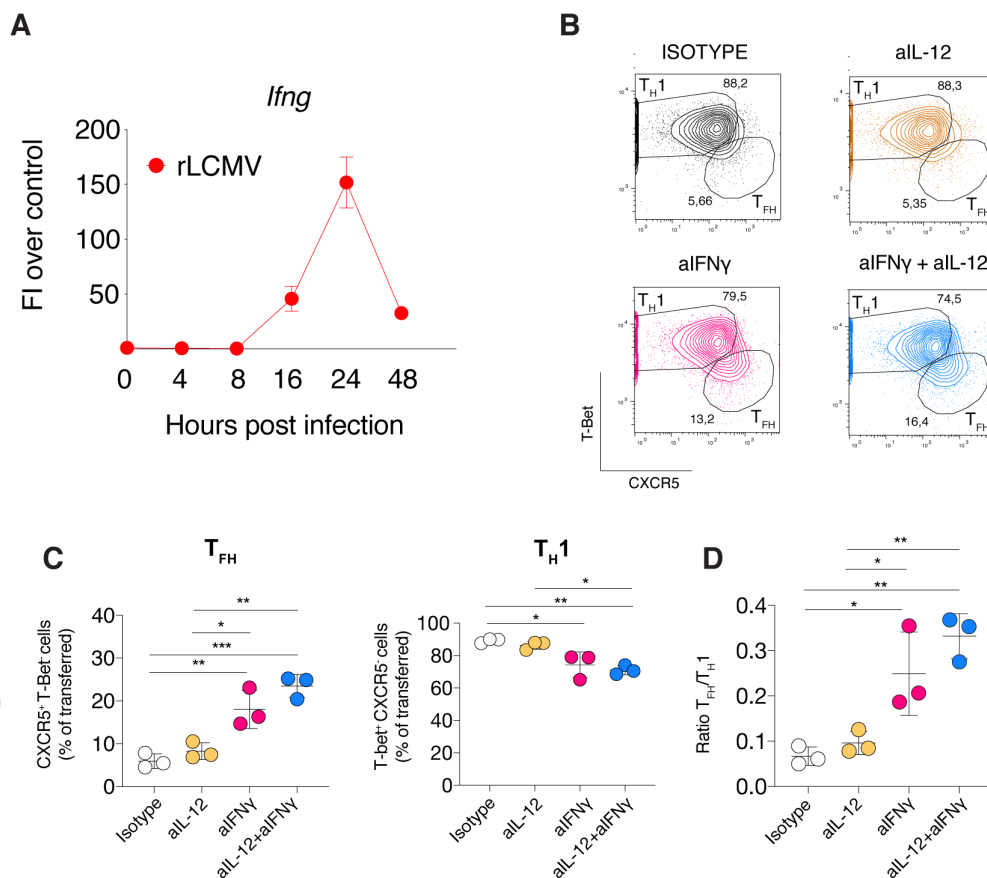


Figure 27. IFN- γ induces SMARTA T_H1 differentiation and suppresses SMARTA T_{FH} development upon LCMV infection.

(A) Analysis of *Ifng* gene expression in dLN at 0, 4, 8, 16, 24 and 48 h after rLCMV infection by qPCR. $n = 3$ (0 h), 4 (4 h), 4 (8 h), 4 (16 h), 3 (24 h), and 4 (48 h). Data were pooled from two independent experiments. The mean \pm s.e.m. is shown. FI, fold increase.

(B) 1×10^6 purified CD45.1⁺ SMARTA CD4⁺ T cells were transferred into CD45.2⁺ WT recipients 1 day before s.c. rLCMV infection (2×10^5 F.F.U). In some conditions, WT recipient mice were also treated with anti-IL-12 (d0, d3), or IFN- γ (d0) blocking antibody (or isotype control) alone or in combination. pLNs were analyzed 5 days post infection.

Representative flow cytometry plots showing T_{H1} (T-bet⁺ CXCR5⁻) and T_{FH} (T-bet⁺ CXCR5⁺) cells among SMARTA antigen-specific CD4⁺ T cells, in the dLNs. Numbers represent the percentage of cells within the indicated gate.

(C) Quantification of T_{H1} (right) and T_{FH} (left), expressed as percentages of antigen-specific CD4⁺ T cells out of total transferred cells, in dLNs of mice described in (B). $n=3$. Mean \pm s.e.m. is shown. Data are representative of at least three independent experiments. One-way ANOVA with Bonferroni's post test was applied: * $P < 0.05$, ** $P < 0.01$, *** $P < 0.001$.

(D) T_{FH}-to-T_{H1} ratio obtained from frequencies of T_{FH} and T_{H1} from (C). One-way ANOVA with Bonferroni's post test was applied: * $P < 0.05$, ** $P < 0.01$.

To further confirm the role of IFN- γ upon LCMV infection, we asked whether a similar phenotype could be observed also in the context of endogenous CD4⁺ T cells polarization. To test this, C57BL/6 mice were treated with aIFN- γ blocking antibodies, infected subcutaneously with rLCMV and endogenous CD4⁺ T cell polarization in the draining lymph nodes was assessed at day 7 upon infection. In line with the previous result, we observed the same trend of CD4⁺ T cell polarization with an increase in T_{FH} development coupled with a decrease in T_{H1} differentiation in the group of mice treated with the IFN- γ blocking antibody compared to the isotype control (**Figure 28A-B**). We then determined the ratio between T_{FH} and T_{H1} for the two groups and we could appreciate that, in absence of IFN- γ , there is a partial shift towards T_{FH} in the balancing between T_{FH} and T_{H1} (**Figure 28C**).

This role of IFN- γ was not observed just in terms of frequencies, but also in terms of absolute numbers (**data not shown**).

Overall, these data suggest that IFN- γ partially induces T_{H1} differentiation and suppresses T_{FH} development.

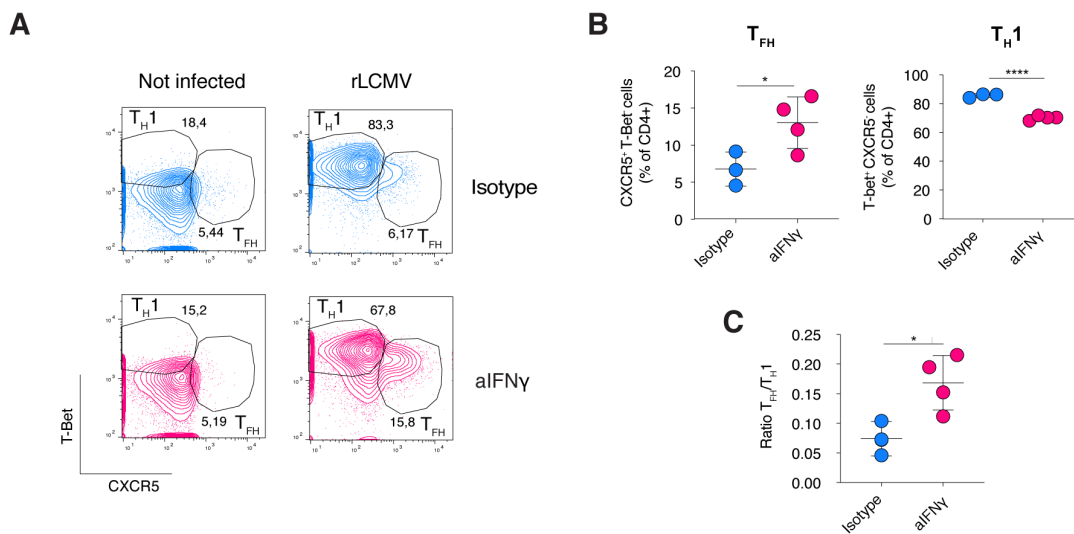


Figure 28. IFN- γ induces endogenous T_{H1} differentiation at the expense of T_{FH} development upon LCMV infection.

CD45.2⁺ WT mice were infected s.c. intrafootpad with rLCMV (2×10^5 F.F.U) and treated with anti-IFN γ blocking antibody (or isotype control) at day 0. pLNs were analyzed 7 days post infection.

(A) Representative flow cytometry plots showing T_{H1} ($T\text{-bet}^+CXCR5^-$) and T_{FH} ($T\text{-bet}^+CXCR5^+$) cells among total $CD4^+$ T cells, in the dLNs of mice described above. Numbers represent the percentage of cells within the indicated gate.

*(B) Quantification of T_{H1} (right) and T_{FH} (left) expressed as percentages of total $CD4^+$ T cells in dLNs of mice described above. Isotype, $n = 3$; aIFN γ , $n = 4$. Mean \pm s.e.m. is shown. Data are representative of at least three independent experiments. An unpaired two-tailed t test was applied: * $P < 0.05$, **** $P < 0.0001$.*

*(C) T_{FH} -to- T_{H1} ratio obtained from frequencies of T_{FH} and T_{H1} from (B). An unpaired two-tailed t test was applied: * $P < 0.05$.*

8.3.3 Sc-RNA-seq and flow cytometry highlight heterogeneity within Ag-specific $CD4^+$ T cells upon LCMV infection

Data presented in the previous paragraph clearly show how in the context of LCMV infection IL-12 and type I IFNs are not relevant in the induction of T_{H1} polarization, whereas IFN- γ plays a key role in skewing $CD4^+$ T cell differentiation towards T_{H1} at the expense of T_{FH} . However, it looks like IFN- γ is able to modulate the fate decision of just a small population of $CD4^+$ T cells. This result prompted us to investigate whether T_{H1} polarization upon LCMV infection could be endowed with a degree of heterogeneity that is characterized by dependence on different polarizing cytokines, some of which unknown.

To investigate the transcriptional heterogeneity of CD4⁺ T cell differentiation in the context of LCMV infection we performed single-cell RNA sequencing (scRNA-seq) on SMARTA CD4⁺ T cells isolated 5 days upon subcutaneous rLCMV infection. To this end, we adoptively transferred naïve SMARTA CD4⁺ CD45.1⁺ T cells into C57BL/6 WT mice 24 h before subcutaneous intrafootpad infection with rLCMV. On day 5 after infection, we sorted SMARTA CD4⁺ T cells from footpad-draining popliteal LNs and performed massively parallel single-cell RNA-sequencing (MARS-seq) on QC-positive single T cells. To be able to compare transcriptional profiles of T_H1 to those of T_{FH} cells, we also sorted either total SMARTA CD4⁺ T cells or CXCR5⁺ ICOS⁺ PD-1^{high} SMARTA CD4⁺ T cells from rVSV infected mice. The dataset was analyzed using the Seurat R package (Stuart *et al*, 2019) and the four groups were visualized using the uniform manifold approximation and projection (UMAP) (Becht *et al*, 2019) (**Figure 29A**). Naïve SMARTA CD4⁺ T cells (n=369, in lightblue) cluster at the upper-left of the UMAP and are characterized by a higher expression of canonical naïve markers such as *Sell* and *Ccr7* (*data not shown*). It is then possible to appreciate an almost complete overlap between rVSV cells (n=498, in green) and the sample composed by the T_{FH} subset of rVSV (n=243, in purple), confirming our previous findings that the majority of CD4⁺ T cells polarize towards T_{FH} upon subcutaneous rVSV infection. The vast majority of SMARTA CD4⁺ T cells from rLCMV-infected mice (n=643, in red) cluster at the right of the UMAP with some of the cells that localize at the interface of rLCMV and rVSV samples. In order to investigate whether there is heterogeneity within SMARTA CD4⁺ T cells from mice infected with LCMV, we focused only on this condition and identified two unbiased clusters (**Figure 29B**). Cluster 0 (n cells=557) showed higher expression of genes such as *Gzmb*, *Nkg7* and *Lgals1*, whereas cluster 1 (n cells=86) was characterized, among other genes, by a higher expression of *Tcf7*, a transcription factor that is needed for T_{FH} differentiation (Xu *et al*, 2015) (**Figure 29D-E**). Confirming the different transcriptional profile of the cells belonging to cluster 1, we observed that in the initial UMAP with all the different samples, the cells of cluster 1 localize at the interface between the cells from rLCMV and rVSV infected mice (**Figure 29C**).

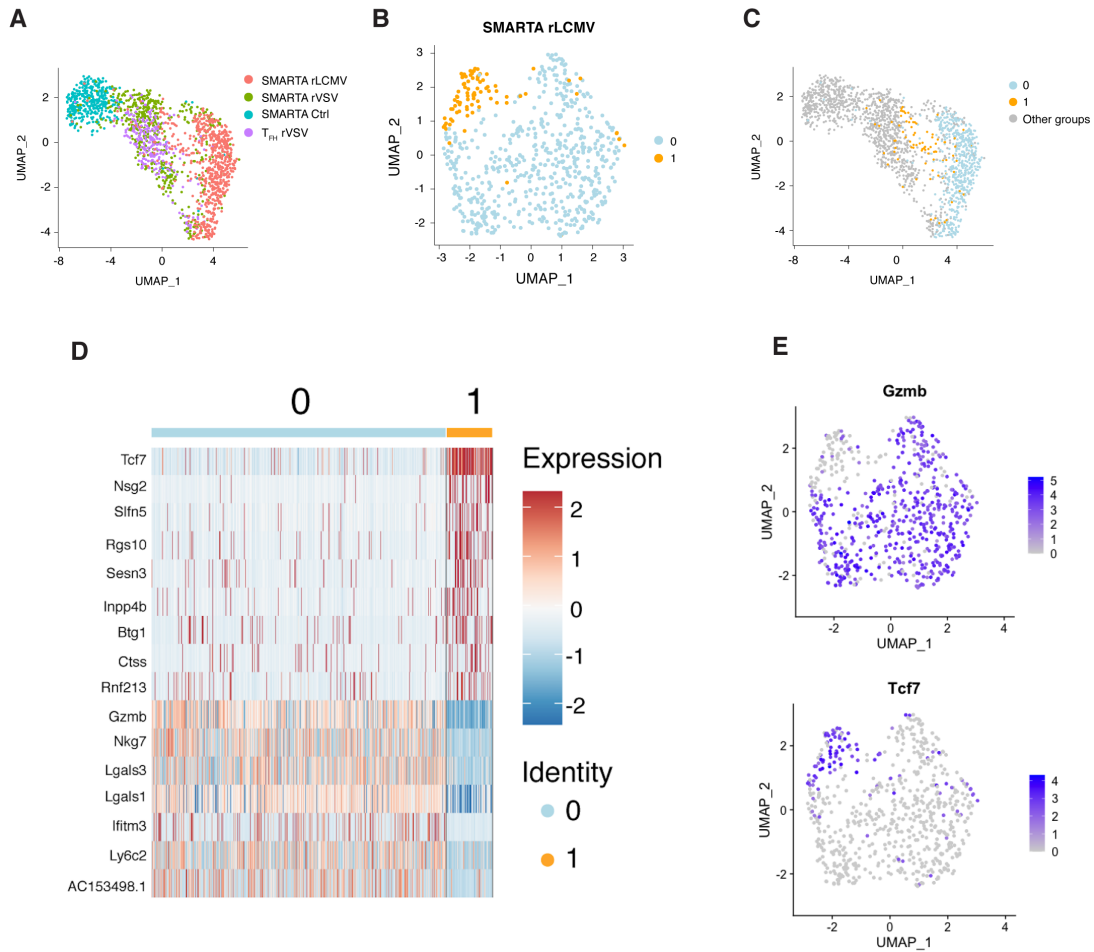


Figure 29. Single-cell RNA-seq identifies two clusters of SMARTA CD4⁺ T cells upon LCMV infection

(A) UMAP projection of sorted cells. Each dot corresponds to a single cell, colored according to different samples. Naïve SMARTA CD4⁺ T cells (lightblue, 369 cells), rVSV cells (green, 498 cells), T_{FH} subset of rVSV (purple, 243 cells), LCMV cells (red, 643 cells).

(B) UMAP projection of SMARTA CD4⁺ T cells sorted from rLCMV infected mice. Each dot corresponds to a single cell, colored according to the unbiased clusters identified: cluster 0 (light blue, 557 cells) and cluster 1 (orange, 86 cells).

(C) UMAP projection of sorted cells. Each dot corresponds to a single cell, colored according to the unbiased clusters identified in the rLCMV setting.

(D) Heatmap of normalized and scaled expression values of the top marker genes identifying the two clusters (logFC threshold: $\pm 1,2$). Color coding of the bar on the top of the heatmap as in **(B)**

(E) Feature plot representation of the normalized expression level of Gzmb and Tcf7 on the scRNAseq dataset described in **(B)**. The expression is measured as the $\ln(TPM+1)$.

These data suggest that there is a certain degree of heterogeneity among the T_{H1} cells that develop upon rLCMV infection and raised the hypothesis that there could be more than

one subset of T_H1 cells arising upon the same infection setting. These different subsets could potentially depend on different cytokine milieu for their polarization and they could play different roles in the immune response.

To validate the scRNA-seq dataset with analysis of the subset-specific proteins, we used flow cytometry to analyze Granzyme B (GzmB) and TCF-1 (encoded by *Tcf7* gene) expression on SMARTA CD4⁺ T cells at day 5 upon sc rLCMV infection. In line with scRNAseq, two populations were identified: one GzmB⁺ TCF-1⁻ and the other TCF-1⁺ GzmB⁻ (**Figure 30A**). Interestingly, the frequencies of the two populations mirror the one observed in the scRNA-seq data, with the GzmB⁺ population that represents nearly 80% of the SMARTA, whereas the TCF-1⁺ population around the 20% (**Figure 30A**).

We further confirmed the presence of these two populations in the endogenous CD4⁺ T cell population at day 7 post infection, and also in this context CD44⁺ CD62L⁻ effector CD4⁺ T cells were either TCF1⁺ or GzmB⁺, with similar frequency compared to SMARTA CD4⁺ T cells (**Figure 30B**). Interestingly, we observed that upon GP-61 peptide restimulation, around the 36% of GzmB⁺ cells produced IFN- γ , whereas just the 13% of TCF-1⁺ cells produce this cytokine, indicating that among the T-bet⁺ population the GzmB⁺ subset represents the major source of IFN- γ and the two populations might be functionally different (**Figure 30C-D**). This was true also per cell basis, since we observed a striking decrease in the expression of IFN- γ (shown as mean fluorescence intensity MFI) in the TCF-1⁺ population compared to the GzmB⁺ cells (**Figure 30E**).

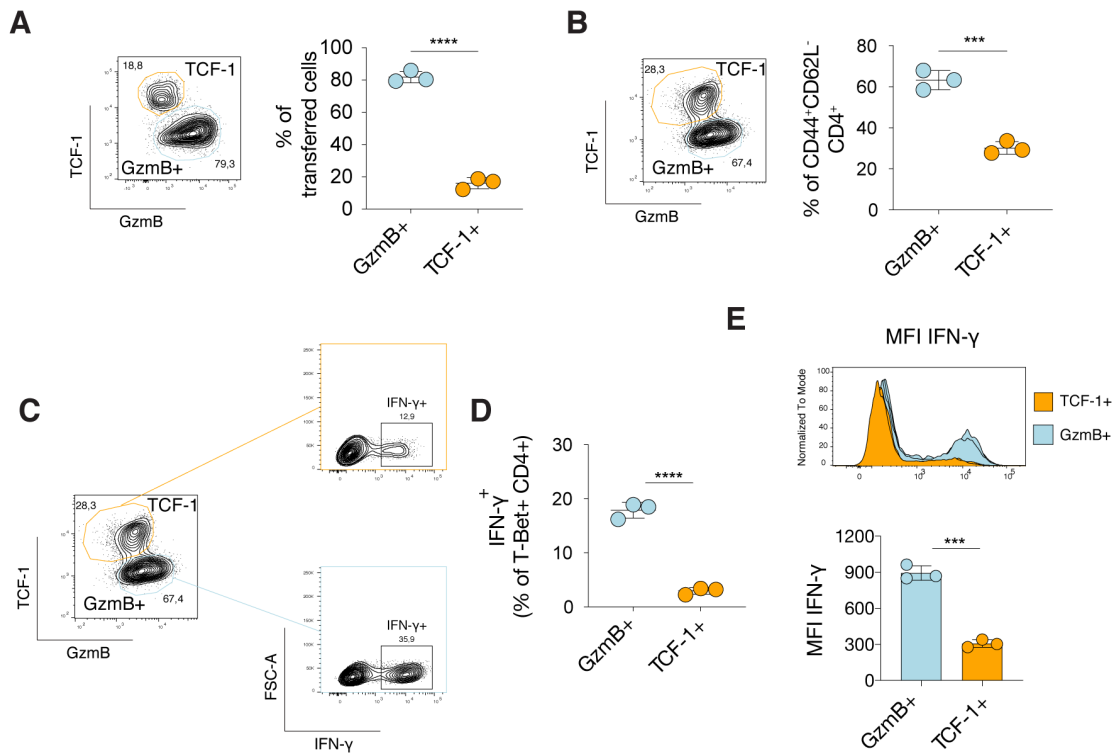


Figure 30. Effector CD4⁺ T cells polarize into TCF-1⁺ and TCF-1⁻ Gzmb⁺ populations and the Gzmb⁺ population represent the major IFN- γ producer.

(A) 1×10^6 purified CD45.1⁺ SMARTA CD4⁺ T cells were transferred into CD45.2⁺ WT recipients 1 day before s.c. rLCMV infection (2×10^5 F.F.U). pLNs were analyzed 5 days post infection.

Representative flow cytometry plots showing TCF-1⁺ and Gzmb⁺ cells among SMARTA antigen-specific CD4⁺ T cells, in the dLNs. Numbers represent the percentage of cells within the indicated gate. On the right quantification of Gzmb⁺ and TCF-1⁺ cells expressed as percentages of antigen-specific CD4⁺ T cells out of total transferred cells in dLNs. $n=3$. Mean \pm s.e.m. is shown. An unpaired two-tailed t test was applied: **** $P < 0.0001$.

(B) CD45.2⁺ WT mice were infected s.c. intrafootpad with rLCMV (2×10^5 F.F.U) and pLNs were analyzed 7 days post infection. Representative flow cytometry plots showing TCF-1⁺ and Gzmb⁺ cells among CD44⁺ CD62L⁻ effector CD4⁺ T cells in the dLNs). Numbers represent the percentage of cells within the indicated gate. On the right quantification of Gzmb⁺ and TCF-1⁺ cells expressed as percentages of effector CD4⁺ T cells in dLNs. $n=3$. Mean \pm s.e.m. is shown. Data are representative of at least three independent experiments. An unpaired two-tailed t test was applied: *** $P < 0.001$.

(C) Representative flow cytometry plots showing the frequencies of IFN- γ ⁺ cells among the Gzmb⁺ or TCF-1⁺ CD4⁺ T cells. Numbers represent the percentage of cells within the indicated gate of mice described in **(B)**.

(D) Quantification of Gzmb⁺ IFN- γ ⁺ and TCF-1⁺ IFN- γ ⁺ CD4⁺ T cells expressed as percentages of T-bet⁺ CD4⁺ T cells in dLNs of mice described in **(B)**. $n = 3$. Mean \pm s.e.m. is shown. Data are representative of at least three independent experiments. An unpaired two-tailed t test was applied: **** $P < 0.0001$.

(E) Flow-cytometric representative histogram of IFN- γ expression within GzmB⁺ or TCF-1⁺ CD4⁺ T cells of mice described in **(B)**. The graphs below the histogram represent the quantification of the mean fluorescence intensity (MFI) of IFN- γ on GzmB⁺ or TCF-1⁺ CD4⁺ T cells. Mean \pm s.e.m. is shown. An unpaired two-tailed *t* test was applied: ****P* < 0.001

Since IFN- γ blockade partially inhibits T_{H1} and increases T_{FH} development, we asked whether IFN- γ might act specifically on the TCF-1⁺ or on the GzmB⁺ population. To address this point, SMARTA CD4⁺ T cells were adoptively transferred in C57BL/6 mice treated with blocking antibody against IFN- γ or PBS. Mice were then infected sc with rLCMV and SMARTA CD4⁺ T cell polarization in the draining lymph nodes was assessed at day 5 upon infection by flow cytometry. As we previously showed, IFN- γ blockade led to an increase SMARTA CD4⁺ T cell differentiation toward T_{FH} compared to PBS-treated mice (**Figure 31A-B**). Strikingly, in the group of mice treated with aIFN- γ blocking antibodies we observed an increase of the TCF-1⁺ population and a change in their phenotype, with the upregulation of the canonical T_{FH} markers CXCR5 and PD-1 (**Figure 31C-E**). These results suggest that IFN- γ inhibits T_{FH} differentiation suppressing the differentiation of the TCF-1⁺ population towards fully differentiated CXCR5⁺ PD-1⁺ T_{FH}.

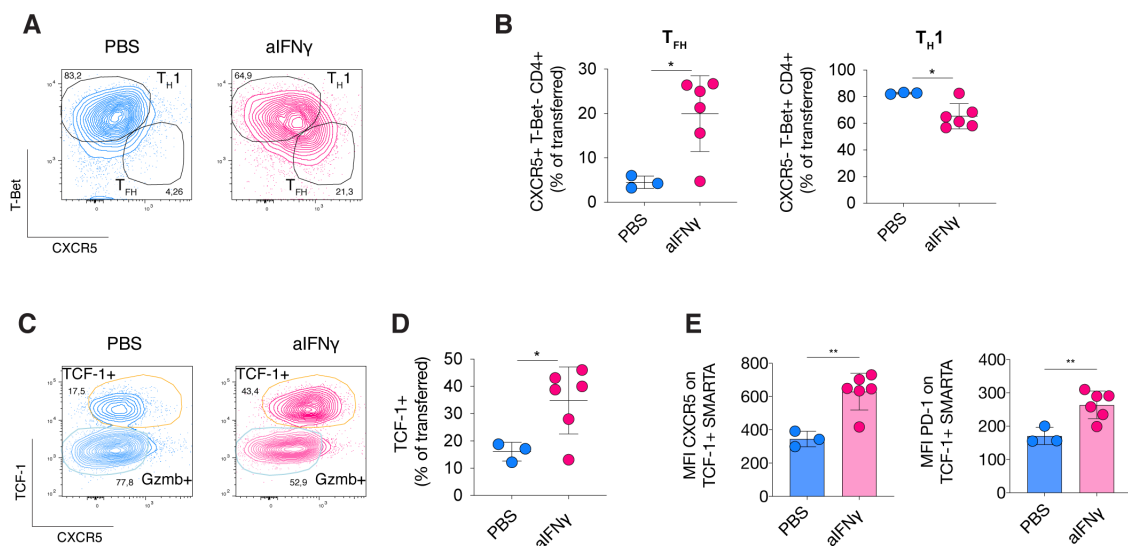


Figure 31. IFN- γ inhibits T_{FH} differentiation suppressing the differentiation of the TCF-1⁺ population towards CXCR5⁺ PD-1⁺ T_{FH}.

*1*10⁶ purified CD45.1⁺ SMARTA CD4⁺ T cells were transferred into CD45.2⁺ WT recipients 1 day before s.c. intrafootpad rLCMV infection (2*10⁵ F.F.U). CD45.2⁺ WT recipient mice were also treated with anti-IFN γ blocking antibody (or PBS) at d0 after infection. pLNs were analyzed 5 days post infection.*

(A) Representative flow cytometry plots showing T_{H1} ($T\text{-bet}^+CXCR5^+$) and T_{FH} ($T\text{-bet}^+CXCR5^+$) cells among antigen-specific $CD4^+$ T cells in dLNs of mice described above. Numbers represent the percentage of cells within the indicated gate.

(B) Quantification of T_{H1} (right) and T_{FH} (left), expressed as percentages of antigen-specific $CD4^+$ T cells out of total transferred cells, in dLNs of mice described above. PBS $n=3$; $aIFN\gamma$ $n=6$. Mean \pm s.e.m. is shown. An unpaired two-tailed t test was applied: $*P < 0.05$.

(C) Representative flow cytometry plots showing $TCF-1^+$ and $TCF1^-GzmB^+$ cells among antigen-specific $CD4^+$ T cells in dLNs of mice described above. Numbers represent the percentage of cells within the indicated gate.

(D) Quantification of $TCF-1^+$ cells expressed as percentages of antigen-specific $CD4^+$ T cells out of total transferred cells, in dLNs of mice described above. PBS $n=3$; $aIFN\gamma$ $n=6$. Mean \pm s.e.m. is shown. An unpaired two-tailed t test was applied: $*P < 0.05$.

(E) Quantification of the mean fluorescence intensity (MFI) of $CXCR5$ and $PD-1$ on $TCF-1^+$ cells in dLNs of mice described above. Mean \pm s.e.m. is shown. An unpaired two-tailed t test was applied: $**P < 0.01$.

8.4 Molecular mechanism whereby $IFN-\gamma$ induces T_{H1} polarization and suppresses T_{FH} development

Data presented in the previous paragraphs clearly highlight a role of $IFN-\gamma$ as an important determinant of $CD4^+$ T cell differentiation by partially supporting T_{H1} differentiation and suppressing T_{FH} differentiation. Our next step is to define the molecular mechanisms whereby this process occurs, for example by identifying the relevant cellular source for $IFN-\gamma$.

Many cell types, including Group I ILCs, DCs, and innate $CD8^+$ T cells have been described to produce $IFN-\gamma$ early upon infection, whereas late $IFN-\gamma$ producers include $CD8^+$ T cells and T_{H1} themselves that can support and stabilize their differentiation in a positive feedback loop (Vremec *et al*, 2007); (Schoenborn & Wilson, 2007); (Kastenmüller *et al*, 2012). In this section I will present data aimed at determining which, among the $IFN-\gamma$ cellular sources, plays a major role in T_{H1} differentiation and T_{FH} inhibition.

8.4.1 SMARTA-derived $IFN-\gamma$ is sufficient, but not necessary to drive T_{H1} $CD4^+$ T cell polarization upon LCMV infection

We first focused our attention on the role of $IFN-\gamma$ produced by $CD4^+$ T cells since they are not just able to produce this cytokine, but they can also sense it in a positive

feedback fashion that further enhances and maintains T_{H1} polarization (Wakil *et al*, 1998). Given the strong polarization of LCMV-specific $CD4^+$ T cells into T_{H1} , an interesting question would be whether an excessive T_{H1} polarization (and IFN- γ production) could induce the maintenance of T_{H1} cell polarization and interfere with the development of a T_{FH} response. To dissect the role of CD4-derived IFN- γ we took advantage of SMARTA IFN- $\gamma^{-/-}$ mice. We adoptively transfer SMARTA WT or SMARTA IFN- $\gamma^{-/-}$ $CD4^+$ T cells in WT or IFN- $\gamma^{-/-}$ recipients, we infected them subcutaneously and we assessed SMARTA polarization at day 5 upon infection in the pLNs (**Figure 32A**). We found that, although SMARTA-derived IFN- γ was sufficient to drive T_{H1} polarization in IFN- $\gamma^{-/-}$ recipients, when adoptively transferred SMARTA were not able to produce IFN- γ , they still differentiated into T_{H1} but not T_{FH} cells, indicating that also IFN- γ produced by other cell types was sufficient to promote T_{H1} polarization. Only total absence of IFN- γ (from both recipient and donor cells) increased T_{FH} differentiation and decreased T_{H1} development (**Figure 32B**). These data suggest that IFN- γ derived from $CD4^+$ T cells is sufficient, but not necessary to drive T_{H1} polarization and suppress T_{FH} development. In addition, we measured viral titers in the dLNs of the mice of the different groups, but they were undetectable since in this setting of acute infection the virus is cleared very fast by the efficient CTL response (**Figure 32C**). To this regard, in order to use viral titers as a functional readout of the increase T_{FH} response observed in absence of IFN- γ , we have planned to perform the same experimental setup in the context of chronic infection.

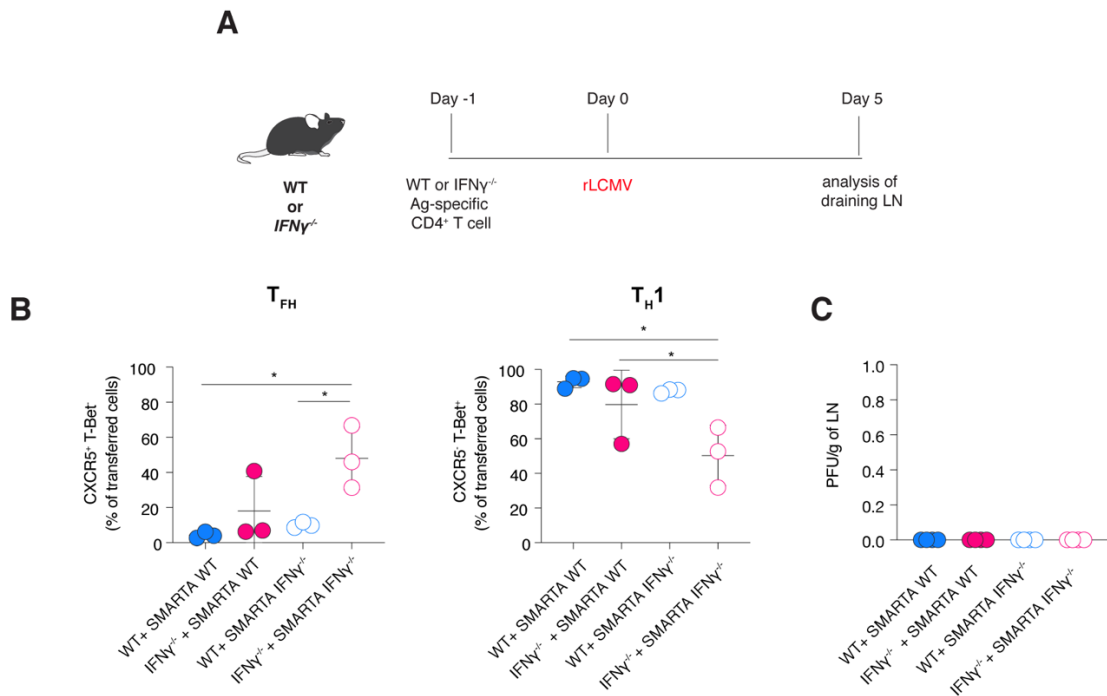


Figure 32. SMARTA-derived $IFN\text{-}\gamma$ is sufficient, but not necessary, to drive T_{H1} $CD4^{+}$ T cell polarization upon LCMV infection

(A) Schematic representation of experimental procedure for the results described in (B). 1×10^6 purified $CD45.1^{+}$ SMARTA $CD4^{+}$ T cells WT or $IFN\text{-}\gamma^{-/-}$ were transferred into $CD45.2^{+}$ WT or $IFN\text{-}\gamma^{-/-}$ recipients 1 day before s.c. rLCMV infection (2×10^5 F.F.U). dLNs were analyzed 5 days post infection.

(B) Quantification of T_{H1} (right) and T_{FH} (left), expressed as percentages of antigen-specific $CD4^{+}$ T cells out of total transferred cells, in dLNs of mice described in (A). $n=3$. Mean \pm s.e.m is shown. Data are representative of at least three independent experiments. One-way ANOVA with Bonferroni's post test was applied: $*P < 0.05$.

(C) Virus titers were determined in the LNs ($n = 3$) of mice described in (A).

8.4.2 The early wave of $IFN\text{-}\gamma$ drives T_{H1} polarization at the expense of T_{FH} differentiation

The caveat of the previous experiment is that when SMARTA $IFN\text{-}\gamma^{-/-}$ $CD4^{+}$ T cells were transferred in WT recipients, activated endogenous $CD4^{+}$ T cells might have produced $IFN\text{-}\gamma$ and promoted T_{H1} development. Thus, we asked whether $IFN\text{-}\gamma$ plays a role in the early hours after infection (likely produced by innate cells in the environment) or a few days after infection (thus likely produced by antigen-specific $CD4^{+}$ or $CD8^{+}$ T

cells). In the first case scenario, this would mean that the equilibrium between humoral and cellular responses could be determined already at the CD4⁺ T cell priming phase. To dissect at which time point IFN- γ important for CD4⁺ T cell polarization is produced, we blocked IFN- γ either at day 0 or at day 3 post infection. Administration of the blocking antibodies against IFN- γ on day 3 after LCMV infection did not affect the differentiation of SMARTA CD4⁺ T cells in comparison to untreated controls (**Figure 33A-B**) indicating that only IFN- γ sensing within the first 3 days after infection was essential for the shaping of CD4⁺ T cell polarization.

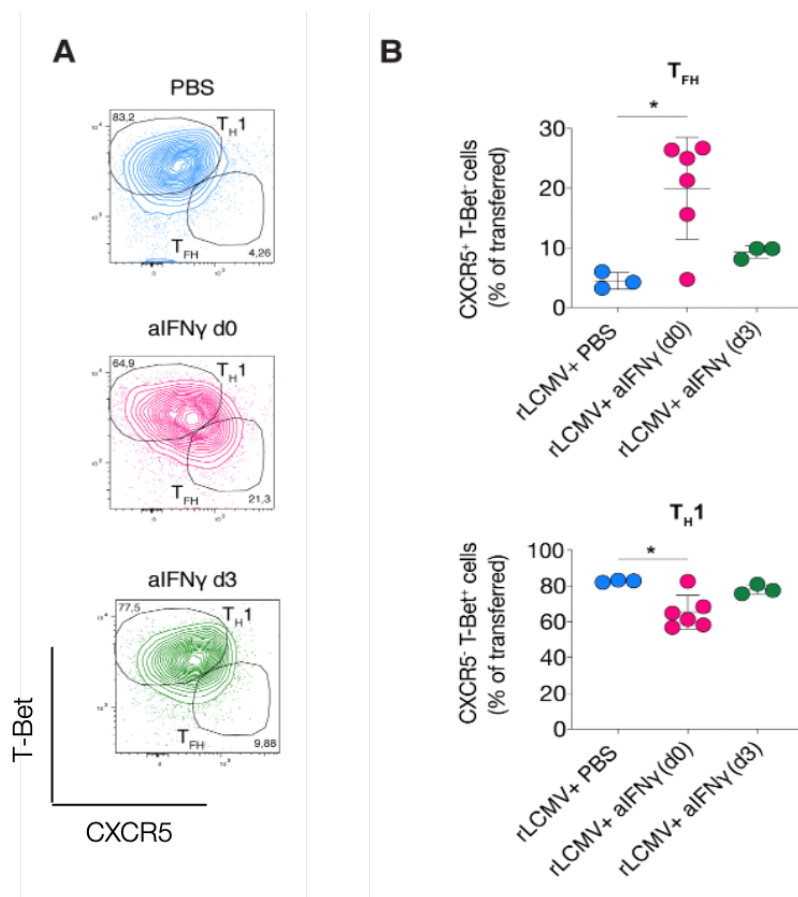


Figure 33. The early sensing of IFN- γ influences CD4⁺ T cell polarization upon LCMV infection

*1*10⁶ purified CD45.1⁺ SMARTA CD4⁺ T cells were transferred into CD45.2⁺ WT recipients 1 day before s.c. intrafootpad rLCMV infection (2*10⁵ F.F.U). CD45.2⁺ WT recipient mice were also treated with anti-IFN γ blocking antibody (or PBS) at d0 or d3 after infection. pLNs were analyzed 5 days post infection.*

(A) Representative flow cytometry plot showing T_H1 (T-bet⁺CXCR5⁻) and T_{FH} (T-bet⁻CXCR5⁺) among SMARTA antigen-specific CD4⁺ T cells in dLNs. Numbers represent the percentage of cells within the indicated gate.

(B) Quantification of T_{H1} and T_{FH} , expressed as percentages of antigen-specific $CD4^+$ T cells out of total transferred cells, in dLNs of mice described above. PBS, aIFN γ d3 n=3; aIFN γ d0 n=6. Mean \pm s.e.m. is shown. One-way ANOVA with Bonferroni's post test was applied: * $P < 0.05$,

We next checked if the IFN- γ blockade could influence $CD4^+$ T cell responses by changing the cellular composition of the LNs early upon infection. To this end, we first investigated if IFN- γ could indirectly act on the abundance of the early interaction partners of $CD4^+$ T cells, such as DCs, monocytes and neutrophils. To address this point, we infected WT mice subcutaneously and we checked neutrophils, inflammatory monocytes, cDC1 and cDC2 expansion 2 days upon infection. IFN- γ blockade did not alter the cellular composition of the LNs (**Figure 34A-F**), indicating that the effect on $CD4^+$ T cell differentiation could be ascribed more to a change in the phenotype of the early interaction partners of $CD4^+$ T cells rather than to a change in their frequencies.

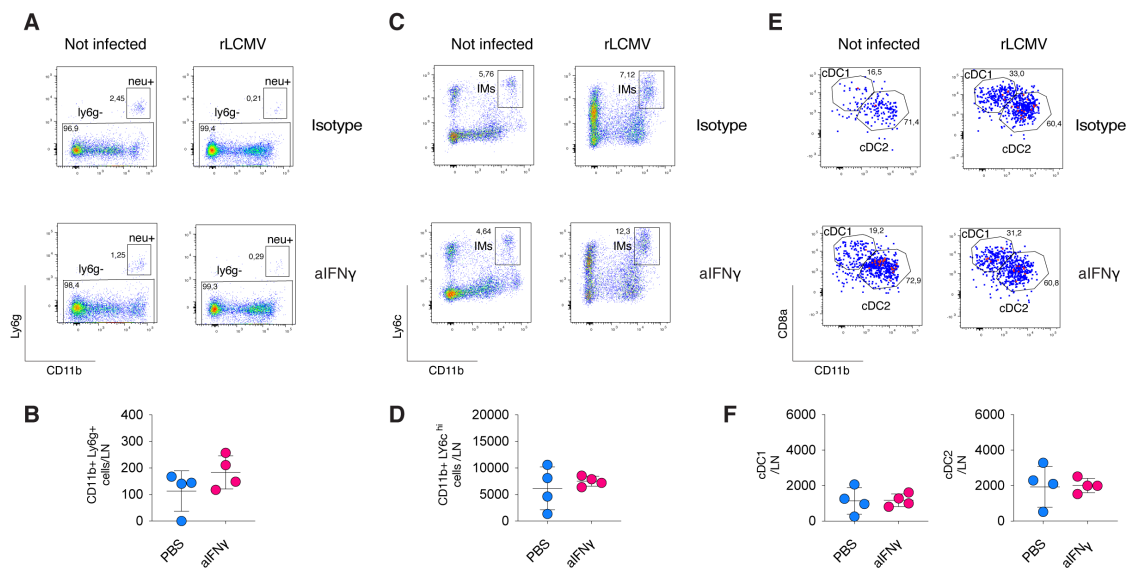


Figure 34. IFN- γ blockade does not affect the expansion of neutrophils, inflammatory monocytes or cDCs

$CD45.2^+$ WT mice were infected s.c. intrafootpad with rLCMV (2×10^5 F.F.U) and treated with anti-IFN γ blocking antibody (or isotype control) at day 0. pLNs were analyzed 2 days post infection.

(A) Representative flow cytometry plots showing the frequencies of neutrophils ($CD11b^+$ $Ly6g^+$) gated on $B220^- CD3^-$ cells in dLNs. Numbers represent the percentage of cells within the indicated gate.

(B) Quantification of neutrophils ($CD11b^+$ $Ly6g^+$) absolute numbers, in dLNs of mice described in (A). n=4. Mean \pm s.e.m is shown.

(C) Representative flow cytometry plots showing the frequencies of inflammatory monocytes (IMs) ($CD11b^+ Ly6c^{hi}$) gated on $B220^- CD3^- Ly6g^-$ cells in dLNs of mice described above. Numbers represent the percentage of cells within the indicated gate.

(D) Quantification of inflammatory monocytes (IMs) ($CD11b^+ Ly6c^{hi}$) absolute numbers, in dLNs of mice described above. $n=4$. Mean \pm s.e.m is shown.

(E) Representative flow cytometry plots showing the frequencies of cDC1 ($CD8a^+ CD11b^-$) and cDC2 ($CD8a^- CD11b^+$) gated on $B220^- CD3^- Ly6g^- NK1.1^-$ cells in dLNs of mice described above. Numbers represent the percentage of cells within the indicated gate.

(F) Quantification of cDC1 ($CD8a^+ CD11b^-$) and cDC2 ($CD8a^- CD11b^+$) absolute numbers, in dLNs of mice described above.. $n=4$. Mean \pm s.e.m is shown.

To understand which cells in the draining LNs express IFN- γ early upon LCMV infection, we took advantage of the IFN- γ -(Yellow Fluorescent Protein) YFP mouse reporter model, which faithfully reports endogenous IFN- γ expression in all major immune cell subsets (Reinhardt *et al*, 2009). In this model, all cells activating the transcription of *Ifng* will also start to express YFP and thus can be detected by flow cytometry or fluorescence microscopy. In a first set of experiments, IFN- γ -YFP mice were infected s.c. with rLCMV and dLNs were analyzed by flow cytometry 1- and 2-days post infection to test the early producers of IFN- γ . The gating strategy performed to define YFP $^+$ cells took into account only the SSC $^{int/hi}$ cells, to avoid the YFP background signal coming from SSC lo cells present also in not infected mice. We noticed that, although the YFP signal was not very strong and defined, the frequency of YFP $^+$ cells increased over time, reaching about 0.24% of all LN cells by day 2 post infection (**Figure 35A**). Among all YFP $^+$ cells, the main producers of IFN- γ were NK1.1 $^+$ Group 1 ILCs (that include NK cells) (**Figure 35B**). These data were further confirmed by confocal microscopy analysis, which revealed many NK1.1 $^+$ cells co-expressing YFP 2 days after LCMV infection (**Figure 36B**). Moreover, to understand which IFN- γ -producer cells interact with antigen-specific CD4 $^+$ T cells, in this experiment we had adoptively transferred SMARTA CD4 $^+$ T cell fluorescently labelled with CMTMR prior to s.c. infection with rLCMV. In contrast to the non-infected LNs where SMARTA CD4 $^+$ T cells do not undergo clonal expansion and IFN- γ signal seems almost undetectable and not specific, on day 2 post infection CD4 $^+$ T cells expand and localize into T cell zone (**Figure 36A**). However, in the sections analyzed till now we could not detect any substantial interactions between Group I ILCs and SMARTA CD4 $^+$ T cells.

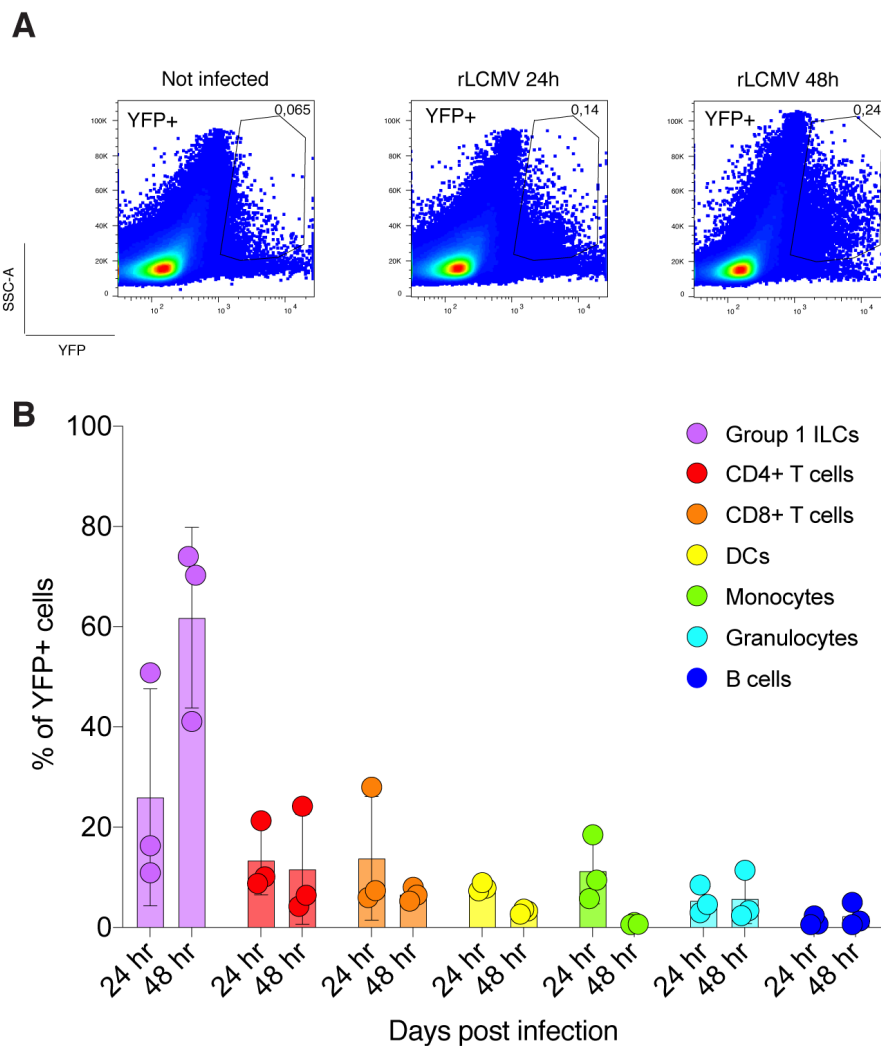


Figure 35. IFN- γ producers upon rLCMV infection

(A) Representative flow cytometry plots showing YFP⁺ cells (IFN- γ ⁺ cells) in the dLNs of IFN- γ - YFP recipient mice 24 and 48 h d after intrafootpad infection with rLCMV (2×10^5 F.F.U). Numbers represent the percentage of cells within the indicated gate.

(B) Frequencies of Group 1 ILCs, CD4⁺, CD8⁺, DCs, monocytes, granulocytes and B cells expressed as percentages out of the total YFP⁺ cells in the dLNs at 24h and 48h upon rLCMV infection. $n = 3$. Mean \pm s.e.m. is shown.

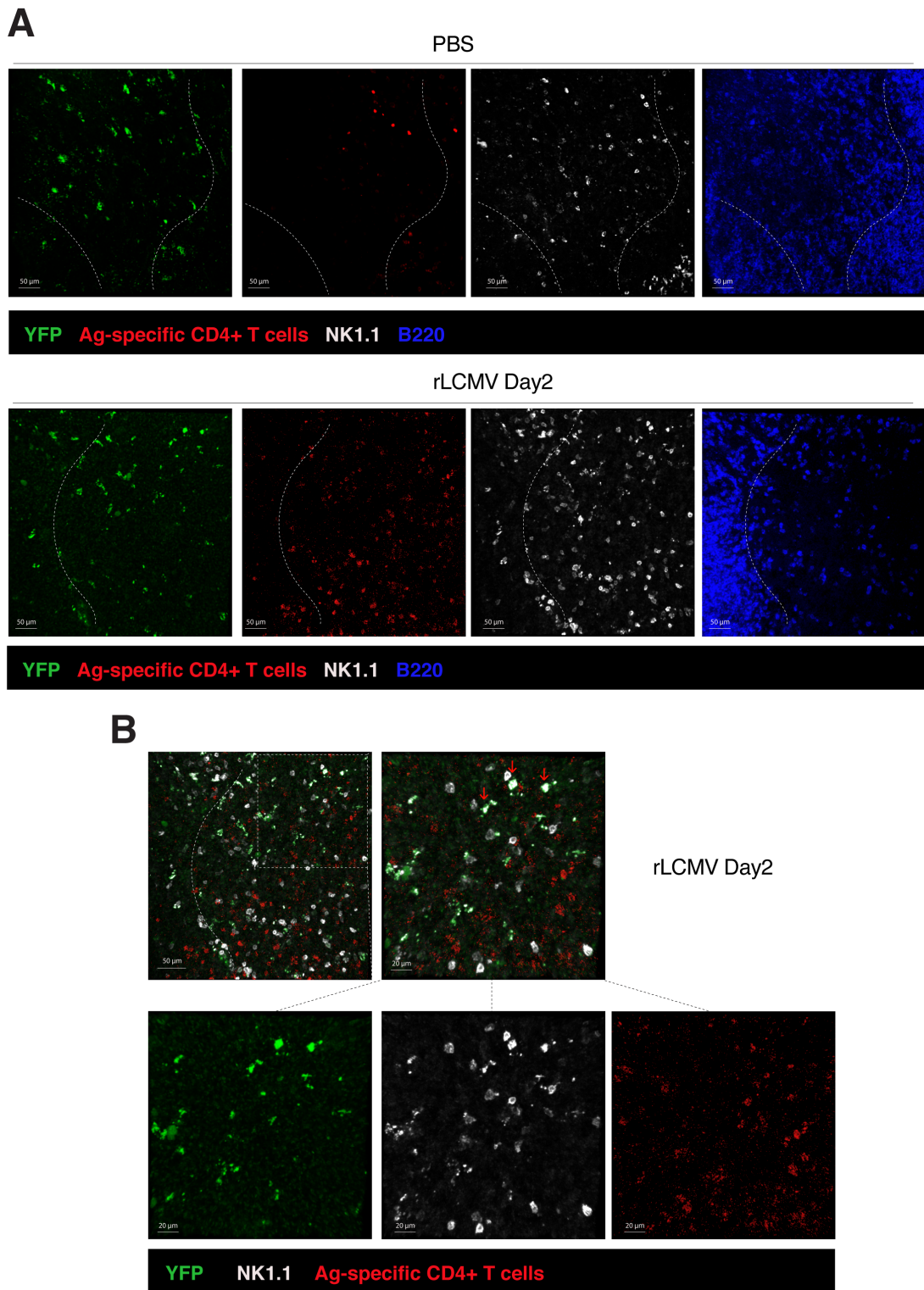


Figure 36. IFN- γ expression by Group I ILCs in dLNs upon LCMV infection

Confocal micrographs in the popliteal LNs of IFN- γ -YFP mice injected with 1×10^6 purified CD45.1⁺ SMARTA CD4⁺ T cells fluorescently labelled with CMTMR (red), 48h post rLCMV (2×10^5 F.F.U) infection. IFN- γ -producing cells are depicted in green (YFP), Group I ILCs in white (NK1.1), and B cells in blue (B220). Data are representative of two independent experiments. Scale bars represent 50 μ m (A) or 20 μ m (B). (B) is a magnification of the same section shown in (A). YFP⁺ NK1.1⁺ cells are indicated by red arrows.

8.4.3 Group I ILCs-derived IFN- γ does not influence CD4⁺ T cell differentiation upon LCMV infection

We then proceeded to some functional experiments aimed at understanding if Group I ILCs could be responsible for supporting T_H1 differentiation and suppressing T_{FH} development. To investigate whether, upon LCMV infection, IFN- γ produced by Group I ILCs is instrumental for CD4⁺ T cell polarization, WT mice were adoptively transferred with SMARTA CD4⁺ T cells 24 hours before s.c. rLCMV infection and treated with neutralizing antibodies towards either IFN- γ or NK1.1 or with the combination of both. On day 5 post infection SMARTA CD4⁺ T cell polarization was assessed in the dLNs. In line with previous results, treatment with IFN- γ neutralizing antibody led to a shift towards the T_{FH} cell subset. Surprisingly, treatment with anti-NK1.1 antibody alone, did not significantly impact polarization of T helper cell subsets. On the contrary, the polarization of CD4⁺ T cells in the group of mice treated with the combination of the two antibodies mirrored the one observed with anti-IFN- γ alone (**Figure 37A-B**). Together these results suggest that Group I ILCs derived IFN- γ is not involved in CD4⁺ T cell polarization, at least in this infection setting.

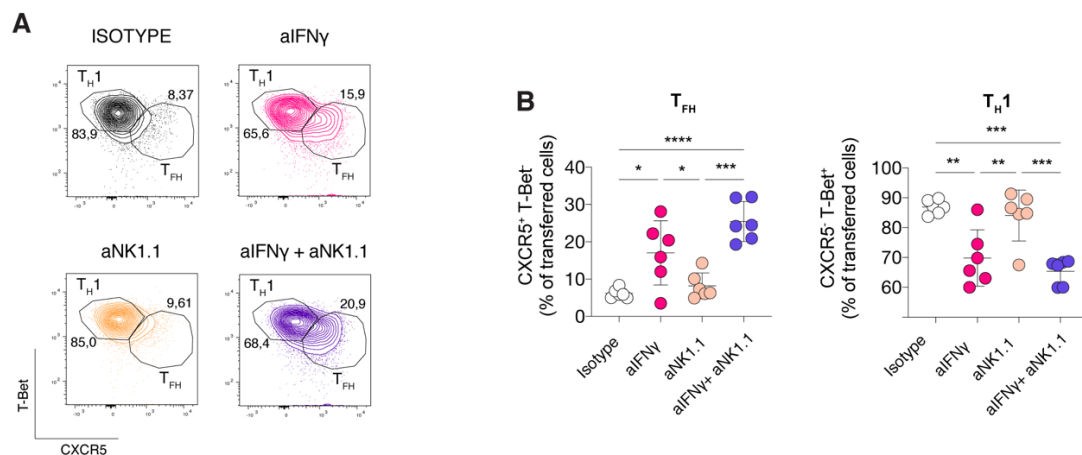


Figure 37. Group I ILCs-derived IFN- γ does not influence CD4⁺ T cell polarization upon LCMV infection

*1*10⁶ purified CD45.1⁺ SMARTA CD4⁺ T cells were transferred into CD45.2⁺ WT recipients 1 day before s.c. rLCMV infection (2*10⁵ F.F.U). In some conditions CD45.2⁺ WT recipient mice were also treated with anti-IFN- γ (d0), anti-NK1.1 (d-1, d0) blocking antibodies (or isotype control) alone or in combination. dLNs were analyzed 5 days post infection.*

(A) Representative flow cytometry plots showing T_{H1} ($T\text{-bet}^+CXCR5^-$) and T_{FH} ($T\text{-bet}^-CXCR5^+$) cells among SMARTA antigen-specific $CD4^+$ T cells, in the dLNs. Numbers represent the percentage of cells within the indicated gate.

*(B) Quantification of T_{H1} (right) and T_{FH} (left), expressed as percentages of antigen-specific $CD4^+$ T cells out of total transferred cells, in dLNs of mice described above. $n=6$. Mean \pm s.e.m is shown. Data from two independent experiments were pooled. One-way ANOVA with Bonferroni's post test was applied: * $P < 0.05$, ** $P < 0.01$, *** $P < 0.001$, **** $P < 0.0001$.*

8.4.4 Confocal analysis identifies DCs as early producers of IFN- γ upon LCMV infection

The finding that Group 1 ILCs-derived IFN- γ is dispensable for T_{H1} differentiation prompted us to analyze other possible relevant cellular sources for this cytokine. Among the other cell types analyzed 1 and 2 days after LCMV infection, low amounts of IFN- γ were produced also by $CD4$ and $CD8$ T cells, monocytes, granulocytes and DCs (**Figure 35B**). Of note, the number of DCs obtained after LN processing is usually suboptimal, so we reasoned that we might have underestimated the contribution of DCs using this technical approach. Given the key role of DCs in naïve T cell priming, we decided to investigate whether DCs can produce IFN- γ by taking advantage of confocal microscopy.

Confocal analysis was performed at day 2 post infection, a time-point which has been previously shown by us and others as optimal for analysis of $CD4^+$ T cell priming (De Giovanni et al, 2020). Interestingly, we found a substantial amount of $CD11c^+ YFP^+$ cells in the T cell area of the dLNs (**Figure 38A**), suggesting that the early IFN- γ -producer cells include also some DCs, a phenomenon that can be certainly underestimated when looking at flow cytometry analysis only. Moreover, we detected some interactions between DCs and LCMV-specific $CD4^+$ T cells, although it is not clear whether these interacting DCs are the same producing IFN- γ (**Figure 38A-B**). We are currently analyzing more sections to draw a clear conclusion on this very important point.

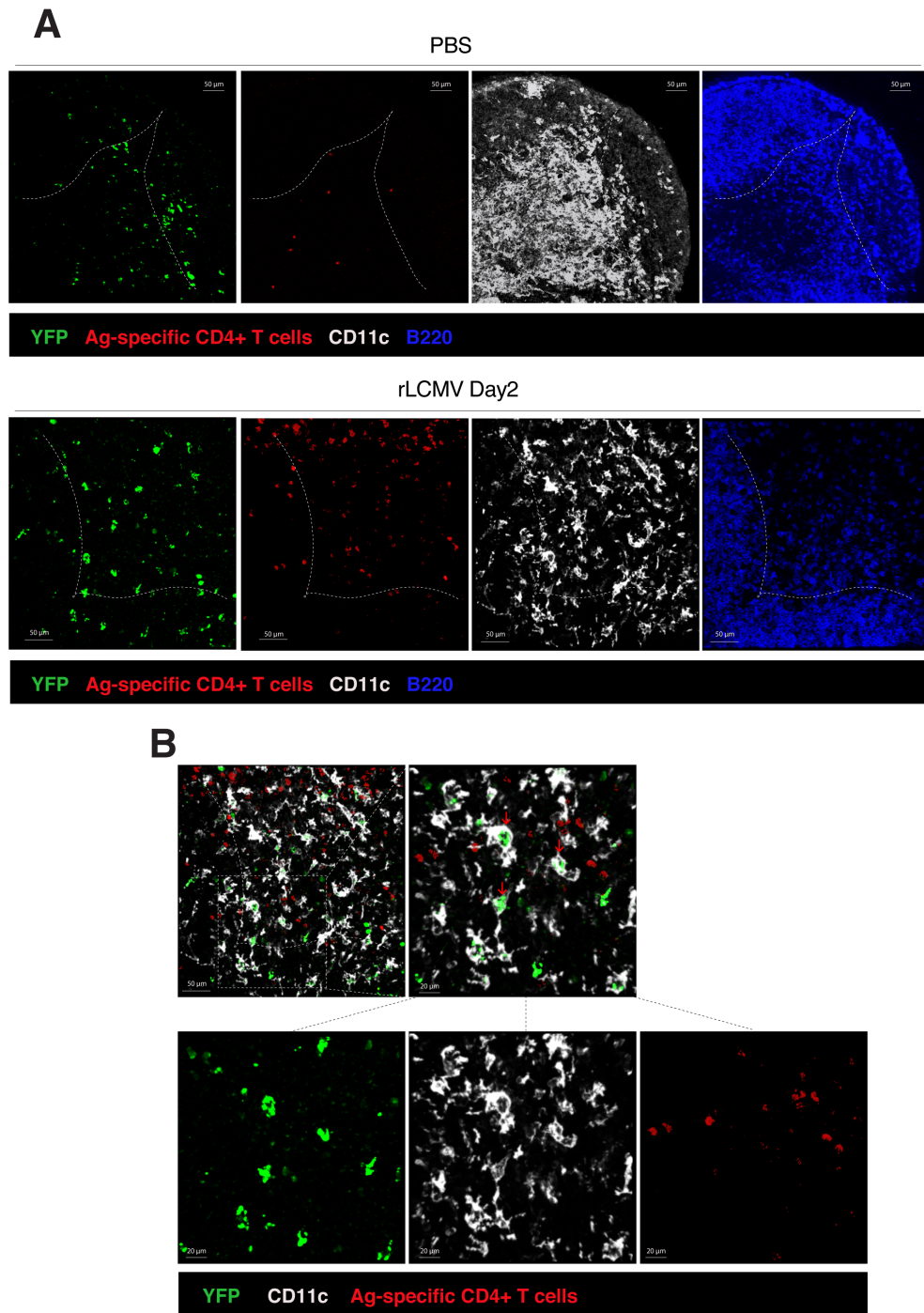


Figure 38. IFN- γ expression by DCs in dLNs upon LCMV infection.

Confocal micrographs in the popliteal LNs of IFN- γ -YFP mice injected with 1×10^6 purified CD45.1⁺ SMARTA CD4⁺ T cells fluorescently labelled with CMTMR (red), 48h post rLCMV (2×10^5 F.F.U) infection. IFN- γ -producing cells are depicted in green (YFP), DCs in white (CD11c), and B cells in blue (B220). Data are representative of two independent experiments; Scale bars represent 50 μ m (A) or 20 μ m (B). (B) is a magnification of the same section shown in (A). YFP⁺ CD11c⁺ cells are indicated by red arrows.

Since we couldn't use any cDC-depleting antibodies, experiments with BM chimeras are ongoing to determine the role of DC-derived IFN- γ . In particular, the mixed BM chimera will be reconstituted by 50% of the BM deriving from CD11c-Cre-iDTR mice and 50% of the BM deriving from IFN- γ $-/-$ mice. Injection of the DT in these mice will kill only DCs derived from the CD11c-Cre-iDTR BM but not DCs derived from the IFN- γ $-/-$ BM. As a result, the only available DCs for T cell priming cannot produce IFN- γ , whereas all other cell types will. As a control, a mixed BM chimera constituted by 50% CD11c-Cre-iDTR BM and 50% WT BM will be prepared.

8.5 Dissecting a possible cross-inhibition between the T_{H1} and T_{FH} subsets

In contrast to other infections, such as influenza, where CD4⁺ T cell polarization results in the coevolution of T_{FH} and T_{H1} (Krueger *et al*, 2021), in the context of LCMV and VSV infection CD4⁺ T cell differentiation is compartmentalized, with virtually no T_{H1} found in VSV-infected mice and very few T_{FH} found in LCMV-infected mice. One explanation for this phenotype might be that besides initial polarization cues, early T_{H1} and T_{FH} subsets might compete or cross-antagonize each other. The CD4⁺ T cell phenotype that we observe in the absence of IFN- γ with a decreased T_{H1} differentiation coupled to an increase T_{FH} development may support this hypothesis and prompted us to investigate the possible molecular mechanisms whereby T_{FH} are inhibited by this T_{H1}-related cytokine.

8.5.1 IFN- γ does not affect expression of T_{FH} polarizing cytokines

One possible hypothesis on the mechanism through which IFN- γ could hinder T_{FH} development could be by antagonizing the expression of T_{FH}-polarizing cytokines. We previously observed that, upon VSV infection, the early wave of type I IFNs sensed by DCs is crucial in promoting IL-6 production that is instrumental for T_{FH} development. On the contrary, in the context of LCMV infection the induction of type I IFNs is delayed and, even if still sensed by DCs, it results in the absence of early IL-6 production. Thus, we asked whether IFN- γ might counteract type I IFNs or IL-6 expression and thus inhibit T_{FH} development through this mechanism. To test this hypothesis, we performed a kinetic analysis of *Ifna4*, *Ifnb1* and *Il6* expression in LNs from wild-type mice infected with rLCMV and treated with IFN- γ -blocking antibodies or PBS, to measure the expression

level of this cytokine at different time-points. Popliteal LNs were collected and analyzed at 0h, 4h, 8h, 16h, 24h, and 48h post infection by qPCR. We did not observe any difference in the induction of *Il6* and type I IFNs expression at the mRNA level, indicating that the molecular inhibitory mechanism exerted by IFN- γ does not imply the suppression of type I IFNs or IL-6 expression (**Figure 39**).

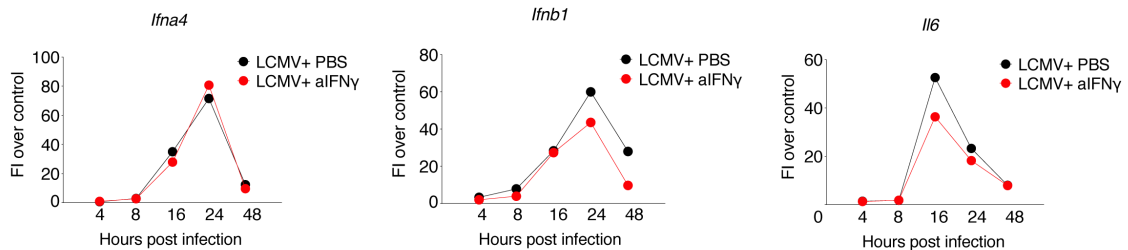


Figure 39. IFN- γ does not affect the expression of type I IFNs and IL-6.

*Analysis of *Ifna4*, *Ifnb1* and *Il6* gene expression at 0, 4, 8, 16, 24 and 48h after rLCMV infection in dLNs of mice treated with PBS (black) or with anti-IFN γ blocking antibody (red). n= 4 (0 h), 4 (4 h), 4 (8 h), 4 (16 h), 4 (24 h) and 4 (48 h). FI, fold increase.*

8.5.2 B cells as possible mediators of T_{FH} inhibition

Another mechanism whereby IFN- γ could inhibit T_{FH} might rely on B cells. Indeed, T_{FH} cell development is a multi-step differentiation process that comprises two different APCs: DCs and cognate B cells. Cognate B cells interact with pre-T_{FH} at the T-B border driving their full commitment and the initiation of GC responses (Crotty, 2011). Since B cells express the IFN γ R, they could sense IFN- γ and this cytokine could potentially shape their phenotype and their crosstalk with T helper cells. Different studies have shown that IFN- γ can induce T-bet in a subset of so-called atypical B cells, which play dichotomous roles in immunity, including being pathogenic in autoimmune settings (Obeng-Adjei *et al*, 2017); (Rubtsova *et al*, 2017), but its role in the context of LCMV infection has never been studied.

To investigate this hypothesis, we first tested the role of IFN- γ in B cell activation upon LCMV infection. WT mice were treated with IFN- γ nAbs (or isotype control) and infected with rLCMV. pLNs were collected at day 7 upon infection, and endogenous B cells analyzed for T-bet and Bcl-6 expression. We found that 16-20% of B cells in rLCMV-infected mice express high levels of T-bet whereas very few of them (about 1%)

express low levels of T-bet and high levels of Bcl-6. By contrast, blockade of IFN- γ antibody treatment resulted in an increase in the frequency of Bcl-6⁺ B cells and a decrease in the T-bet⁺ B cells (**Figure 40A-B**). In agreement with this observation, total GP-binding IgG antibodies were found at higher levels in absence of IFN- γ (**Figure 40C**). Thus, IFN- γ does not influence only CD4⁺ T cell polarization but also the B cell phenotype, restraining on one side the development of Bcl-6⁺ B cells, widely defined as GC-B cells (Cattoretti *et al*, 1995) and on the other side inducing the expression of T-bet on these cells, resulting in an impairment of humoral responses. This result is line with the role of IFN- γ in inducing T_H1 differentiation and suppressing T_{FH} development, but the spatiotemporal mechanism exerted by this cytokine remains unclear. Indeed, IFN- γ could potentially suppress T_{FH} development acting directly on CD4⁺ T cells, or it could restrain GC B cell differentiation that indirectly results in the inhibition of T_{FH} development. A third hypothesis implies a broader role of IFN- γ that could inhibit at the same time T_{FH} and GC B cells differentiation, driving cellular responses at the expense of humoral responses. Future experiments will clarify the cellular targets of this cytokine. In detail, we are planning to test the role of IFN- γ receptor signaling in CD4⁺ T and B cells using CRISPR-Cas9 to delete IFN γ R1 in naïve SMARTA CD4⁺ T cells or KL25 B cells, in order to block their capacity to sense IFN- γ .

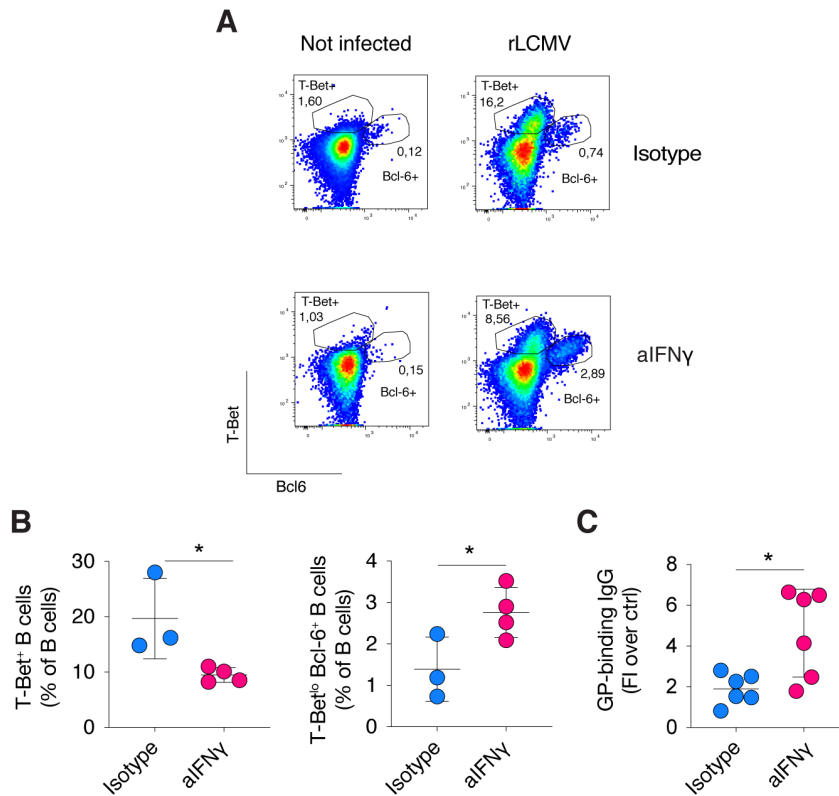


Figure 40. IFN- γ suppresses GC-B cell development and hinders humoral response upon LCMV infection.

(A) CD45.2⁺ WT mice were infected s.c. intrafootpad with rLCMV (2×10^5 F.F.U) and treated with anti-IFN- γ blocking antibody (or isotype control) at day 0. pLNs were analyzed 7 days post infection.

Representative flow cytometry plots showing T-bet⁺ Bcl-6⁻ and Bcl-6⁺ T-bet^{lo} B cells expressed as percentages among total B cells, in the dLNs. Numbers represent the percentage of cells within the indicated gate.

(B) Quantification of T-bet⁺ B cells (left) and Bcl-6⁺ T-bet^{lo} B cells (left) expressed as percentages of total B cells in dLNs of mice described in (A). Isotype n=3; a-IFN γ n=4. Mean \pm s.e.m. is shown. Data are representative of at least three independent experiments. An unpaired two-tailed t test was applied: *P < 0.05

(C) GP-binding IgG Abs were measured in the sera of mice described in (A) and expressed as fold induction over uninfected controls. Data are representative of three independent experiments. n=6 Mean \pm s.e.m. is shown. An unpaired two-tailed t test was applied: *P < 0.05

8.5.3 IL-6 blocks IFN- γ -mediated induction of T_H1 polarization upon VSV infection

We further asked whether IFN- γ might play a role in CD4⁺ T cell polarization in other infection contexts. Kinetic analysis of the best known T_H1-polarizing cytokines, such as *Ifna4*, *Ifnb*, *Il12b* and *IFN γ* in total RNA isolated from LNs at 4, 8, 16, 24 and 48 h after infection with rVSV or rLCMV indicated that the T_H1 milieu is triggered also upon rVSV

infection (**Figure 41**). In particular, IFN γ expression was even higher in VSV in respect to LCMV infection.

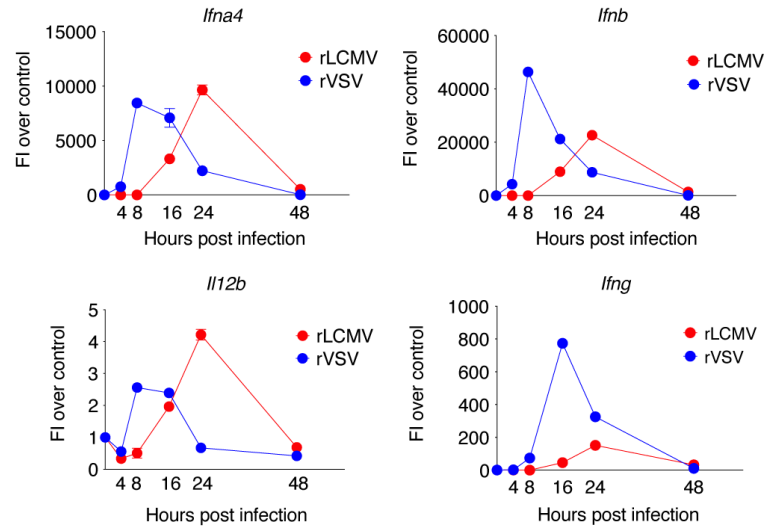


Figure 41. T_H1 polarizing cytokines expression is induced upon rVSV infection

Analysis of Ifna4, Ifnb, Il12b and Ifng gene expression in dLNs at 0, 4, 8, 16, 24 and 48h after rLCMV (red) or rVSV (blue) infection. n= 4 (0 h), 4 (4 h), 4 (8 h), 4 (16 h), 4 (24 h) and 4 (48 h). Data were pooled from two independent experiments. The mean \pm s.e.m. is shown. The same sample was measured repeatedly for the four genes. FI, fold increase.

However, this early wave of T_H1-polarizing cytokines did not result in the induction of T_H1 differentiation upon VSV infection, since the vast majority of VSV-specific CD4⁺ T cells polarize into T_{FH} cell with virtually no detectable T_H1. The only experimental condition in which T_H1 were detectable upon VSV infection was following early blockade of IL-6, as showed previously (**Figure 22B**). Therefore, we asked whether a cross-inhibition mechanism between IL-6 and IFN- γ might be taking place during viral infections, and whether the T_H1 cells that arise upon IL-6 blockade depend on IFN- γ . To address this hypothesis, WT mice were treated with neutralizing antibodies towards IL-6 and IFN- γ , alone or in combination, and infected s.c. with rVSV. As usual, adoptive transfer of SMARTA CD4⁺ T cell (which recognize rVSV since it expresses the LCMV glycoprotein) was performed 24 hours before rVSV infection and pLNs were collected and processed 5 days after infection. As expected, the majority of CD4⁺ T cells in rVSV-infected mice differentiated into T_{FH} and very few of them into T_H1. However, upon IL-6 blockade there was a decrease of T_{FH} polarization and a strong increase of T_H1 cell

differentiation, thus confirming previously published results. Blockade of IFN- γ alone showed a slight increase of T_{FH} and a decrease in T_{H1}. Finally, when both cytokines were blocked simultaneously, the T_{H1} cell polarization observed upon the IL-6 blockade was no longer induced (**Figure 42A-B**), meaning that the molecular determinant that induces T_{H1} differentiation in the absence of IL-6 is IFN- γ . Taken together, these results indicate that the T_{H1} cells that should develop upon VSV infection are IFN- γ dependent and IL-6 can inhibit T_{H1} differentiation through a mechanism that still needs to be investigated in depth, but almost certainly is related to a crosstalk with IFN- γ .

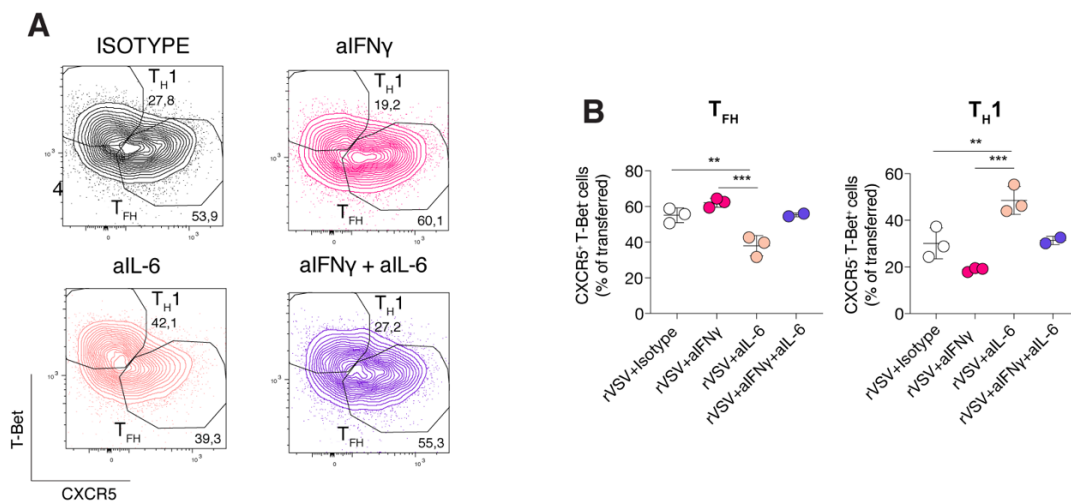


Figure 42. The early production of IL-6 upon rVSV infection antagonizes the IFN- γ mediated induction of T_{H1} polarization.

1×10^6 purified CD45.1⁺ SMARTA CD4⁺ T cells were transferred into CD45.2⁺ WT recipients 1 day before s.c. rVSV infection (2×10^5 P.F.U). In some conditions CD45.2⁺ WT recipient mice were also treated with anti-IFN γ (d0), anti-IL-6 (d-1, d0, d1, d3) blocking antibodies (or isotype control) alone or in combination. dLNs were analyzed 5 days post infection.

(A) Representative flow cytometry plots showing T_{H1} (T-bet⁺CXCR5⁻) and T_{FH} (T-bet⁺CXCR5⁺) cells among SMARTA antigen-specific CD4⁺ T cells, in the dLNs of mice described above. Numbers represent the percentage of cells within the indicated gate.

(B) Quantification of T_{H1} (right) and T_{FH} (left), expressed as percentages of antigen-specific CD4⁺ T cells out of total transferred cells, in dLNs of mice described above. Isotype, aIFN γ , aIL-6 n=3; aIFN γ +aIL-6 n=2. Mean \pm s.e.m. is shown. Data are representative of at least three independent experiments. One-way ANOVA with Bonferroni's post test was applied: *P < 0.05, **P < 0.01, ***P < 0.001.

DISCUSSION

9. DISCUSSION

Antigen-specific effector CD4⁺ T cells subsets play a critical role in shaping antiviral adaptive immune responses and might contribute to the equilibrium between humoral and cellular responses. Interestingly, data obtained in our lab show a striking compartmentalization of CD4⁺ T helper responses in VSV and LCMV infection models. In particular, subcutaneous infection with VSV results in the polarization of CD4⁺ T cells towards the T_{FH} phenotype, with almost no T_{H1} development. In contrast, LCMV infection results in almost complete T_{H1} differentiation, with little or no T_{FH} induction. This dichotomy was quite surprising, since in other infection contexts (i.e. IAV infection) T_{H1} and T_{FH} responses co-exist (Krueger *et al*, 2021). Further investigation on the factors that drive the observed compartmentalization led to the identification of the spatiotemporal regulation of type I IFNs as critical determinants of CD4⁺ T cell polarization. In particular, in the context of VSV infection, early type I IFNs sensing by migratory cDC2s and/ or moDCs leads to the production of IL-6 that in turn promotes T_{FH} differentiation and humoral responses (**Figure 43**).

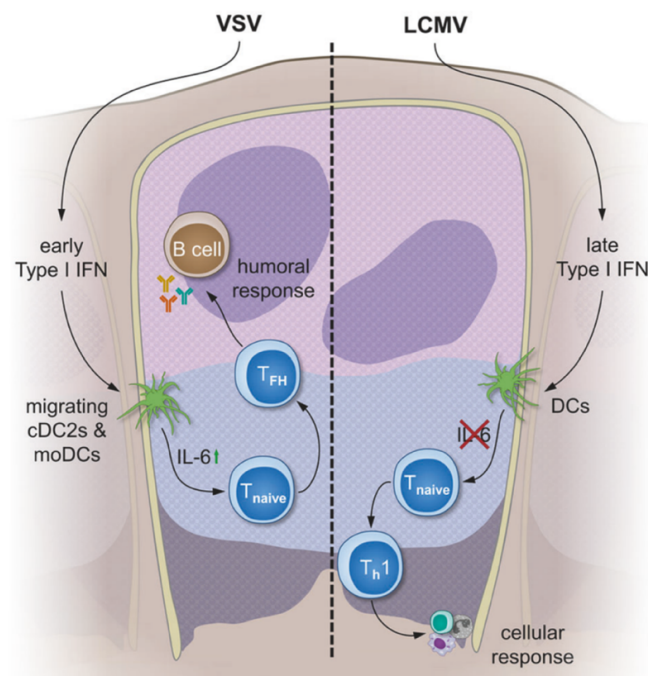


Figure 43. Spatiotemporal regulation of type I interferon expression determines the antiviral polarization of CD4⁺ T cells

(Adapted from Wedekind *et al.*, *Cellular & Molecular Immunology*, 2020. License Number_ 5252971215143)

These results offer an additional molecular mechanism that might explain why different viruses induce a wide spectrum of antibody responses. The role of type I IFNs in shaping CD4⁺ T cell differentiation is not a new concept. Several publications previously showed their involvement in T_{H1} or T_{FH} differentiation, but their role is strictly context-dependent. For example, CD4⁺ T cells cultured *in vitro* with type I IFNs start to upregulate the canonical T_{FH} markers CXCR5 and PD-1, but they are functionally impaired since they do not produce IL-21, the main T_{FH} cytokine responsible for IgG1 class switching (Nakayamada *et al*, 2014). These data suggest that other factors, such as IL-6, are necessary to drive the full commitment of T_{FH}. *In vivo*, the picture is far more complex, since it involves the interplay of many cytokines secreted in the environment and the coordinated migration and positioning of several cell types (Cucak *et al*, 2009) (Ray *et al*, 2014);(Barbet *et al*, 2018);(Ugur & Mueller, 2019) ; Together, these studies highlight a multifaceted role of type I IFNs that could be linked to the different cellular sources, expression kinetics, and cellular targets (Kuka *et al*, 2019). Our results suggest that spatial and temporal regulation of type I IFN is critical for its effect on adaptive immune responses, thus providing a potential explanation for the above-mentioned conflicting results.

The cellular source of type I IFN in the two infections remains to be elucidated. However, this question is difficult to address because of the many isoforms of type I IFN and the absence of an efficient type I IFN reporter mouse that would allow the clear identification of the cellular source of these cytokines. Whereas it was previously shown that VSV induces the production of type I IFNs by SSMs and pDCs, the relative contribution of each LN cell type to the production of type I IFNs after subcutaneous infection with LCMV is unknown.

The assessment of the composition and the transcriptional state of DC subsets upon early and late type I IFN sensing led to the conclusion that IL-6 expression by DCs drives T_{FH} cell polarization in response to early (VSV) but not to late (LCMV) type I IFN signaling. These findings are supported by previous data showing that adjuvantation with CpG-B enhances GC reactions by increasing the ability of Ag-presenting moDCs to produce IL-6 that promotes T_{FH} differentiation (Chakarov & Fazilleau, 2014). Like for type I IFNs, blockade of early IL-6 (which is also an ISG) results in reduced generation of T_{FH} cells. However, it is important to point out that IFNAR blockade has a larger

impact on T_{FH} cell differentiation than IL-6 blockade, suggesting that IL-6 induction by type I IFNs is only one of the mechanisms whereby type I IFN drives T_{FH} differentiation upon VSV infection. Indeed, other T_{FH} polarizing cytokines, such as IL-27, could promote T_{FH} differentiation in synergy with the IL-6 (Batten *et al*, 2010). In addition, even though the results reported here unravel DCs as key producers of IL-6 that promotes T_{FH} differentiation, the role of IL-6 produced by other cellular sources remains to be elucidated. A possible caveat that must be taken into consideration is that we analyzed the DC composition of the entire LN, rather than from the $CD4^+$ T cell priming niche, thus potentially underestimating the localized production of IL-6 by DCs.

Lack of early type I IFN and IL-6 sensing does explain the impaired T_{FH} differentiation in the context of LCMV infection, but the mechanisms leading to the extreme T_{H1} differentiation remain unclear. Interestingly, we identified that LCMV-specific T_{H1} cells are IL-12 and type I IFNs independent. Instead, we identified IFN- γ as an important determinant for $CD4^+$ T cell differentiation, partially driving T_{H1} differentiation and suppressing T_{FH} , $Bcl-6^+$ GC-B cells and antibody responses (**Figure 44**).

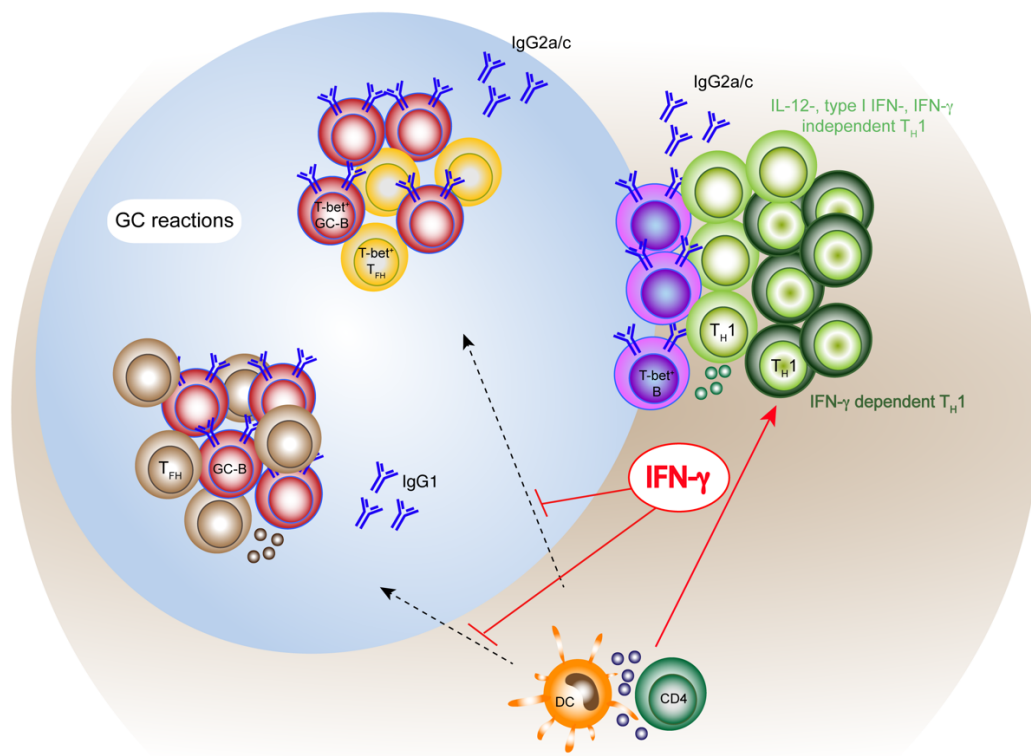


Figure 44. Graphical Abstract showing the role of IFN- γ in shaping $CD4^+$ T cell responses.

The role of IFN- γ in T_{H1} cell polarization is not a completely new concept. Indeed, IFN- γ can act both as an effector cytokine and as an autocrine T_{H1} differentiation signal (Zhang *et al*, 2001a);(Schroder *et al*, 2004);. Previous work has shown that IFN- γ can either cooperate with IL-12 in inducing T-bet upregulation in naïve CD4⁺ T cells or can stabilize an already established T_{H1} phenotype (Lighvani *et al*, 2001);(Schulz *et al*, 2009). Moreover, IFN- γ R^{-/-}CD4⁺ T cells lose the capacity to develop into effector T_{H1} cells, indicating that IFN- γ exerts a crucial role in the differentiation of CD4⁺ T cells (Diehl *et al*, 2000). Despite this important evidence, the role of IFN- γ in T helper cell differentiation remains controversial. Indeed, it has been shown in the setting of autoimmune disease that excess of IFN- γ leads to pathogenic accumulation of T_{FH} and GCs, suggesting that IFN- γ might promote also T_{FH} polarization (Lee *et al*, 2012).

Despite acting as a molecular switch between T_{H1} and T_{FH}, IFN- γ blockade did not affect the entire T_{H1} population. This observation brings in mind two important points. The first one is that the T-bet expressing cells remaining after the IFN- γ blockade are IL-12-, type I IFN- and IFN- γ - independent. Despite the numerous studies reporting IL-12 as the main T_{H1}-polarizing cytokine in different contexts, our data clearly highlight that upon LCMV infection T_{H1} cells arise independently of IL-12. These results are supported by other studies that confirm the hypothesis that T_{H1} cells generated during viral infections are not dependent on IL-12 for their development. The possible explanation for this IL-12-independent T_{H1} formation remains elusive and might potentially be related to redundant mechanisms arising in the absence of high levels of IL-12. This opens an important question on which might be the key T_{H1} polarizing cytokines upon viral infections.

The second point is that a certain degree of heterogeneity might occur within the T_{H1} cells developing upon the same viral infection. The heterogeneity within the T helper subsets is not a new concept. Indeed, T_{FH} cells arising in the context of different infections are quite different and their phenotype is shaped in a pathogen-dependent manner (Kuka & Iannacone, 2021);(Tuzlak *et al*, 2021). For example, T_{FH} generated upon IAV infection express low levels of T-bet; by contrast, T_{FH} generated upon systemic LCMV infection express high levels of T-bet at their peak of expansion and differentiation (Sheikh *et al*, 2019). The same concept could be applied for T_{H1} cells, whose development is IL-12 dependent in the context of bacterial infection, but not for viral infections (Athie-Morales

et al, 2004);(Heufler *et al*, 1996). Moreover, Krueger *et al*. recently showed that there are two types of T_{H1} and only the T_{H1} that develop upon Salmonella infection, but not upon Influenza infection, need IL-12 for their full commitment (Krueger *et al*, 2021).

ScRNAseq analysis performed on antiviral $CD4^+$ T cells revealed that there can be heterogeneity even within the same infection contexts, like LCMV, that induces the differentiation of two T-bet-expressing subsets: $TCF-1^+$ and $TCF-1^-$ populations. The $TCF-1^-$ population retains some cytotoxic characteristics since it expresses a high amount of GzmB, however, future studies will formally test their cytotoxic ability. Interestingly, in the single-cell UMAP, the $TCF-1^+$ population clustered at the interface between LCMV and VSV samples, demonstrating that, from the transcriptional point of view, this population carries a mixed T_{H1}/T_{FH} signature, further functionally confirmed by their lower capacity to secrete IFN- γ . Future experiments will characterize the spatiotemporal dynamics of differentiation of these $TCF-1^+$ and $TCF-1^-$ $GzmB^+ CD4^+$ T cells in more detail. In particular, we will perform a time-course analysis to define the temporal development of these two populations upon LCMV infection.

This observation prompted us to consider the hypothesis that T-bet induction in the context of LCMV infection is a feature of the virus since it is present on all the $CD4^+$ T cells that develop upon infection. However, the $TCF-1^+ T-bet^+ CD4^+$ T cell population could be a more plastic population that adapts its phenotype to the inflammatory milieu to which it is exposed to optimize the antiviral response. This hypothesis was partially corroborated by the role of IFN- γ on these two populations that arise upon LCMV infection. Flow cytometric analysis hinted towards IFN- γ acting on the $TCF-1^+$ population, preventing its differentiation towards fully committed $CXCR5^+ PD-1^+ T_{FH}$. Our results strongly suggest that IFN- γ could act as a molecular switch on this intermediate $TCF-1^+$ population. This $TCF-1^+$ population resembles the recently described T progenitor exhausted (TPEX) population observed for $CD8^+$ T cells, which retains some stem-like properties, it expresses high levels of TCF-1 and it is critical for enhanced antiviral immunity (Utzschneider *et al*, 2016). Since we observed that the $TCF-1^+$ population upregulates the T_{FH} markers CXCR5 and PD-1 in absence of IFN- γ , we will also check if it will develop entirely into fully differentiated T_{FH} at late time points post-infection (day 7-10). RNA velocity analysis and selective adoptive transfer experiments will be performed to further confirm that the T_{FH} that develop in absence of IFN- γ arise

from the TCF-1⁺ population that changes its phenotype. In addition, we will perform a confocal analysis to define if these two populations of effector CD4⁺ T cells occupy distinct LN niches and to further confirm that the CXCR5⁺ population that arises in absence of IFN- γ localizes inside B cell follicles.

Our study raises the question of which could be the relevant IFN- γ producers upon LCMV infection. We show that the IFN- γ produced by Ag-specific CD4⁺ T cells is sufficient, but not necessary to drive their differentiation in a positive feedback loop. This result was further corroborated by data showing that the late blocking of IFN- γ at day 3 post-infection did not result in any change of the phenotype of CD4⁺ T cells, ruling out a potential role of the late IFN- γ producers (mainly CD4⁺ T cells and CD8⁺ T cells) in inducing the phenotype that we observe. Focusing our attention on the early IFN- γ producers upon LCMV infection, we identified Group I ILCs as the major IFN- γ producers upon LCMV infection. Surprisingly, the high amount of IFN- γ produced by Group I ILCs was not the one responsible for CD4⁺ T cell polarization. This result is in contrast with previously published data that showed a role of NK-derived IFN- γ in inducing T_H1 differentiation. However, these different outcomes could be ascribed to the different contexts, since in the published study mice were immunized with OVA-pulsed DCs (Martín-Fontecha *et al*, 2004). Interestingly, we also identified DCs as early IFN- γ producers upon LCMV infection, but their role in shaping CD4⁺ T cell differentiation still needs further investigation. It is worth pointing out that there could be more than one cellular source of this cytokine and given this redundancy of the system, it will be a difficult question to address.

Even though we have highlighted this important role of IFN- γ in shaping CD4⁺ T cells responses, the cellular target of this cytokine remains unclear. Indeed, IFN- γ could potentially suppress T_{FH} development leading as a consequence to an impaired GC B cell differentiation, otherwise, it could directly act in restraining GC B cell differentiation that in turn results in the inhibition of T_{FH} development. A third hypothesis implies a broader role of IFN- γ that could inhibit at the same time T_{FH} and GC B cell differentiation, driving cellular responses at the expense of humoral responses. Future experiments are needed to clarify the cellular targets of this cytokine.

Our preliminary data suggest that IFN- γ is responsible for the polarization of T_H1 cells also in VSV-infected mice. In this setting, T_H1 cells are detectable only upon the

conditions of type I IFN and IL-6 blockade (which lead to decreased T_{FH} polarization). This could imply the existence of a possible cross-antagonism between T_{H1} and T_{FH} subsets, in this case mediated by IL-6 at the expense of IFN- γ . In line with this hypothesis, Diehl et al., have shown that IL-6 inhibits T_{H1} differentiation interfering with the IFN- γ -R signaling pathway and gene expression during differentiation of naïve CD4⁺ T cells, by reducing IFN- γ gene expression. Specifically, the molecular mechanism relies on the activation of STAT3 in response to IL-6 signaling during the activation of naïve CD4⁺ T cells, which leads to upregulation of SOCS1 gene expression that inhibits STAT1 phosphorylation thus preventing its positive autoregulation of IFN- γ gene expression. Data from this study also showed that SOCS1-deficient mice produced more IFN- γ , indicating that IFN- γ signaling upregulates its own expression and that IL-6 interferes with IFN- γ production through this mechanism (Diehl *et al*, 2000). Future studies will determine if this mechanism of action occurs also upon VSV infection.

MATERIALS AND METHODS

10. MATERIALS AND METHODS

Sections of Material and Methods (10.11, 10.12, 10.13) have been published in the paper: “De Giovanni M, Cutillo V, Giladi A, et al. Spatiotemporal regulation of type I interferon expression determines the antiviral polarization of CD4⁺ T cells. *Nat Immunol.* 2020;21(3):321-330”.

10.1. Mice

C57BL/6 and C57BL/6-Ly5.1 (CD45.1) (inbred C57BL/6) mice were purchased from Charles River. Mice bearing LCMV-specific transgenic CD4⁺ T cells (SMARTA), mice bearing VSV-specific transgenic CD4⁺ T cells (Tg7) and mice lacking the IFNAR1 receptor (*Ifnar1*^{-/-}) were obtained through the Swiss Immunological Mouse Repository (SwImMR). *Cd11c*-Cre and *Ifnar1*^{fl/fl} mice have been described previously (Yamazaki *et al*, 2013); (Prigge *et al*, 2015). 129S4(B6)-Ifn γ tm3-1Lky/J (IFN γ -YFP) mice were purchased from The Jackson Laboratory; these mice express the bicistronic IFN γ -IRES-eYFP mRNA under control of the endogenous IFN γ promoter/enhancer regions (Reinhardt *et al*, 2009).

Mice were housed under specific pathogen-free conditions and used at 8-10 weeks of age, unless otherwise indicated. In all experiments mice were matched for age and sex before experimental manipulation. All experimental animal procedures were approved by the Institutional Animal Committee of the San Raffaele Scientific Institute and by Italian Ministry of Health.

10.2. Bone marrow transplantation

WT recipient mice were lethally irradiated (one dose of 900 rad), and were supplied with antibiotic-supplemented water. Tibia and femur bones from donor mice were collected and bone marrow (BM) cells were isolated using HBSS and syringes: 10⁷ cells were resuspended in 200 μ l and injected i.v. into each recipient mice. BM chimeras were used for experiments 2 months after transplantation. In experiments described in Section 8.2 BM chimeras were generated by lethally-irradiation of WT mice (background C57BL/6N

CD45.2) that were reconstituted for at least 6/8 weeks with BM from CD45.1 *Cd11c*-Cre x *Ifnar1^{fl/fl}* mice.

In experiments described in Section 8.4.4 BM chimeras were generated by lethally-irradiation of WT mice (background C57BL/6N CD45.1) that were reconstituted for at least 6/8 weeks with BM from *Cd11c*-Cre-iDTR and IFN- $\gamma^{-/-}$ mice.

10.3. Infections and immunizations

Mice were infected via the footpad with 1×10^5 Plaque-Forming Unit (PFU) of VSV serotype Ind or rVSV (a recombinant VSV expressing a GP derived from the LCMV WE strain and recognized by SMARTA TCR-transgenic instead of the VSV GP) or with 2×10^5 Focus-Forming Unit (FFU) of LCMV WE or rLCMV (a recombinant LCMV clone 13 expressing a GP derived from the LCMV WE strain and recognized by SMARTA TCR-transgenic instead of the LCMV C113 GP). Viruses were propagated and quantified as described in previous studies (Sammicheli et al., 2016) and were diluted in 25 μ l of HBBS before subcutaneous footpad injection. All infectious work was performed in designated Biosafety Level 2 (BSL-2) and BSL-3 workspaces in accordance with institutional guidelines.

10.4. T cell isolation and adoptive transfer

Naïve CD4⁺ T cells from the spleens of SMARTA CD45.1⁺ transgenic mice were negatively selected by magnetic isolation (Miltenyi Biotec), with purity always above 98% as determined by flow cytometry. Unless otherwise indicated, 1×10^6 SMARTA T cells were injected intravenously into indicated recipients 1d before intrafootpad infection. In experiment described in Section 8.5, 10^6 LCMV-specific SMARTA CD4⁺ T cells were labelled with 5 μ M CMTMR before adoptive transfer.

10.5 Cell labelling

In experiment described in Section 8.5, cells were labelled using CMTMR (Thermo Fisher Scientific, #C34571) according to the manufacturer's instructions. In brief, SMARTA CD4⁺ T cells were washed with PBS and resuspended at 10^6 cells/mL in working dye solution (5 μ M in PBS) for 20 minutes at 37°C. Five volumes of cell

complete medium were then added and cell mixtures were allowed to rest for 5 minutes to remove free dyes. The labelled cells were centrifuged, resuspended in HBSS to be injected.

10.6 Ex Vivo Restimulation of SMARTA CD4+ T cells

Cell suspensions from the LNs were plated in round-bottom 96-well plates (2×10^6 cells/well) and restimulated for 4 hours with 1 mM GP61–80 peptide from LCMV (GLKGPDIYKGVYQFKSVEFD) in the presence of Brefeldin A (GolgiPlug, 1 ml/ml), in RPMI supplemented with 10% fetal bovine serum (Section 8.3.3).

10.7 Administration of antibodies and toxins

In indicated experiments, mice were treated with:

- InVivoMab α IFN γ blocking antibody (BioXcell Clone XMG1.2 #BE0055) or rat IgG1 isotype control (BioXcell Clone HRPN #BE0088): 250ug i.p. at day 0;
- InVivoMab α IL-6 blocking antibody (BioXcell Clone MP5-20F3 #BE0046) or rat IgG1 isotype control (BioXcell Clone HRPN #BE0088): 0.5mg i.p. 1 or 3 days after infection and 0.25mg every other day;
- InVivoMab α IL-12 blocking antibody (BioXcell Clone R2-9A5 #BE0233) or rat IgG2b isotype control, (BioXcell Clone LFT-2 #BE0090): 1 mg i.p. at day 0 or 3 after infection;
- InVivoMab α NK1.1 depleting antibody (BioXcell Clone PK136 #BE0036): 1mg i.p. at day 0 or 1d after infection.

To deplete DCs 500ng of diphtheria toxin (DTX, Millipore, # 322326) diluted in 200 μ l of PBS was administered intraperitoneally 1d before the infection and every other day thereafter to CD11c-CRE-iDTR/IFN γ ^{-/-} and CD11c-CRE-iDTR/WT BM chimeras, respectively.

10.8 Organ processing to obtain cell suspension

10.8.1 Peripheral Blood

Blood was collected from the retro-orbital sinus of anesthetized mice into sodium heparin-coated hematocrit capillaries. Single cell suspensions were obtained as

previously described (Iannacone et al, 2005). Briefly, cells were prepared from whole anticoagulated blood by lysis of red blood cells with ammonium chloride (ACK) lysis buffer (0.15 M NH₄Cl, 1.0 mM KHCO₃, 0.1 mM Na₂EDTA; pH 7.2). Cells were washed twice with PBS and used for further analysis.

10.8.2 Spleen

Spleen was smashed in Hanks' Balanced Salt Solution (HBSS). Aggregates and debris were removed by passing cell suspension through a 40-um cell strainer (BD Labware). After, cells were resuspended in ACK to lyse red blood cells. After washing cells were counted using trypan blue dye and used for further analysis.

10.8.3 Lymph Nodes

Popliteal lymph nodes were harvested in Hanks' Balanced Salt Solution (HBSS) and mechanically smashed in 6mm petri dish. Aggregated and debris were removed by passing cell suspension in 2x75mm tubes with 35 µm mesh nylon strainer (Corning).

10.9 Flow Cytometry

All flow cytometry staining of surface-expressed markers was performed in FACS Buffer containing PBS and 2% FBS at 4°C, while intracellular molecule staining was performed using Foxp3/Transcription Factor Staining Buffer set (eBioscience, #00-5523-00), following the manufacturer's instructions at room temperature. Anti-CD16/32 antibody (Invitrogen # 14-0161-82) was added to cell pellets prior to staining with fluorochrome-conjugated antibodies to block Fc receptors. Antibodies (Abs) used are indicated in **Table 1**. Flow cytometry analysis were performed on BD FACSCanto II or BD FACSymphony A5 and analysed with FlowJo software (Treestar). To genotype SMARTA mice blood was collected, ACK-lysed and stained for flow cytometry using the following antibodies: CD4 (RM4-5), CD45.1 (A20), Vβ8.3 TCR (1B3.3), Vα2 TCR (B20.1).

REAGENTS	SUPPLIER	CATALOGUE NUMBER
Antibodies		
APC Rat anti-Mouse CD185 (CXCR5) (2G8)	BD Bioscience	Cat#560615;
Alexa Fluor® 488 Mouse anti-Bcl-6 (K112-91)	BD Bioscience	Cat# 561524;
APC/Cyanine7 anti-mouse CD45.1 (A20)	Biolegend	Cat# 110716;
eFluor450 CD4 Monoclonal Antibody (RM4-5)	Invitrogen	Cat# 48-0042-82;
PerCP/Cyanine5.5 anti-T-bet Antibody	Biolegend	Cat# 644806;
PE Rat anti-Mouse CD4 (RM4-5)	BD Bioscience	Cat# 553049;
PE/Cyanine7 anti-mouse CD8a (53-6.7)	Biolegend	Cat# 00722;
eFluor450 CD19 Monoclonal Antibody (eBio1D3 (1D3))	Invitrogen	Cat# 48-0193-82;
APC/Cyanine7 anti-mouse CD62L (MEL-14)	Biolegend	Cat# 104428;
V500 Rat anti-Mouse CD44 (Pgp-1/Ly-24)	BD Bioscience	Cat# 560781;
PerCP/Cyanine5.5 anti-mouse I-A ^b (AF6-120.1)	Biolegend	Cat#116416
Alexa Fluor® 647 anti-mouse CD3ε (145-2C11)	Biolegend	Cat#100322
APC/Cyanine7 anti-mouse CD8a (53-6.7)	Biolegend	Cat#100714
Pacific Blue™ anti-mouse Ly-6C (HK1.4)	Biolegend	Cat#128014
Brilliant Violet 650™ anti-mouse/human CD11b (M1/70)	Biolegend	Cat#101259

Brilliant Violet 785™ anti-mouse NK-1.1 (PK136)	Biolegend	Cat# 108749
BUV395 Rat Anti-Mouse CD4 (RM4-5)	BD Bioscience	Cat# 740208
BUV496 Rat Anti-Mouse CD45R/B220 (RA3-6B2)	BD Bioscience	Cat# 612950
BUV805 Rat Anti-Mouse Ly-6G (1A8)	BD Bioscience	Cat# 741994
PE anti-mouse CD11c (N418)	Biolegend	Cat#117308
PE/Cyanine7 anti-mouse CD335 (NKp46) (29A1.4)	Biolegend	Cat#137618
FITC Rat Anti-Mouse Ly-6C (AL-21)	BD Bioscience	Cat#561085
Brilliant Violet 421™ anti-mouse NK-1.1 (PK136)	Biolegend	Cat#108741
Brilliant Violet 711™ anti-mouse CD335 (NKp46) (29A1.4)	Biolegend	Cat#137621
Brilliant Violet 711™ anti-mouse CD8a (53-6.7)	Biolegend	Cat#100759
BV786 Hamster Anti-Mouse CD11c (HL3)	BD Bioscience	Cat#563735
PE-CF594 Rat Anti-Mouse CD19 (1D3)	BD Bioscience	Cat#562291
PE-Cy™7 Hamster Anti-Mouse CD3e (145-2C11)	BD Bioscience	Cat#552774
APC TCR V alpha 2 Monoclonal Antibody (B20.1)	Invitrogen	Cat#17-5812-82
BV605 Rat Anti-Mouse CD119 (IFNγR1) (GR20)	BD Bioscience	Cat#745111
Alexa Fluor® 488 Rabbit Anti-mouse TCF1/TCF7 (C63D9)		

	Cell Signaling	Cat#6444S
Brilliant Violet 421™ anti-mouse IFN- γ (XMG1.2)	Biolegend	Cat#505830
Brilliant Violet 605™ anti-mouse CD4 (RM4-5)	Biolegend	Cat#100548
Brilliant Violet 711™ anti-mouse CD186 (CXCR6) (<u>SA051D1</u>)	Biolegend	Cat#151111
Brilliant Violet 785™ anti-mouse CD366 (Tim-3) (RMT3-23)	Biolegend	Cat#119725
BUV395 Hamster Anti-Mouse CD279 (PD-1) (J43)	BD Bioscience	Cat#744549
BUV563 Rat Anti-Mouse CD44 (IM7)	BD Bioscience	Cat#741227
BUV737 Hamster Anti-Mouse CD183 (CXCR3-173)	BD Bioscience	Cat#741895
BUV805 Rat Anti-Mouse CD8a (53-6.7)	BD Bioscience	Cat#612898
PE Granzyme B Monoclonal Antibody (GB11)	Invitrogen	Cat#12-8899-41
PE-CF594 Mouse Anti-Bcl-6 (K112-91)	BD Bioscience	Cat#562401
PE-Cy™7 Rat Anti-Mouse CD45R/B220 (RA3-6B2)	BD Bioscience	Cat#552772

Table 1. List of Antibodies for Flow Cytometry

10.10. Immunofluorescence Staining

For confocal microscopy analysis LNs were directly collected and incubated for 90 min at room temperature in Antigen Fix (Diapath #P0016), and then washed in DPBS and dehydrated in 30% Sucrose at 4°C. LNs were embedded in OCT freezing media (Killik Bio-Optica #05-9801) and 20 μ m cryosections were prepared on a CM1520 cryostat (Leica), adhered to Superfrost Plus slides (Thermo Scientific) and stored at -20°C.

Sections were permeabilized and blocked with Blocking Buffer composed of DPBS, 10% FCS and 0.3% Triton X-100 (Sigma-Aldrich) and stained in the same buffer. Before staining with fluorochrome-conjugated antibodies, slides were stained with Anti-mouse Fc Block antibody to block non-specific binding sites. The following fluorochrome-conjugated antibodies were used for cryosections staining: rat α B220 (RA3-6B2), rabbit α GFP (Invitrogen), mouse α NK1.1 (PK136), α CD11c (HL3). Stained slides were mounted with FluorSaveTM Reagent (Merck Millipore, #345789) and Images were acquired on an inverted Leica microscope (SP5, Leica Microsystems) with a motorized stage for tiled imaging using an HC PL APO CS 20X (NA 0.7) Dry or HCX PL APO λ blue 40X (NA 1.25) Oil objectives. To minimize fluorophore spectral spillover, we used the Leica sequential laser excitation and detection modality. B cell follicles were defined on the basis of the position of polyclonal B cells or B220 staining. For three-dimensional image acquisition, 6-10 xy stacks (1,024 \times 1,024 pixels) sampled with 2- μ m z spacing were acquired to provide image volumes that were 20 μ m in depth.

REAGENTS	SUPPLIER	CATALOGUE NUMBER
Antibodies		
Alexa Fluor® 647 anti-mouse NK-1.1 (PK136)	Biolegend	Cat#108720
Alexa Fluor® 647 anti-mouse CD11c (N418)	Biolegend	Cat#117312
Brilliant Violet 421 TM anti-mouse/human CD45R/B220 (RA3-6B2)	Biolegend	Cat#103251

Table 2. List of Antibodies for Immunofluorescence

10.11. qPCR

Total RNA was isolated from frozen LNs with the ReliaPrep RNA Miniprep system (Promega), following the manufacturer's instructions. One microgram of total RNA was reverse transcribed before qPCR analyses for *Ifna4* (Mm00833969_S1), *Ifnb* (Mm00439552_S1), *Isg15* (Mm01705338_S1), *Oas2* (Mm00460961_m1), *Il6* (Mm00446190_M1), *Il12a* (*Mm01208555_m1*) and *Il12b* (Mm01288989_m1), *Ifng* (Mm01168134_m1) in a QuantStudio 5 Real-Time PCR

System (all from Thermo Fisher Scientific). All experiments were done in duplicate, and data were normalized to the housekeeping gene **Gapdh** (Mm99999915_g1, Thermo Fisher Scientific).

10.12. Statistical analyses

Results are expressed as the mean±s.e.m. All statistical analyses were performed in Prism 5 (GraphPad Software). Means between two groups were compared with unpaired two-tailed t tests. Means among three or more groups were compared with one-way or two-way ANOVA. The Bonferroni or LSD post test were used to correct for multiple comparisons.

10.13 DCs Single-cell RNA sequencing

DCs were sorted with a BD FACSAria fusion (BD Biosciences). After exclusion of doublets, cells positive for CD11c and MHC-II but negative for CD3 and B220 underwent single-cell sorting into 384-well cell capture plates containing 2 µl of lysis solution and barcoded poly(T) reverse transcription primers for scRNA-seq. Immediately after sorting, each plate was spun down to ensure cell immersion in the lysis solution, snap frozen on dry ice and stored at –80 °C until processing.

10.13.1 Massively parallel single-cell RNA sequencing library preparation

Single-cell libraries were prepared as previously described (Jaitin *et al*, 2014). Briefly, mRNA from cells sorted into cell capture plates was barcoded, converted to cDNA and pooled with an automated pipeline. The pooled sample was then linearly amplified by T7 in vitro transcription, and the resulting RNA was fragmented and converted to a sequencing-ready library by tagging the samples with pool barcodes and Illumina sequences during ligation, reverse transcription and PCR. Each pool of cells was tested for library quality, and the concentration was assessed as described (Jaitin *et al*, 2014). All RNA-seq libraries (pooled at equimolar concentrations) were sequenced on the Illumina NextSeq 500 platform at a median sequencing depth of 38,323 reads per cell. Sequences were mapped to the mouse genome (mm9), demultiplexed and filtered as described (Jaitin *et al*, 2014), extracting a set of unique molecular identifiers that defined

distinct transcripts in single cells for further processing. We estimated the level of spurious UMIs in the data with statistics on empty MARS-seq wells and excluded all plates with estimated noise of >5%. Mapping of reads was done with HISAT (v0.1.6); reads with multiple mapping positions were excluded. Reads were associated with genes if they were mapped to an exon, using the UCSC Genome Browser for reference. Exons of different genes that shared a genomic position on the same strand were considered to represent a single gene with a concatenated gene symbol. Cells with fewer than 500 UMIs were discarded from the analysis.

10.13.2 Clustering of dendritic cells

For clustering of scRNA-seq data from CD11c⁺MHC-II^{hi} DCs, we used the R package MetaCell (Baran *et al*, 2018), as previously described. Cells from rVSV- and rLCMV-infected LNs, from all time points and genetic backgrounds, were clustered. Meta-cells were annotated by pooled differential expression of marker genes, as described above. The selected genes, priorities and fold change threshold parameters were as follows:

Group	Gene	Priority	Fold change
Migratory cDC2	<i>Fscn1</i>	1	5
Migratory cDC2	<i>Il12b</i>	1	2
cDC1	<i>Naaa</i>	1	3
cDC1	<i>Cd24a</i>	1	2.5
cDC2	<i>Cd209a</i>	2	5
cDC2	<i>Cd209d</i>	2	1.8
MoDC	<i>Csf1r</i>	4	3
MoDC	<i>Tgfb1</i>	4	2
MoDC	<i>Fcer1g</i>	4	2
Macrophage	<i>Clqb</i>	5	4

10.14 SMARTA Single-cell RNA sequencing

Single cell populations from rVSV-infected mice (CD4⁺CD45.1⁺ or CD4⁺ CD45.1⁺ PD-1⁺ ICOS⁺ 405 cells) rLCMV-infected mice or not infected SMARTA mice (CD4⁺CD45.1⁺) were sorted by using the following flow cytometry antibodies: APC-CXCR5 (2G8; BD Biosciences), APC-Cy7-CD45.1 (A20; Biolegend), eFluor450-CD4 (RM4-5; eBioscience), BV605-ICOS (C398.4A; Biolegend), PE-PD-1 (J43; eBioscience), AxFl488-B220 (RA3-6B2; Biolegend), AxFl488-NK1.1 (PK136; Biolegend), PE-Cy7-CD8a (53-6.7; Biolegend). LIVE/DEAD Fixable Aqua Dead Cell Stain (ThermoFisher Scientific) was used to exclude dead cells. Sorting was performed following exclusion of doublets, dead cells, and B220⁺ B cells, NK1.1⁺ NK cells, CD8a⁺ T cells, and Ter119⁺ erythrocytes.

10.14.1 MARS-seq low level data processing

Single-cell libraries were prepared as described in the paragraph 10.13.1 and were sequenced on an Illumina NextSeq 500 or NOVA-seq, at a median sequencing depth of 15,054 reads per cell. Sequences were mapped to the mouse genome (mm10), demultiplexed, and filtered as previously described (Berglund *et al*, 2018); (Oxenius *et al*, 1998), with the following adaptations. Mapping of reads was done using HISAT (version 0.1.6); reads with multiple mapping positions were excluded. Reads were associated with genes if they were mapped to an exon, using the UCSC genome browser for reference. We estimated a median of 2% spurious UMI in the data using statistics on empty MARS-seq wells. Cells with less **than 500 UMI**, **more than 500,000 UMI**, or with more than 10% mitochondrial genes were excluded from analysis. We used the Seurat package(ref) to analyze scRNA-seq data. Default parameters were used unless otherwise stated.

10.15 GP-1-IgG ELISA

The ELISA was carried out in 96-well half-volume polystyrene plates. Plates were coated overnight at 4°C with goat α -human IgG Fc capturing Ab (Jackson ImmunoResearch #109005098) diluted 1:1000 in 0.1 M sodium carbonate buffer (pH 9.6). Afterward, the plates were blocked for 1 h with 5% milk diluted in PBS-T. Thereafter, the plates were

incubated with 50 μ l per well of GP-1-IgG-containing cell supernatant for 1 h. Sera were diluted 1:4 in 5% milk in the first 96-well row and then 1:2 serial dilution were carried out in the GP-1-IgG-saturated plates, followed by incubation for 1 h. Finally, the plates were incubated for 1h with HRP Goat anti-mouse IgG (Biolegend #405306) diluted 1:500 in 0,5% BFA. HRP was detected by using TMB Substrate Reagent set (BD Bioscience #555214). All steps were carried out at room temperature. Between each step the plates were washed five times with PBS-T. Titers represent double-above-background values.

11 REFERENCES

- Abdel-Hakeem MS (2019) Viruses teaching immunology: Role of LCMV model and human viral infections in immunological discoveries. *Viruses* 11
- Akiba H, Takeda K, Kojima Y, Usui Y, Harada N, Yamazaki T, Ma J, Tezuka K, Yagita H & Okumura K (2005) The Role of ICOS in the CXCR5 + Follicular B Helper T Cell Maintenance In Vivo . *J Immunol* 175: 2340–2348
- Allen CD, Okada T & Cyster JG (2008) Germinal Center Organization and Cellular Dynamics Role of the GC in Antibody Responses. *Immunity* 27: 190–202
- Allen CDC, Okada T, Tang HL & Cyster JG (2007) Imaging of germinal center selection events during affinity maturation. *Science (80-)* 315: 528–531
- Althaus CL, Ganusov V V. & De Boer RJ (2007) Dynamics of CD8 + T Cell Responses during Acute and Chronic Lymphocytic Choriomeningitis Virus Infection . *J Immunol* 179: 2944–2951
- Andersen C, Jensen T, Nansen A, Marker O & Thomsen AR (1999) CD4+ T cell-mediated protection against a lethal outcome of systemic infection with vesicular stomatitis virus requires CD40 ligand expression, but not IFN- γ or IL-4. *Int Immunol* 11: 2035–2042
- Anderson AO & Anderson ND (1975) Studies on the structure and permeability of the microvasculature in normal rat lymph nodes. *Am J Pathol* 80: 387–418
- Anderson J, Byrne JA, Schreiber R, Patterson S & Oldstone MB (1985) Biology of cloned cytotoxic T lymphocytes specific for lymphocytic choriomeningitis virus: clearance of virus and in vitro properties. *J Virol* 53: 552–560
- Arguni E, Arima M, Tsuruoka N, Sakamoto A, Hatano M & Tokuhisa T (2006) JunD/AP-1 and STAT3 are the major enhancer molecules for high Bcl6 expression in germinal center B cells. *Int Immunol* 18: 1079–1089
- Arnaut RA & Nowak MA (2000) Competitive coexistence in antiviral immunity. *J Theor Biol* 204: 431–441
- Athie-Morales V, Smits HH, Cantrell DA & Hilkens CMU (2004) Sustained IL-12 Signaling Is Required for Th1 Development. *J Immunol* 172: 61–69
- Ballesteros-tato A, León B, Graf BA, Moquin A, Scott P, Lund FE & Randall TD (2013) Follicular Helper Differentiation. 36: 847–856
- Baran Y, Sebe-Pedros A, Lubling Y, Giladi A, Chomsky E, Meir Z, Hoichman M,

- Lifshitz A & Tanay A (2018) MetaCell: Analysis of single cell RNA-seq data using k-NN graph partitions. *bioRxiv*: 1–19
- Baranek T, Manh TPV, Alexandre Y, Maqbool MA, Cabeza JZ, Tomasello E, Crozat K, Bessou G, Zucchini N, Robbins SH, *et al* (2012) Differential responses of immune cells to type i interferon contribute to host resistance to viral infection. *Cell Host Microbe* 12: 571–584
- Barbet G, Sander LE, Geswell M, Leonardi I, Iliev I, Blander JM, Medicine WC, Division H, Medicine WC, Medicine WC, *et al* (2018) Follicular Helper Cell and Antibody Responses. *Immunity* 48: 584–598
- Barnett BE, Staupe RP, Odorizzi PM, Palko O, Tomov VT, Mahan AE, Gunn B, Chen D, Paley MA, Alter G, *et al* (2016) Cutting Edge: B Cell–Intrinsic T-bet Expression Is Required To Control Chronic Viral Infection. *J Immunol* 197: 1017–1022
- Barreto VM, Ramiro AR & Nussenzweig MC (2005) Activation-induced deaminase: Controversies and open questions. *Trends Immunol* 26: 90–96
- Batten M, Ramamoorthi N, Kljavin NM, Ma CS, Cox JH, Dengler HS, Danilenko DM, Caplazi P, Wong M, Fulcher DA, *et al* (2010) IL-27 supports germinal center function by enhancing IL-21 production and the function of T follicular helper cells. *J Exp Med* 207: 2895–2906
- Baumjohann D, Preite S, Reboldi A, Ronchi F, Ansel KM, Lanzavecchia A & Sallusto F (2013) Persistent Antigen and Germinal Center B Cells Sustain T Follicular Helper Cell Responses and Phenotype. *Immunity* 38: 596–605
- Becht E, McInnes L, Healy J, Dutertre CA, Kwok IWH, Ng LG, Ginhoux F & Newell EW (2019) Dimensionality reduction for visualizing single-cell data using UMAP. *Nat Biotechnol* 37: 38–47
- Berglund E, Maaskola J, Schultz N, Friedrich S, Marklund M, Bergenstråhle J, Tarish F, Tanoglidi A, Vickovic S, Larsson L, *et al* (2018) Spatial maps of prostate cancer transcriptomes reveal an unexplored landscape of heterogeneity. *Nat Commun* 9
- Bergthaler A, Flatz L, Hegazy AN, Johnson S, Horvath E, Löhning M & Pinschewer DD (2010) Viral replicative capacity is the primary determinant of lymphocytic choriomeningitis virus persistence and immunosuppression. *Proc Natl Acad Sci U S A* 107: 21641–21646

- Bergtold A, Desai DD, Gavhane A & Clynes R (2005) Cell surface recycling of internalized antigen permits dendritic cell priming of B cells. *Immunity* 23: 503–514
- Borrow P, Evans CF & Oldstone MB (1995) Virus-induced immunosuppression: immune system-mediated destruction of virus-infected dendritic cells results in generalized immune suppression. *J Virol* 69: 1059–1070
- Bradley LM, Dalton DK & Croft M (1996) A direct role for IFN- γ in regulation of Th1 cell development. *J Immunol* 157: 1350–8
- Braun A, Worbs T, Moschovakis GL, Halle S, Hoffmann K, Bölter J, Münk A & Förster R (2011) Afferent lymph-derived T cells and DCs use different chemokine receptor CCR7-dependent routes for entry into the lymph node and intranodal migration. *Nat Immunol* 12: 879–887
- Braun D, Caramalho I & Demengeot J (2002) IFN- α/β enhances BCR-dependent B cell responses. *Int Immunol* 14: 411–419
- Breitfeld D, Ohl L, Kremmer E, Ellwart J, Sallusto F, Lipp M & Förster R (2000) Follicular B helper T cells express CXC chemokine receptor 5, localize to B cell follicles, and support immunoglobulin production. *J Exp Med* 192: 1545–1551
- Cabeza-Cabrerizo M, Cardoso A, Minutti CM, Pereira da Costa M & Reis Sousa C (2021) Annual Review of Immunology Dendritic Cells Revisited.
- Cano-Gamez E, Soskic B, Roumeliotis TI, So E, Smyth DJ, Baldrighi M, Willé D, Nakic N, Esparza-Gordillo J, Larminie CGC, *et al* (2020) Single-cell transcriptomics identifies an effectorness gradient shaping the response of CD4⁺ T cells to cytokines. *Nat Commun* 11: 1–15
- Carrasco YR & Batista FD (2007) B Cells Acquire Particulate Antigen in a Macrophage-Rich Area at the Boundary between the Follicle and the Subcapsular Sinus of the Lymph Node. *Immunity* 27: 160–171
- Cattoretti G, Chang CC, Cechova K, Zhang J, Ye BH, Falini B, Louie DC, Offit K, Chaganti RSK & Dalla-Favera R (1995) BCL-6 protein is expressed in germinal-center B cells. *Blood* 86: 45–53
- Chakarov S & Fazilleau N (2014) Monocyte-derived dendritic cells promote T follicular helper cell differentiation. *EMBO Mol Med* 6: 590–603
- Chen LL, Frank AM, Adams JC & Steinman RM (1978) Distribution of horseradish

- peroxidase (HRP)- anti-HRP immune complexes in mouse spleen with special reference to follicular dendritic cells. *J Cell Biol* 79: 184–199
- Chevrier S, Kratina T, Emslie D, Tarlinton DM & Corcoran LM (2017) IL4 and IL21 cooperate to induce the high Bcl6 protein level required for germinal center formation. *Immunol Cell Biol* 95: 925–932
- Cho SS, Bacon CM, Sudarshan C, Rees RC, Finbloom D, Pine R & O’Shea JJ (1996) Activation of STAT4 by IL-12 and IFN-alpha: evidence for the involvement of ligand-induced tyrosine and serine phosphorylation. *J Immunol* 157: 4781–9
- Choi YS, Eto D, Yang JA, Lao C & Crotty S (2013) Cutting Edge: STAT1 Is Required for IL-6–Mediated Bcl6 Induction for Early Follicular Helper Cell Differentiation. *J Immunol* 190: 3049–3053
- Clark SL (1962) The reticulum of lymph nodes in mice studied with the electron microscope. *Am J Anat* 110: 217–257
- Croft M & Swain SL (1991) B cell response to fresh and effector T helper cells: Role of cognate T-B interaction and the cytokines IL-2, IL-4, and IL-6. *J Immunol* 146
- Crotty S (2011) Follicular Helper CD4 T Cells (T_{FH}) . *Annu Rev Immunol* 29: 621–663
- Crotty S (2014) T Follicular Helper Cell Differentiation, Function, and Roles in Disease. *Immunity* 41: 529–542
- Crotty S (2019) T Follicular Helper Cell Biology: A Decade of Discovery and Diseases. *Immunity* 50: 1132–1148
- Cucak H, Yrlid U, Reizis B, Kalinke U & Johansson-Lindbom B (2009) Type I Interferon Signaling in Dendritic Cells Stimulates the Development of Lymph-Node-Resident T Follicular Helper Cells. *Immunity* 31: 491–501
- Cyster JG (2010) B cell follicles and antigen encounters of the third kind. *Nat Immunol* 11: 989–996
- Cyster JG, Dang E V., Reboldi A & Yi T (2014) 25-Hydroxycholesterols in innate and adaptive immunity. *Nat Rev Immunol* 14: 731–743
- Dasoveanu DC, Park HJ, Ly CL, Shipman WD, Chyou S, Kumar V, Tarlinton D, Ludewig B, Mehrara BJ, Lu TT, *et al* (2020) Lymph node stromal CCL2 limits antibody responses. 5
- De Giovanni M, Cutillo V, Giladi A, Sala E, Maganuco CG, Medaglia C, Di Lucia P,

- Bono E, Cristofani C, Consolo E, *et al* (2020) Spatiotemporal regulation of type I interferon expression determines the antiviral polarization of CD4⁺ T cells. *Nat Immunol* 21: 321–330
- De Guinoa JS, Barrio L, Mellado M & Carrasco YR (2011) CXCL13/CXCR5 signaling enhances BCR-triggered B-cell activation by shaping cell dynamics. *Blood* 118: 1560–1569
- DeKruyff RH, Ju ST, Hunt AJ, Mosmann TR & Umetsu DT (1989) Induction of antigen-specific antibody responses in primed and unprimed B cells. Functional heterogeneity among Th1 and Th2 T cell clones. *J Immunol* 142: 2575–82
- Del Prete G, Maggi E, Parronchi P, Chretien I, Tiri A, Macchia D, Ricci M, Banchereau J, De Vries J & Romagnani S (1988) IL-4 is an essential factor for the IgE synthesis induced in vitro by human T cell clones and their supernatants. *J Immunol* 140
- Detje CN, Meyer T, Schmidt H, Kreuz D, Rose JK, Bechmann I, Prinz M & Kalinke U (2009) Local Type I IFN Receptor Signaling Protects against Virus Spread within the Central Nervous System. *J Immunol* 182: 2297–2304
- Diehl S, Anguita J, Hoffmeyer A, Zapton T, Ihle JN, Fikrig E & Rincón M (2000) Inhibition of Th1 differentiation by IL-6 is mediated by SOCS1. *Immunity* 13: 805–815
- Dituro D, Winstead C, Pham D, Witte S, Andargachew R, Singer JR, Wilson CG, Zindl CL, Luther RJ, Silberger DJ, *et al* (2018) Differential IL-2 expression defines developmental fates of follicular versus nonfollicular helper T cells. *Science* (80-) 361
- Eisenbarth SC (2019) Dendritic cell subsets in T cell programming: location dictates function. *Nat Rev Immunol* 19: 89–103
- Eschli B, Quirin K, Wepf A, Weber J, Zinkernagel R & Hengartner H (2006) Identification of an N-Terminal Trimeric Coiled-Coil Core within Arenavirus Glycoprotein 2 Permits Assignment to Class I Viral Fusion Proteins. *J Virol* 80: 5897–5907
- Espéli M & Linterman M (2015) T follicular helper cells: Methods and protocols. *T Follicular Help Cells Methods Protoc* 1291: 1–226
- Eto D, Lao C, DiToro D, Barnett B, Escobar TC, Kageyama R, Yusuf I & Crotty S

- (2011) IL-21 and IL-6 are critical for different aspects of B cell immunity and redundantly induce optimal follicular helper CD4 T cell (T_{fh}) differentiation. *PLoS One* 6
- Fallet B, Narr K, Ertuna YI, Remy M, Sommerstein R, Cornille K, Kreutzfeldt M, Page N, Zimmer G, Geier F, *et al* (2016) Interferon-driven deletion of antiviral B cells at the onset of chronic infection. *Sci Immunol* 1: 1–23
- Garside P, Ingulli E, Merica RR, Johnson JG, Noelle RJ & Jenkins MK (1998) Visualization of specific B and T lymphocyte interactions in the lymph node. *Science* (80-) 281: 96–99
- Gatto D & Brink R (2013) B cell localization: Regulation by EBI2 and its oxysterol ligand. *Trends Immunol* 34: 336–341
- Gerner MY, Torabi-Parizi P & Germain RN (2015a) Strategically Localized Dendritic Cells Promote Rapid T Cell Responses to Lymph-Borne Particulate Antigens. *Immunity* 42: 172–185
- Gerner MY, Torabi-Parizi P & Germain RN (2015b) Strategically Localized Dendritic Cells Promote Rapid T Cell Responses to Lymph-Borne Particulate Antigens. *Immunity* 42: 172–185
- Girard JP, Moussion C & Förster R (2012) HEVs, lymphatics and homeostatic immune cell trafficking in lymph nodes. *Nat Rev Immunol* 12: 762–773
- Golnaz Vahedi S, Sun H, Kanno Y, Hirahara JJ, Cannons JL, Schwartzberg PL, Takahashi H, Kato M, Iwata S, Shingo Nakayamada K, *et al* (2014) Helper Cell Genetic Program Transcription Factors in the T Follicular Bcl6: Divergent Roles of STAT Family Type I IFN Induces Binding of STAT1 to.
- Gray EE & Cyster JG (2012) Lymph node macrophages. *J Innate Immun* 4: 424–436
- Groom JR, Richmond J, Murooka TT, Sorensen EW, Sung JH, Bankert K, von Andrian UH, Moon JJ, Mempel TR & Luster AD (2012) CXCR3 Chemokine Receptor-Ligand Interactions in the Lymph Node Optimize CD4⁺ T Helper 1 Cell Differentiation. *Immunity* 37: 1091–1103
- Gunn MD, Tangemann K, Tam C, Cyster JG, Rosen SD & Williams LT (1998) A chemokine expressed in lymphoid high endothelial venules promotes the adhesion and chemotaxis of naive T lymphocytes. *Proc Natl Acad Sci U S A* 95: 258–263
- Guo ZS (2018) The 2018 Nobel Prize in medicine goes to cancer immunotherapy

- (editorial for BMC cancer). *BMC Cancer* 18: 1–2
- Hale JS, Youngblood B, Latner DR, Mohammed AUR, Ye L, Akondy RS, Wu T, Iyer SS & Ahmed R (2013) Distinct memory cd4+ t cells with commitment to t follicular helper- and t helper 1-cell lineages are generated after acute viral infection. *Immunity* 38: 805–817
- Hamilton SE & Jameson SC (2007) CD8+ T Cell Differentiation: Choosing a Path through T-bet. *Immunity* 27: 180–182
- Hangartner L, Zinkernagel RM & Hengartner H (2006) Antiviral antibody responses: The two extremes of a wide spectrum. *Nat Rev Immunol* 6: 231–243
- Hardtke S, Ohl L & Förster R (2005) Balanced expression of CXCR5 and CCR7 on follicular T helper cells determines their transient positioning to lymph node follicles and is essential for efficient B-cell help. *Blood* 106: 1924–1931
- Harker JA, Lewis GM, Mack L & Zuniga EI (2011) Late interleukin-6 escalates T follicular helper cell responses and controls a chronic viral infection. *Science (80-)* 334: 825–829
- Hastie E, Cataldi M, Marriott I & Grzelishvili VZ (2013) Understanding and altering cell tropism of vesicular stomatitis virus. *Virus Res* 176: 16–32
- Hatzi K, Philip Nance J, Kroenke MA, Bothwell M, Haddad EK, Melnick A & Crotty S (2015) BCL6 orchestrates Tfh cell differentiation via multiple distinct mechanisms. *J Exp Med* 212: 539–553
- Herold S, Steinmueller M, Von Wulffen W, Cakarova L, Pinto R, Pleschka S, Mack M, Kuziel WA, Corazza N, Brunner T, *et al* (2008) Lung epithelial apoptosis in influenza virus pneumonia: The role of macrophage-expressed TNF-related apoptosis-inducing ligand. *J Exp Med* 205: 3065–3077
- Heufler C, Koch F, Stanzl U, Topar G, Wysocka M, Trinchieri G, Enk A, Steinman RM, Romani N & Schuler G (1996) Interleukin-12 is produced by dendritic cells and mediates T helper 1 development as well as interferon- γ production by T helper 1 cells. *Eur J Immunol* 26: 659–668
- Hickman HD (2017) New insights into antiviral immunity gained through intravital imaging. *Curr Opin Virol* 22: 59–63
- Hilligan KL & Ronchese F (2020) Antigen presentation by dendritic cells and their instruction of CD4+ T helper cell responses. *Cell Mol Immunol* 17: 587–599

- Hotson AN, Hardy JW, Hale MB, Contag CH & Nolan GP (2009) The T Cell STAT Signaling Network Is Reprogrammed within Hours of Bacteremia via Secondary Signals. *J Immunol* 182: 7558–7568
- Huang HY, Rivas-Caicedo A, Renevey F, Cannelle H, Peranzoni E, Scarpellino L, Hardie DL, Pommier A, Schaeuble K, Favre S, *et al* (2018) Identification of a new subset of lymph node stromal cells involved in regulating plasma cell homeostasis. *Proc Natl Acad Sci U S A* 115: E6826–E6835
- Huang S, Hendriks W, Althage A, Hemmi S, Bluethmann H, Kamijo R, Vilček J, Zinkernagel RM & Aguet M (1993) Immune response in mice that lack the interferon- γ receptor. *Science (80-)* 259: 1742–1745
- Hunziker L, Recher M, Macpherson AJ, Ciurea A, Freigang S, Hengartner H & Zinkernagel RM (2003) Hypergammaglobulinemia and autoantibody induction mechanisms in viral infections. *Nat Immunol* 4: 343–349
- Iannacone M, Moseman EA, Tonti E, Bosurgi L, Junt T, Henrickson SE, Whelan SP, Guidotti LG & Von Andrian UH (2010) Subcapsular sinus macrophages prevent CNS invasion on peripheral infection with a neurotropic virus. *Nature* 465: 1079–1083
- Iannacone M, Sitia G, Isogawa M, Marchese P, Castro MG, Lowenstein PR, Chisari F V., Ruggeri ZM & Guidotti LG (2005) Platelets mediate cytotoxic T lymphocyte-induced liver damage. *Nat Med* 11: 1167–1169
- Ichii H, Sakamoto A, Hatano M, Okada S, Toyama H, Taki S, Arima M, Kuroda Y & Tokuhisa T (2002) Role for Bcl-6 in the generation and maintenance of memory CD8⁺ T cells. *Nat Immunol* 3: 558–563
- Jacobsen JT, Hu W, Castro TBR, Solem S, Galante A, Lin Z, Allon SJ, Mesin L, Bilate AM, Schiepers A, *et al* (2021) Expression of Foxp3 by T follicular helper cells in end-stage germinal centers. *Science (80-)* 373
- Jaitin DA, Kenigsberg E, Keren-Shaul H, Elefant N, Paul F, Zaretsky I, Mildner A, Cohen N, Jung S, Tanay A, *et al* (2014) Massively parallel single cell RNA-Seq for marker-free decomposition of tissues into cell types HHS Public Access. *Science (80-)* 343: 776–779
- Jarjour M, Jorquera A, Mondor I, Wienert S, Narang P, Coles MC, Klauschen F & Bajénoff M (2014) Fate mapping reveals origin and dynamics of lymph node

- follicular dendritic cells. *J Exp Med* 211: 1109–1122
- Jego G, Palucka AK, Blanck JP, Chalouni C, Pascual V & Banchereau J (2003) Plasmacytoid dendritic cells induce plasma cell differentiation through type I interferon and interleukin 6. *Immunity* 19: 225–234
- Johnson JE, Nasar F, Coleman JW, Price RE, Javadian A, Draper K, Lee M, Reilly PA, Clarke DK, Hendry RM, *et al* (2007) Neurovirulence properties of recombinant vesicular stomatitis virus vectors in non-human primates. *Virology* 360: 36–49
- Johnston RJ, Choi YS, Diamond JA, Yang JA & Crotty S (2012) STAT5 is a potent negative regulator of T FH cell differentiation. *J Exp Med* 209: 243–250
- Johnston RJ, Poholek AC, Ditoro D, Yusuf I, Eto D, Barnett B, Dent AL, Craft J & Crotty S (2009) Bcl6 and Blimp-1 Are Reciprocal and Antagonistic Regulators of T Follicular Helper Cell Differentiation. *Science (80-)* 325: 1006–1010
- Junt T, Moseman EA, Iannacone M, Massberg S, Lang PA, Boes M, Fink K, Henrickson SE, Shayakhmetov DM, Di Paolo NC, *et al* (2007) Subcapsular sinus macrophages in lymph nodes clear lymph-borne viruses and present them to antiviral B cells. *Nature* 450: 110–114
- Kallies A & Good-Jacobson KL (2017) Transcription Factor T-bet Orchestrates Lineage Development and Function in the Immune System. *Trends Immunol* 38: 287–297
- Kamath AT, Pooley J, O’Keeffe MA, Vremec D, Zhan Y, Lew AM, D’Amico A, Wu L, Tough DF & Shortman K (2000) The Development, Maturation, and Turnover Rate of Mouse Spleen Dendritic Cell Populations. *J Immunol* 165: 6762–6770
- Kastenmüller W, Torabi-Parizi P, Subramanian N, Lämmermann T & Germain RN (2012) A spatially-organized multicellular innate immune response in lymph nodes limits systemic pathogen spread. *Cell* 150: 1235–1248
- Katakai T, Hara T, Lee JH, Gonda H, Sugai M & Shimizu A (2004) A novel reticular stromal structure in lymph node cortex: An immuno-platform for interactions among dendritic cells, T cells and B cells. *Int Immunol* 16: 1133–1142
- Kim CH, Rott LS, Clark-Lewis I, Campbell DJ, Wu L & Butcher EC (2001) Subspecialization of CXCR5⁺ T cells: B helper activity is focused in a germinal center-localized subset of CXCR5⁺ T cells. *J Exp Med* 193: 1373–1381
- Kiner E, Willie E, Vijaykumar B, Chowdhary K, Schmutz H, Chandler J, Schnell A, Thakore PI, LeGros G, Mostafavi S, *et al* (2021) Gut CD4⁺ T cell phenotypes are a

- continuum molded by microbes, not by TH archetypes. *Nat Immunol* 22: 216–228
- Kitano M, Moriyama S, Ando Y, Hikida M, Mori Y, Kurosaki T & Okada T (2011) Bcl6 Protein Expression Shapes Pre-Germinal Center B Cell Dynamics and Follicular Helper T Cell Heterogeneity. *Immunity* 34: 961–972
- Krueger PD, Goldberg MF, Hong S-W, Osum KC, Langlois RA, Kotov DI, Dileepan T & Jenkins MK (2021) Two sequential activation modules control the differentiation of protective T helper-1 (Th1) cells. *Immunity* 1: 1–15
- Kuka M, De Giovanni M & Iannacone M (2019) The role of type I interferons in CD4+ T cell differentiation. *Immunol Lett* 215: 19–23
- Kuka M & Iannacone M (2014) The role of lymph node sinus macrophages in host defense. *Ann N Y Acad Sci* 1319: 38–46
- Kuka M & Iannacone M (2021) Heterogeneity in antiviral B cell responses: Lessons from the movies*. *Immunol Rev* 306: 224–233
- Kunz S, Edelmann KH, de la Torre JC, Gorney R & Oldstone MBA (2003) Mechanisms for lymphocytic choriomeningitis virus glycoprotein cleavage, transport, and incorporation into virions. *Virology* 314: 168–178
- Lazarevic V, Chen X, Shim JH, Hwang ES, Jang E, Bolm AN, Oukka M, Kuchroo VK & Glimcher LH (2011) T-bet represses TH 17 differentiation by preventing Runx1-mediated activation of the gene encoding ROR γ t. *Nat Immunol* 12: 96–104
- Lee SK, Silva DG, Martin JL, Pratama A, Hu X, Chang PP, Walters G & Vinuesa CG (2012) Interferon- γ Excess Leads to Pathogenic Accumulation of Follicular Helper T Cells and Germinal Centers. *Immunity* 37: 880–892
- Liang H, Tang J, Liu Z, Liu Y, Huang Y, Xu Y, Hao P, Yin Z, Zhong J, Ye L, *et al* (2019) ZIKV infection induces robust Th1-like Tfh cell and long-term protective antibody responses in immunocompetent mice. *Nat Commun* 10: 1–16
- Lighvani AA, Frucht DM, Jankovic D, Yamane H, Aliberti J, Hissong BD, Nguyen B V., Gadina M, Sher A, Paul WE, *et al* (2001) T-bet is rapidly induced by interferon- γ in lymphoid and myeloid cells. *Proc Natl Acad Sci U S A* 98: 15137–15142
- Liu D, Xu H, Shih C, Wan Z, Ma X, Ma W, Luo D & Qi H (2015) T-B-cell entanglement and ICOSL-driven feed-forward regulation of germinal centre reaction. *Nature* 517: 214–218

- Lönnberg T, Svensson V, James KR, Fernandez-Ruiz D, Sebina I, Montandon R, Soon MSF, Fogg LG, Nair AS, Liligeto U, *et al* Single-cell RNA-seq and computational analysis using temporal mixture modelling resolves Th1/Tfh fate bifurcation in malaria denotes equal contribution † denotes equal contribution Author contributions TL and KRJ performed the single-cell RNA-seq experiments. VS developed the GPfates model in collaboration with MZ Europe PMC Funders Group. *Sci Immunol* 2
- Louie DAP & Liao S (2019) Lymph node subcapsular sinus macrophages as the frontline of lymphatic immune defense. *Front Immunol* 10: 1–9
- Ly A, Liao Y, Pietrzak H, Ioannidis LJ, Sidwell T, Gloury R, Doerflinger M, Triglia T, Qin RZ, Groom JR, *et al* (2019) Transcription Factor T-bet in B Cells Modulates Germinal Center Polarization and Antibody Affinity Maturation in Response to Malaria. *Cell Rep* 29: 2257–2269.e6
- Ma B, Jablonska J, Lindenmaier W & Dittmar KEJ (2007) Immunohistochemical study of the reticular and vascular network of mouse lymph node using vibratome sections. *Acta Histochem* 109: 15–28
- Maloy KJ, Burkhart C, Freer G, Rüllicke T, Pircher H, Kono DH, Theofilopoulos AN, Ludewig B, Hoffmann-Rohrer U, Zinkernagel RM, *et al* (1999) Qualitative and quantitative requirements for CD4+ T cell-mediated antiviral protection. *J Immunol* 162: 2867–74
- Mandels TE, Phippsi RP, Abbot A & Tew JG (1980) The Follicular Dendritic Cell: Long Term Antigen Retention During Immunity. *Immunol Rev* 53: 29–59
- Marshall HD, Urban SL & Welsh RM (2011) Virus-Induced Transient Immune Suppression and the Inhibition of T Cell Proliferation by Type I Interferon. *J Virol* 85: 5929–5939
- Marshall JD, Heeke DS, Abbate C, Yee P & Van Nest G (2006) Induction of interferon- γ from natural killer cells by immunostimulatory CpG DNA is mediated through plasmacytoid-dendritic-cell- produced interferon- α and tumour necrosis factor- α . *Immunology* 117: 38–46
- Martín-Fontecha A, Thomsen LL, Brett S, Gerard C, Lipp M, Lanzavecchia A & Sallusto F (2004) Induced recruitment of NK cells to lymph nodes provides IFN- γ for TH1 priming. *Nat Immunol* 5: 1260–1265

- McDevitt HO, Askonas BA, Humphrey JH, Schechter I & Sela M (1966) The localization of antigen in relation to specific antibody-producing cells. I. Use of a synthetic polypeptide [(T,G)-A--L] labelled with iodine-125. *Immunology* 11: 337–51
- McNab F, Mayer-Barber K, Sher A, Wack A & O’Garra A (2015) Type I interferons in infectious disease. *Nat Rev Immunol* 15: 87–103
- Medaglia C, Giladi A, Stoler-Barak L, De Giovanni M, Salame TM, Biram A, David E, Li H, Iannacone M, Shulman Z, *et al* (2017) Spatial reconstruction of immune niches by combining photoactivatable reporters and scRNA-seq. *Science (80-)* 358: 1622–1626
- Mendoza A, Yewdell WT, Hoyos B, Schizas M, Bou-Puerto R, Michaels AJ, Brown CC, Chaudhuri J & Rudensky AY (2021) Assembly of a spatial circuit of T-bet-expressing T and B lymphocytes is required for antiviral humoral immunity. *Sci Immunol* 6
- Meredith MM, Liu K, Darrasse-Jeze G, Kamphorst AO, Schreiber HA, Guermonprez P, Idoyaga J, Cheong C, Yao KH, Niec RE, *et al* (2012) Expression of the zinc finger transcription factor zDC (Zbtb46, Btbd4) defines the classical dendritic cell lineage. *J Exp Med* 209: 1153–1165
- Min J, Yang D, Kim M, Haam K, Yoo A, Choi JH, Schraml BU, Kim YS, Kim D & Kang SJ (2018) Inflammation induces two types of inflammatory dendritic cells in inflamed lymph nodes. *Exp Mol Med* 50
- Misumi I & Whitmire JK (2014) B Cell Depletion Curtails CD4 + T Cell Memory and Reduces Protection against Disseminating Virus Infection . *J Immunol* 192: 1597–1608
- Moseman EA, Wu T, Carlos De La Torre J, Schwartzberg PL & MCGavern DB (2016) Type I interferon suppresses virus-specific B cell responses by modulating CD8 + T cell differentiation LCMV-specific B cells in a perforin-dependent manner within the first few days of infection. Blockade of IFN-I signaling protected LCMV-specific B cell. *Sci Immunol* 1: 1–31
- Mosmann TR, Cherwinski H, Bond MW, Giedlin MA & Coffman RL (1986) Two types of murine helper T cell clone. I. Definition according to profiles of lymphokine activities and secreted proteins. *J Immunol* 136: 2348–57

- Mueller SN & Rouse BT (2008) Immune responses to viruses. *Clin Immunol*: 421–431
- Nakayamada S, Kanno Y, Takahashi H, Jankovic D, Lu KT, Johnson TA, Sun H wei, Vahedi G, Hakim O, Handon R, *et al* (2011) Early Th1 Cell Differentiation Is Marked by a Tfh Cell-like Transition. *Immunity* 35: 919–931
- Nguyen KB, Watford WT, Salomon R, Hofmann SR, Pien GC, Morinobu A, Gadina M, O’Shea JJ & Biron CA (2002) Critical role for STAT4 activation by type 1 interferons in the interferon- γ response to viral infection. *Science (80-)* 297: 2063–2066
- Noelle RJ, McCann J, Marshall L & Bartlett WC (1989) Cognate interactions between helper T cells and B cells. III. Contact-dependent, lymphokine-independent induction of B cell cycle entry by activated helper T cells. *J Immunol* 143
- Novelli F & Casanova JL (2004) The role of IL-12, IL-23 and IFN- γ in immunity to viruses. *Cytokine Growth Factor Rev* 15: 367–377
doi:10.1016/j.cytogfr.2004.03.009 [PREPRINT]
- Nurieva RI, Chung Y, Martinez GJ, Yang XO, Tanaka S, Matskevitch TD, Wang Y-H & Dong C (2009) Bcl6 Mediates the Development of T Follicular Helper Cells. *Science (80-)* 325: 1001–1005
- Obeng-Adjei N, Portugal S, Holla P, Li S, Sohn H, Ambegaonkar A, Skinner J, Bowyer G, Doumbo OK, Traore B, *et al* (2017) Malaria-induced interferon- γ drives the expansion of Tbethiatypical memory B cells. *PLoS Pathog* 13
- Ochsenbein AF, Pinschewer DD, Sierro S, Horvath E, Hengartner H & Zinkernagel RM (2000) Protective long-term antibody memory by antigen-driven and T help-dependent differentiation of long-lived memory B cells to short-lived plasma cells independent of secondary lymphoid organs. *Proc Natl Acad Sci U S A* 97: 13263–13268
- Odermatt B, Eppler M, Leist TP, Hengartner H & Zinkernagel RM (1991) Virus-triggered acquired immunodeficiency by cytotoxic T-cell-dependent destruction of antigen-presenting cells and lymph follicle structure. *Proc Natl Acad Sci U S A* 88: 8252–8256
- Oestreich KJ, Huang AC & Weinmann AS (2011) The lineage-defining factors T-bet and Bcl-6 collaborate to regulate Th1 gene expression patterns. *J Exp Med* 208: 1001–1013

- Oestreich KJ, Mohn SE & Weinmann AS (2012) Molecular mechanisms that control the expression and activity of Bcl-6 in T H1 cells to regulate flexibility with a T FH-like gene profile. *Nat Immunol* 13: 405–411
- Okada T, Miller MJ, Parker I, Krummel MF, Neighbors M, Hartley SB, O’Garra A, Cahalan MD & Cyster JG (2005) Antigen-engaged B cells undergo chemotaxis toward the T zone and form motile conjugates with helper T cells. *PLoS Biol* 3: 1047–1061
- Olatunde AC, Hale JS & Lamb TJ (2021) Cytokine-skewed Tfh cells: functional consequences for B cell help. *Trends Immunol* 42: 536–550
- Onai N, Obata-Onai A, Schmid MA, Ohteki T, Jarrossay D & Manz MG (2007) Identification of clonogenic common Flt3⁺M-CSFR⁺ plasmacytoid and conventional dendritic cell progenitors in mouse bone marrow. *Nat Immunol* 8: 1207–1216
- Osokine I, Snell LM, Cunningham CR, Yamada DH, Wilson EB, Elsaesser HJ, De La Torre JC & Brooks D (2014) Type I interferon suppresses de novo virus-specific CD4 Th1 immunity during an established persistent viral infection. *Proc Natl Acad Sci U S A* 111: 7409–7414
- Oxenius A, Bachmann MF, Zinkernagel RM & Hengartner H (1998) Virus-specific MHC class II-restricted TCR-transgenic mice: Effects on humoral and cellular immune responses after viral infection. *Eur J Immunol* 28: 390–400
- Oxenius A, Karrer U, Zinkernagel RM & Hengartner H (1999) IL-12 is not required for induction of type 1 cytokine responses in viral infections. *J Immunol* 162: 965–973
- Ozaki K, Spolski R, Feng CG, Qi CF, Cheng J, Sher A, Morse HC, Liu C, Schwartzberg PL & Leonard WJ (2002) A critical role for IL-21 in regulating immunoglobulin production. *Science (80-)* 298: 1630–1634
- Pene J, Rousset F, Briere F, Chretien I, Bonnefoy JY, Spits H, Yokota T, Arai N, Arai K, Banchereau J, *et al* (1988) IgE production by normal human lymphocytes is induced by interleukin 4 and suppressed by interferons γ and α and prostaglandin E2. *Proc Natl Acad Sci U S A* 85: 6880–6884
- Phan TG, Grigorova I, Okada T & Cyster JG (2007) Subcapsular encounter and complement-dependent transport of immune complexes by lymph node B cells. *Nat Immunol* 8: 992–1000

- Phan TG, Paus D, Chan TD, Turner ML, Nutt SL, Basten A & Brink R (2006) High affinity germinal center B cells are actively selected into the plasma cell compartment. *J Exp Med* 203: 2419–2424
- Pinschewer DD, Perez M, Jeetendra E, Bächli T, Horvath E, Hengartner H, Whitt MA, de la Torre JC & Zinkernagel RM (2004) Kinetics of protective antibodies are determined by the viral surface antigen. *J Clin Invest* 114: 988–993
- Planz O, Seiler P, Hengartner H & Zinkernagel RM (1996) Specific cytotoxic T cells eliminate cells producing neutralizing antibodies. *Nature* 382: 726–729
- Platanias LC (2005) Mechanisms of type-I- and type-II-interferon-mediated signalling. *Nat Rev Immunol* 5: 375–386
- Preite S, Huang B, Cannons JL, McGavern DB & Schwartzberg PL (2019) PI3K orchestrates T follicular helper cell differentiation in a context dependent manner: Implications for autoimmunity. *Front Immunol* 10: 1–10
- Purkerson JM & Isakson PC (1992) Interleukin 5 (IL-5) Provides a Signal That Is Required in Addition to ID4 for Isotype Switching to Immunoglobulin (Ig) G1 and IgE. *J Exp Med* 175: 973–982
- Ray JP, Marshall HD, Laidlaw BJ, Staron MM, Kaech SM & Craft J (2014) Transcription factor STAT3 and type I interferons are corepressive insulators for differentiation of follicular helper and T helper 1 cells. *Immunity* 40: 367–377
- Reinhardt RL, Liang HE & Locksley RM (2009) Cytokine-secreting follicular T cells shape the antibody repertoire. *Nat Immunol* 10: 385–393
- Reljic R, Wagner SD, Peakman LJ & Fearon DT (2000) Suppression of signal transducer and activator of transcription 3-dependent B lymphocyte terminal differentiation by BCL-6. *J Exp Med* 192: 1841–1847
- Rouse BT & Sehrawat S (2010) Immunity and immunopathology to viruses: What decides the outcome? *Nat Rev Immunol* 10: 514–526
- Rubtsova K, Rubtsov A V., Thurman JM, Mennona JM, Kappler JW & Murrack P (2017) B cells expressing the transcription factor T-bet drive lupus-like autoimmunity. *J Clin Invest* 127: 1392–1404
- Sammicheli S, Kuka M, Di Lucia P, Jimenez De Oya N, De Giovanni M, Fioravanti J, Cristofani C, Maganuco CG, Fallet B, Ganzer L, *et al* (2016) Inflammatory monocytes hinder antiviral B cell responses Europe PMC Funders Group. *October*

21: 1–11

- Schaerli P, Willimann K, Lang AB, Lipp M, Loetscher P & Moser B (2000) CXC chemokine receptor 5 expression defines follicular homing T cells with B cell helper function. *J Exp Med* 192: 1553–1562
- Schijns VECJ, Haagmans BL, Wierda CMH, Kruithof B, Horzinek MC, Heijnen IAFM & Alber G (1998) Mice lacking IL-12 develop polarized Th1 cells during viral infection. *J Immunol* 160: 3958–3964
- Schoenborn JR & Wilson CB (2007) Regulation of Interferon- γ During Innate and Adaptive Immune Responses. *Adv Immunol* 96: 41–101
- Schroder K, Hertzog PJ, Ravasi T & Hume DA (2004) Interferon- γ : an overview of signals, mechanisms and functions. *J Leukoc Biol* 75: 163–189
- Schulz EG, Mariani L, Radbruch A & Höfer T (2009) Sequential Polarization and Imprinting of Type 1 T Helper Lymphocytes by Interferon- γ and Interleukin-12. *Immunity* 30: 673–683
- Schwickert TA, Lindquist RL, Shakhar G, Livshits G, Skokos D, Kosco-Vilbois MH, Dustin ML & Nussenzweig MC (2007) In vivo imaging of germinal centres reveals a dynamic open structure. *Nature* 446: 83–87
- Seiler P, Kalinke U, Rüllicke T, Bucher EM, Böse C, Zinkernagel RM & Hengartner H (1998) Enhanced Virus Clearance by Early Inducible Lymphocytic Choriomeningitis Virus-Neutralizing Antibodies in Immunoglobulin-Transgenic Mice. *J Virol* 72: 2253–2258
- Shao P, Li F, Wang J, Chen X, Liu C & Xue H-H (2019) Cutting Edge: Tcf1 Instructs T Follicular Helper Cell Differentiation by Repressing Blimp1 in Response to Acute Viral Infection. *J Immunol* 203: 801–806
- Sheikh AA, Cooper L, Feng M, Souza-Fonseca-Guimaraes F, Lafouresse F, Duckworth BC, Huntington ND, Moon JJ, Pellegrini M, Nutt SL, *et al* (2019) Context-Dependent Role for T-bet in T Follicular Helper Differentiation and Germinal Center Function following Viral Infection. *Cell Rep* 28: 1758-1772.e4
- Sheikh AA & Groom JR (2020) Transcription tipping points for T follicular helper cell and T-helper 1 cell fate commitment. *Cell Mol Immunol*: 1–11
- Smelt SC, Borrow P, Kunz S, Cao W, Tishon A, Lewicki H, Campbell KP & Oldstone MBA (2001) Differences in Affinity of Binding of Lymphocytic Choriomeningitis

- Virus Strains to the Cellular Receptor α -Dystroglycan Correlate with Viral Tropism and Disease Kinetics. *J Virol* 75: 448–457
- Snapper CM & Paul WE (1987) Interferon- γ and B cell stimulatory factor-1 reciprocally regulate Ig isotype production. *Science* (80-) 236: 944–947
- Solmaz G, Puttur F, Francozo M, Lindenberg M, Guderian M, Swallow M, Duhan V, Khairnar V, Kalinke U, Ludewig B, *et al* (2019) TLR7 controls VSV replication in CD169⁺ SCS macrophages and associated viral neuroinvasion. *Front Immunol* 10: 1–18
- Staniek J, Lorenzetti R, Heller B, Janowska I, Schneider P, Unger S, Warnatz K, Seidl M, Venhoff N, Thiel J, *et al* (2019) TRAIL-R1 and TRAIL-R2 mediate TRAIL-dependent apoptosis in activated primary human B lymphocytes. *Front Immunol* 10: 1–13
- Steinman RM & Cohn ZA (1973) Identification of a novel cell type in peripheral lymphoid organs of mice: I. Morphology, quantitation, tissue distribution. *J Exp Med* 137: 1142–1162
- Stuart T, Butler A, Hoffman P, Hafemeister C, Papalexi E, Mauck WM, Hao Y, Stoeckius M, Smibert P & Satija R (2019) Comprehensive Integration of Single-Cell Data. *Cell* 177: 1888-1902.e21
- Summers WC (2009) Virus Infection. *Encycl Microbiol* 13: 546–552
- Suzuki K, Grigorova I, Phan TG, Kelly LM & Cyster JG (2009) Visualizing B cell capture of cognate antigen from follicular dendritic cells. *J Exp Med* 206: 1485–1493
- Swain SL, McKinstry KK & Strutt TM (2012) Expanding roles for CD4⁺ T cells in immunity to viruses. *Nat Rev Immunol* 12: 136–148
- Swiecki M, Gilfillan S, Vermi W, Wang Y & Colonna M (2010) Plasmacytoid Dendritic Cell Ablation Impacts Early Interferon Responses and Antiviral NK and CD8⁺ T Cell Accrual. *Immunity* 33: 955–966
- Szabo SJ, Kim ST, Costa GL, Zhang X, Fathman CG & Glimcher LH (2000) A novel transcription factor, T-bet, directs Th1 lineage commitment. *Cell* 100: 655–669
- Takahashi Y, Dutta PR, Cerasoli DM & Kelsoe G (1998) In situ studies of the primary immune response to (4-hydroxy-3-nitrophenyl)acetyl. v. affinity maturation develops in two stages of clonal selection. *J Exp Med* 187: 885–895

- Thieu VT, Yu Q, Chang H-C, Yeh N, Nguyen ET, Sehra S & Kaplan MH (2008) Stat4 is required for T-bet to promote IL-12-dependent Th1 fate determination. *Immunity* 29: 679–690
- Tpw JG, Phipps RP & Mandel TE (1980) The Maintenance and Regulation of the Humoral Immune Response: Persisting Antigen and the Role of Follicular Antigen-Binding Dendritic Cells as Accessory Cells. *Immunol Rev* 53: 175–201
- Tuzlak S, Dejean AS, Iannacone M, Quintana FJ, Waisman A, Ginhoux F, Korn T & Becher B (2021) Repositioning TH cell polarization from single cytokines to complex help. *Nat Immunol* 22: 1210–1217
- Ugur M & Mueller SN (2019) T cell and dendritic cell interactions in lymphoid organs: More than just being in the right place at the right time. *Immunol Rev* 289: 115–128 doi:10.1111/imr.12753 [PREPRINT]
- Utzschneider DT, Charmoy M, Chennupati V, Pousse L, Ferreira DP, Calderon-Copete S, Danilo M, Alfei F, Hofmann M, Wieland D, *et al* (2016) T Cell Factor 1-Expressing Memory-like CD8+ T Cells Sustain the Immune Response to Chronic Viral Infections. *Immunity* 45: 415–427
- Victoria GD (2014) SnapShot: The Germinal Center Reaction. *Cell* 159: 700-700.e1
- Victoria GD & Nussenzweig MC (2012) Germinal centers. *Annu Rev Immunol* 30: 429–457
- Vilibic-Cavlek T, Savic V, Ferenc T, Mrzljak A, Barbic L, Bogdanic M, Stevanovic V, Tabain I, Ferencak I & Zidovec-Lepej S (2021) Lymphocytic choriomeningitis—emerging trends of a neglected virus: A narrative review. *Trop Med Infect Dis* 6
- Von Andrian UH & Mempel TR (2003) Homing and cellular traffic in lymph nodes. *Nat Rev Immunol* 3: 867–878
- Vremec D, O’Keeffe M, Hochrein H, Fuchsberger M, Caminschi I, Lahoud M & Shortman K (2007) Production of interferons by dendritic cells, plasmacytoid cells, natural killer cells, and interferon-producing killer dendritic cells. *Blood* 109: 1165–1173
- Wakil AE, Wang ZE, Ryan JC, Fowell DJ & Locksley RM (1998) Interferon γ derived from CD4 + T cells is sufficient to mediate T helper cell type 1 development. *J Exp Med* 188: 1651–1656
- Wang P, Wang Y, Xie L, Xiao M, Wu J, Xu L, Bai Q, Hao Y, Huang Q, Chen X, *et al*

- (2019) The transcription factor T-bet is required for optimal type I follicular helper T cell maintenance during acute viral infection. *Front Immunol* 10
- Wang X, Rodda LB, Bannard O & Cyster JG (2014) Integrin-Mediated Interactions between B Cells and Follicular Dendritic Cells Influence Germinal Center B Cell Fitness. *J Immunol* 192: 4601–4609
- Weber JP, Fuhrmann F, Feist RK, Lahmann A, Al Baz MS, Gentz LJ, Vu Van D, Mages HW, Haftmann C, Riedel R, *et al* (2015) ICOS maintains the T follicular helper cell phenotype by down-regulating krüppel-like factor 2. *J Exp Med* 212: 217–233
- Wenner CA, Güler ML, Macatonia SE, O’Garra A & Murphy KM (1996) Roles of IFN-gamma and IFN-alpha in IL-12-induced T helper cell-1 development. *J Immunol* 156: 1442–7
- Whelan SPJ (1972) Vesicular stomatitis virus pseudotypes. *Nature* 240: 129
- Whitmire JK, Eam B, Benning N & Whitton JL (2007) Direct Interferon- γ Signaling Dramatically Enhances CD4 + and CD8 + T Cell Memory . *J Immunol* 179: 1190–1197
- Wilson EB, Yamada DH, Elsaesser H, Herskovitz J, Deng J, Cheng G, Aronow BJ, Karp CL & Brooks DG (2013) Blockade of chronic type I interferon signaling to control persistent LCMV infection. *Science (80-)* 340: 202–207
- Wu T, Shin HM, Moseman EA, Ji Y, Huang B, Harly C, Sen JM, Berg LJ, Gattinoni L, McGavern DB, *et al* (2015) TCF1 Is Required for the T Follicular Helper Cell Response to Viral Infection. *Cell Rep* 12: 2099–2110
- Xu L, Cao Y, Xie Z, Huang Q, Bai Q, Yang X, He R, Hao Y, Wang H, Zhao T, *et al* (2015) The transcription factor TCF-1 initiates the differentiation of TFH cells during acute viral infection. *Nat Immunol* 16: 991–999
- Yamazaki C, Sugiyama M, Ohta T, Hemmi H, Hamada E, Sasaki I, Fukuda Y, Yano T, Nobuoka M, Hirashima T, *et al* (2013) Critical Roles of a Dendritic Cell Subset Expressing a Chemokine Receptor, XCR1. *J Immunol* 190: 6071–6082
- Ye BH, Cattoretti1 G, Shen Q, Zhang1 J, Hawe4 N, De Waard3 R, Leung3 C, Nouri-Shirazi3 M, Orazi A, Chaganti RSK, *et al* (1997) The BCL-6 proto-oncogene controls germinal-centre formation and Th2-type inflammation
- Zhang J, Marotel M, Fauteux-Daniel S, Mathieu AL, Viel S, Marçais A & Walzer T

- (2018) T-bet and Eomes govern differentiation and function of mouse and human NK cells and ILC1. *Eur J Immunol* 48: 738–750
- Zhang Y, Apilado R, Coleman J, Ben-Sasson S, Tsang S, Hu-Li J, Paul WE & Huang H (2001a) Interferon γ stabilizes the T helper cell type 1 phenotype. *J Exp Med* 194: 165–172
- Zhang Y, Apilado R, Coleman J, Ben-Sasson S, Tsang S, Hu-Li J, Paul WE & Huang H (2001b) Interferon γ stabilizes the T helper cell type 1 phenotype. *J Exp Med* 194: 165–172
- Zhou L, Chong MMW & Littman DR (2009) Plasticity of CD4⁺ T Cell Lineage Differentiation. *Immunity* 30: 646–655
- Zhou X, Ramachandran S, Mann M & Popkin DL (2012) Role of lymphocytic choriomeningitis virus (LCMV) in understanding viral immunology: Past, present and future. *Viruses* 4: 2650–2669
- Zhu J, Jankovic D, Oler AJ, Wei G, Sharma S, Hu G, Guo L, Yagi R, Yamane H, Punkosdy G, *et al* (2012) The Transcription Factor T-bet Is Induced by Multiple Pathways and Prevents an Endogenous Th2 Cell Program during Th1 Cell Responses. *Immunity* 37: 660–673
- Zinkernagel RM & Doherty PC (1975) H 2 compatibility requirement for T cell mediated lysis of target cells infected with lymphocytic choriomeningitis virus. Different cytotoxic T cell specificities are associated with structures coded for in H 2K or H 2D. *J Exp Med* 141: 1427–1436